UNIVERSITÉ DE NEUCHÂTEL
FACULTE DES SCIENCES
INSTITUT DE CHIMIE

Iron and Vanadium Complexes for the Catalytic Oxidation of Hydrocarbons : Chemical Catalysts and Biomimetic Models

Thèse présentée à la Faculté des Sciences de l'Université de Neuchâtel par

Laura González Cuervo

Chimiste diplômée de l'Université d'Oviedo (Espagne)

pour l'obtention du titre de Docteur ès Sciences

Institut de Chimie de l'Université de Neuchâtel

Octobre 2003

UNIVERSITÉ DE NEUCHÂTEL
FACULTE DES SCIENCES
INSTITUT DE CHIMIE

Iron and Vanadium Complexes for the Catalytic Oxidation of Hydrocarbons : Chemical Catalysts and Biomimetic Models

Thèse présentée à la Faculté des Sciences de l'Université de Neuchâtel par

Laura González Cuervo

Chimiste diplômée de l'Université d'Oviedo (Espagne)

pour l'obtention du titre de Docteur ès Sciences

Institut de Chimie de l'Université de Neuchâtel

Octobre 2003

IMPRIMATUR POUR LA THESE

Iron and Vanadium Complexes for the Catalytic Oxidation of Hydrocarbons: Chemical Catalysts and Biomimetic Models

Mme Laura GONZALEZ CUERVO

UNIVERSITE DE NEUCHATEL

FACULTE DES SCIENCES

La Faculté des sciences de l'Université de Neuchâtel, sur le rapport des membres du jury

MM. G. Süss-Fink (directeur de thèse), T. Ward et G. Shul'pin

autorise l'impression de la présente thèse.

Neuchâtel, le 28 octobre 2003

La doyenne:

Martine Rahier

« The most exciting phrase to hear in science, the one that heralds new discoveries, is not ‘Eureka!’ (I've found it!), but ‘That's funny’... »

Isaac Asimov (US (Russian-born) writer)

A mis padres

A mi hermana Sara

A mis abuelos

A Ray

Remerciements

Le présent travail de thèse a été effectué d'octobre 1999 à octobre 2003 dans le Département de Chimie Organométallique et de Catalyse Homogène de l'Institut de Chimie de l'Université de Neuchâtel, Suisse, sous la direction de *Monsieur* le *Professeur Dr. Georg Süss-Fink*.

En premier lieu, je tiens à exprimer ma sincère gratitude à *Monsieur* le *Professeur Dr. Süss-Fink*, mon directeur de thèse, pour m'avoir accueilli dans son groupe de recherche comme stagiaire Erasmus pendant l'année 1998-1999, et comme doctorante par la suite. Je tiens à lui remercier pour sa confiance et ses encouragements, ainsi que pour sa disponibilité pour la correction de ma thèse même pendant son semestre de congé scientifique.

Je tiens à remercier *Monsieur* le *Professeur Dr. Georgiy B. Shul'pin* de l'Institut Semenov de Chimie Physique de l'Académie Russe des Sciences (Moscou, Russie) pour avoir accepté d'être membre de mon jury de thèse ainsi que pour son aide inestimable pendant ces quatre ans dans mon sujet de recherche et pour ses encouragements.

Je tiens à remercier *Monsieur* le *Professeur Dr. Thomas Ward* de l'Institut de Chimie de l'Université de Neuchâtel, Suisse, pour avoir accepté d'être membre de mon jury de thèse ainsi que pour ses corrections judicieuses de mon manuscrit de thèse.

J’adresse mes remerciements aussi à *Madame* le *Dr. Galina V. Nizova* et *Monsieur* le *Dr. Yuriy N. Kozlov* de l’Institut Semenov de Chimie Physique de l’Académie Russe des Sciences (Moscou, Russie) pour leur collaboration scientifique pendant ces quatre ans.

Mes remerciements s’adressent aussi à *Monsieur* le *Dr. Bruno Therrien* et le Service de Cristallographie de l’Institut de Chimie dirigé par *Madame* le *Professeur Dr. Helen Stoeckli-Evans* pour leur disponibilité et leur travail afin de déterminer les structures de mes composés. Je remercie également Monsieur Dr. Saturnin Claude et Monsieur Heinz Bursian du service RMN et Messieurs Bernard Jean-Denis et Nicolas Mottier du service de spectrométrie de masse à l’Institut de Chimie, Monsieur Freddy Nydegger du Département de Chimie Organique de Fribourg et Monsieur le Dr. Hansjörg Eder responsable du Service de Microanalyse de Genève.

Il va sans dire que je remercie aussi à tous mes amis et collègues à l’Institut de Chimie, spécialement: Dr. Eva Garcia Fidalgo, Dr. Jessica Pacifico, Deborah Gonzalez Mantero, Dr. Enrique Lozano Diz, Dr. Elena Fernandez Ibañez, Dr. Antonia Neels, Gilles Gasser, Dr. Gaël Labat, Andreas Loosli, Mustapha Tiouabi, Julie Brettar, Marjorie Séverac et Vladimir Romakh. J’ai une pensée spéciale pour mon collègue Dr. Matthieu Fauré, disparu trop tôt.

Je remercie aussi tous les étudiants et étudiantes en première année en Chimie et Biologie qui ont assisté au travaux pratiques de Chimie Analytique I pendant les années 1999-2000 à 2002-2003, pour m’avoir accepté très amicalement comment assistante. Je n’oublie pas non plus Madame Marie-Eve Farine, devenue laborantine

en 2003, qui a fait sa deuxième année de formation avec moi et dont l'aide au laboratoire m'a permis d'avancer plus rapidement et avec bonne humeur dans ma thèse.

Je remercie aussi tout le personnel de l'Institut de Chimie : les secrétaires, les femmes de la cafeteria, et les concierges, spécialement M. Philippe Stauffer, qui était toujours là pour résoudre les problèmes.

Mes remerciements s'adressent aussi à *Monsieur* le *Professeur Dr. Raphaël Tabacchi* et à son groupe pour m'avoir donné la possibilité de commencer un stage post-doctoral dans le Département de Chimie Analytique de l'Institut de Chimie tout de suite après la fin de ma thèse.

Je remercie l'Université de Neuchâtel et le Fonds National Suisse de la Recherche Scientifique qui ont soutenu financièrement ce projet.

Enfin je remercie mes amis et proches à Neuchâtel et en Espagne, et tout particulièrement mes parents et ma sœur pour m'avoir soutenu merveilleusement dans la distance pendant ces quatre ans (os quiero a los tres). Je remercie à Ray pour son soutien, son amour, sa patience et sa bonne humeur, et aussi pour son inestimable aide avec l'anglais.

Table of Contents

Chapter 1

Introduction……1

Chapter 2

Iron and Vanadium Complexes as Chemical and Biological Oxidation Catalysts – State of the Art……...4

2.1 Iron Compounds in Oxidation Catalysis……4

2.1.1 Oxidation Reactions by Molecular Oxygen……4

2.1.2 Oxidation by Peroxides and other Oxygen Atoms Donors……...12

2.2 Iron-Containing Monooxygenases in Living Organisms……17

2.2.1 Cytochrome P450……..18

2.2.2 Methane Monooxygenase……21

2.3 Vanadium Compounds in Oxidation Catalysis……...……25

2.3.1 Alkane Oxidation by Hydrogen Peroxide……...……..25

2.3.2 Alkane Oxidation by Air……...……....31

2.4 Vanadium in Biological Systems……34

2.4.1 Vanadium-Containing Enzymes……...34

2.4.2 Vanadium Compounds in Medicine……37

2.4.3 Toxicity of Vanadium Compounds……...39

Chapter 3

Oxidations of Alkanes Catalyzed by Iron and Vanadium Complexes – Results…….40

3.1 Catalysis by Vanadium(V)-Containing Polyoxomolybdates……...40

3.1.1 Oxidation of Cyclooctane……..41

3.1.2 Oxidation of *n*-Octane and Adamantane: Regioselectivity…...……44

3.1.3 Oxidation of *cis*- and *trans*-Decalin……..47

3.1.4 Oxidation of Light Alkanes……...49

3.1.5 Conclusions……...51

3.2 Synthesis and Characterization of New Vanadium(IV) and (V) Complexes...54

3.2.1 Syntheses……...55

3.2.2 Molecular Structures…….58

3.3 Catalytic Potential of the Vanadium(IV) and (V) Complexes Synthesized….67

3.3.1 Alkane Oxidation with Peroxyacetic Acid Catalyzed by Vanadium Complexes…….…….....……72

3.3.2 Oxidation of Cyclohexane Catalyzed by NBu_4VO_3……..72

3.3.3 Oxidation of Cyclohexane Catalyzed by Vanadium(IV) and (V) Complexes…….……...…….80

3.3.4 Oxidation of Higher Alkanes Catalyzed by NBu_4VO_3…….83

3.3.5 Oxidation of Light Alkanes Catalyzed by NBu_4VO_3……...85

3.3.6 Conclusions……...86

3.4 Catalysis by Simple Iron(III) Salts……...89

3.4.1 Oxidation of Cyclohexane…….89

3.4.2 Oxidation of Higher Alkanes and Benzene……...97

3.4.3 Oxidation of Light Alkanes……...99

3.4.4 Comparison of $FeCl_3$ and $Fe(ClO_4)_3$ as Catalysts……...102

3.5 Catalysis by Iron(III) Complexes Containing *N*- and *N,O*-Chelating Ligands……...107

3.5.1 Alkane Oxidations Catalyzed by $[Fe_2(hptb)(\mu\text{–}OH)(NO_3)_2]^{2+}$…...108

3.5.2 Alkane Oxidations Catalyzed by $[Fe_2(tacn)_2(\mu\text{–}O)(CH_3CO_2)_2]^{2+}$...122

Chapter 4

Experimental Section…….....133

4.1 Solvents and Gases…….133

4.2 Starting Material…….133

4.3 Instrumentation and Analyses……134

4.4 Catalytic Experiments……136

4.5 Syntheses……141

4.6 Crystallographic Data…….145

Chapter 5

Summary……151

Chapter 6

Résumé……...159

Chapter 7

Resumen…….167

Chapter 8

References……..175

Introduction

Saturated hydrocarbons are abundant in nature, they are the main constituents of crude oil and of natural gas, and consequently they are important feedstocks for chemical production [1]. Crude oil contains a considerable amount of higher alkanes, while methane and ethane are the major components of natural gas [2]. Alkanes can also be synthesized from carbon monoxide and hydrogen by Fischer-Tropsch technologies, and cycloalkanes can be obtained from aromatics by catalytic hydrogenation processes [3].

$$CH_4 + 2\,O_2 \longrightarrow CO_2 + 2\,H_2O \quad (\Delta H° = 890\ kJ\ mol^{-1}) \qquad (1.1)$$

On the other hand, alkanes are known to be the least reactive organic compounds, as indicated by the old name "paraffins" (from Latin "parum affinis", meaning "without affinity"); they only react readily with molecular oxygen (air) to give carbon dioxide and water (burning), the example with methane is given in equation 1.1. The combustion of alkanes is one of the principal energy-producing processes, this is why alkanes are important energy resources [1]. However, the use of alkanes as new materials for chemical production is rather limited: Due to their chemical inertness, alkanes can be processed only under drastic conditions, normally at temperatures between 300 and 1200 °C. Thus, the petrochemical cracking process, transforming alkanes mainly into alkenes and hydrogen, requires 800 – 900°C [4]. The chlorination of methane with molecular chlorine to give methylchloride, dichlorometane and chloroform requires temperatures between 400 and 450°C [5] and the nitration of ethane to give nitroethane and nitromethane is carried out at 420°C

[6]. The formation of prussic acid from methane and ammonia (Andrussow process) takes place in the presence of a platinum metal catalyst at 1000 – 1200°C [7].

$$CH_4 + ½\ O_2 \longrightarrow CH_3OH \qquad (1.2)$$

However, nature has found methods to process even methane, the most inert of all alkanes, under mild conditions: Methane oxidizing bacteria (for example, *Methylococcus capsulatus*) transform methane into methanol using molecular oxygen from air, thanks to iron(III) containing enzymes known under the name of methane monooxygenases [8] (Eq. 1.2), but this process is not useful for bulk production. Therefore the development of catalytic processes for the conversion of alkanes, in particular of methane, into valuable oxygenates remains a challenge for the chemical community.

$$CH_4 + H_2O_2 + ½\ O_2 \longrightarrow CH_3OOH + H_2O \qquad (1.3)$$

One of the most interesting catalytic systems for the oxidative functionalization of alkanes comes from our group: A binary system composed of metavanadate, VO_3^-, and pyrazine-2-carboxylic acid (pcaH) turned out to be very active for the reaction of alkanes with hydrogen peroxide and air to give the corresponding alkyl hydroperoxides; the reaction also works with methane either in acetonitrile or in aqueous solution [9, 89, 147] (Eq. 1.3). Detailed synthetic studies on the coordination chemistry of vanadium(V) with *N,O*-coordinating ligand such as pcaH [10] as well as kinetic studies [11] gave a deep insight in the mechanistic aspects of this interesting catalytic reaction.

The aim of the present work was twofold: On the one hand, new vanadium(V) and also vanadium(IV) complexes should be synthesized, characterized and tested for their catalytic performance in the oxidative alkane functionalization, and on the other hand, the catalytic study should be extended to iron(III) complexes in the spirit of mimicking monooxygenase enzymes.

Iron and Vanadium Complexes as Chemical and Biological Oxidation Catalysts - State of the Art

The last two decades have witnessed a steadily increasing interest in the catalytic oxidation of alkanes with iron and vanadium complexes; a deeper insight in biological processes also stimulated research for chemical production [12, 13]. In this chapter the most important results in this area are presented.

2.1 Iron Compounds in Oxidation Catalysis

In the oxidation of alkanes using iron compounds as catalysts, two main types of oxidation reaction can be identified: oxidation reactions using molecular oxygen as the oxidizing agent and oxidation reactions using peroxides or other oxygen donors as the oxidizing agent.

2.1.1 Oxidation Reactions by Molecular Oxygen

Molecular oxygen, present in air, is the most interesting oxidizing agent, since it is readily available, easy to remove, environmentally benign, clean and cheap. Catalytic systems which work with O_2 are therefore very attractive.

2.1.1.1 The Ishii Reaction

In the late nineties, Ishii and coworkers reported a catalytic system formed by *N*-hydroxyphthalimide (pimoH), a transition metal salt [originally $Co(acac)_2$] and air,

that was able to oxidize alkanes like alkylbenzenes [14], adamantanes [15], isobutane [16], cycloalkanes and polycyclic alkanes [17]. Iron(III) acetylacetonate is used for the oxidation of isobutane at 100°C in benzonitrile with 10 atm of air giving *t*-butyl alcohol and acetone in a 52 : 9 ratio [16]. It is also used in adamantane oxidation, giving 63% of adamantan-1-ol after 6 hours of reaction in acetic acid at 75°C.

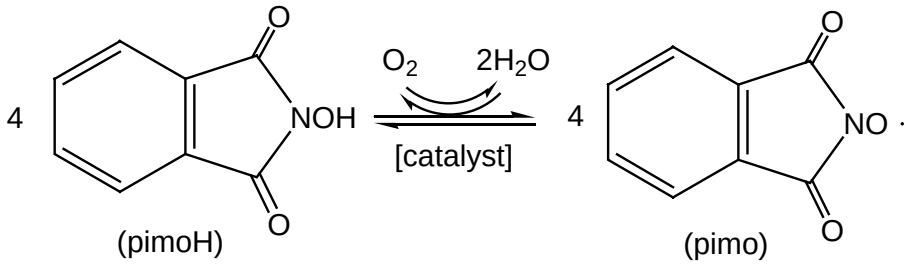

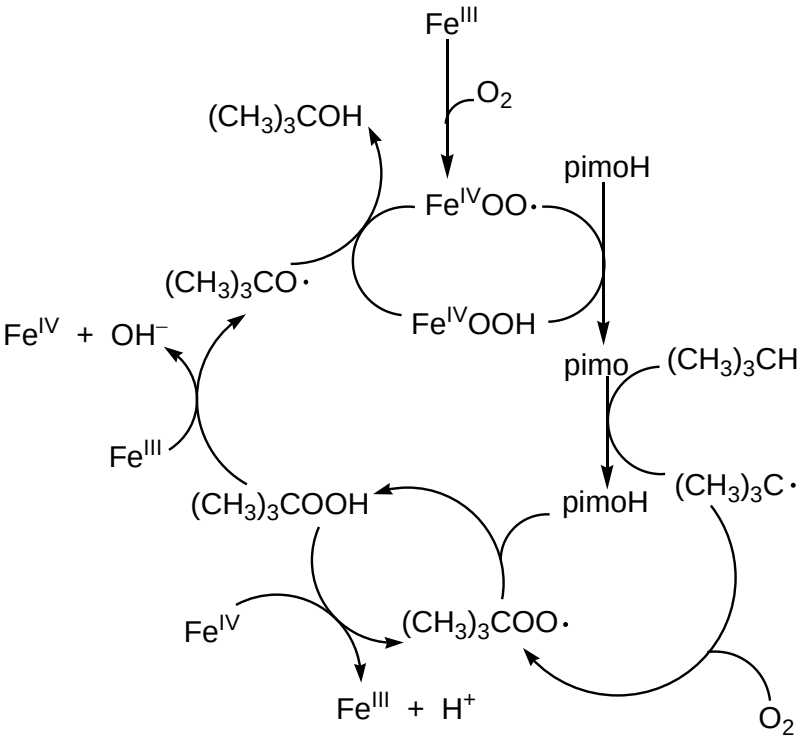

Scheme 2.1.1. The proposed mechanism of *tert*-butyl alcohol formation from isobutane in the Ishii oxidation reaction catalyzed by $Fe(acac)_3$.

The mechanism proposed for the Ishii reaction involves oxidative hydrogen atom abstraction from the alkane by the phthalimidooxyl (pimo) radical formed as intermediate from pimoH under the action of the transition metal catalyst [16] (Scheme 2.1.1).

2.1.1.2 Systems involving a sacrificial co-substrate

In recent years, several catalytic systems for alkane oxygenation composed of oxygen, an iron catalyst and a sacrificial co-substrate have been reported [18-28]. The sacrificial co-substrate is a reducing agent, e.g. an aldehyde, or a metal powder. Thus a dichloromethane solution of $Fe(OAc)_3$ or of $FeCl_3 \cdot 6\ H_2O$ was found to oxidize cyclohexane, cyclooctane, methylcyclohexane, adamantane, *n*-decane and ethylbenzene with molecular oxygen at room temperature, using heptanal as the sacrificial co-substrate; the products obtained are the corresponding ketones and alcohols [18]. Instead of iron(III) complexes, a mixture of metallic iron and acetic acid can also be used under the same conditions [18]. Synthetic iron porphyrine complexes were found to oxidize cyclohexane with O_2 to give cyclohexanol and cyclohexanone in benzene at 30°C, peroxo propionic acid and carbon dioxide being also observed as oxidation products of propionaldehyde [19]. 3-Methyl-butanal was used as sacrificial co-substrate in the $Fe(acac)_3$-catalyzed oxidation of cyclohexane, adamantane, tetraline and indane with O_2 in 1,2-dichloroethane [20].

$$M^{n+} + RCHO \longrightarrow M^{(n-1)+} + RCO\cdot + H^+ \quad (1)$$

$$M^{(n-1)+} + O_2 \longrightarrow [M(OO)]^{(n-1)+\cdot} \quad (2)$$

$$RCO\cdot + O_2 \longrightarrow RCOOO\cdot \quad (3)$$

$$RCOOO\cdot + RCHO \longrightarrow RCOOOH + RCO\cdot \quad (4)$$

$$M^{n+} + RCOOOH \longrightarrow [MO]^{n+} + RCOOH \quad (5)$$

$$[MO]^{n+} + R'–H \longrightarrow M^{n+} + R'OH \quad (6)$$

Scheme 2.1.2. General mechanism of the oxidation of an alkane R'H by a metal ion M^{n+} using an aldehyde, RCHO, as the sacrificial co-substrate.

The frequently proposed mechanistic pathway for the iron-catalyzed oxidations of alkanes in the presence of an aldehyde as the co-substrate involves the metal-catalyzed oxidation of the aldehyde to a peracid species (Eqs. 1–4, Scheme 2.1.2), which consequently form an iron(V) oxo complex (Eq. 5, Scheme 2.1.2); this species can introduce an oxygen atom into the alkane, yielding the corresponding alcohol (Eq. 6, Scheme 2.1.2) [21–24]. This mechanism is in part analogous to that of the alkane oxidation promoted by cytochrome P450 and NADH.

Some metal powders, especially metallic iron, can serve as both, reducing reagents and catalysts. If non-transition metals (e.g., zinc powder) are employed as reducing agents, transition metal complexes are necessary as catalysts. In these reactions, proton donors, such as carboxylic acids, are used to dissolve the solid metal. For example, $FeSO_4 \cdot 7\ H_2O$ fixed on silica gel was found to oxidize cyclohexane with molecular oxygen in the presence of zinc powder and acetic acid [25], and also methane to methanol and formaldehyde [26,27].

Other reducing agents have also been used: The pyridine complex $Fepy_4Cl_2$ catalyzes the oxidation of alkanes with oxygen from air to give the corresponding alcohols using hydrazobenzene as reducing agent [28].

2.1.1.3 Photo-induced oxidations

An alternative method for alkane oxidation that involves radical formation, using $FeCl_3$ as catalyst, molecular oxygen from air as oxidant and UV light was discovered in the nineties. This system oxidizes alkanes to their corresponding alkyl hydroperoxides [29-34].

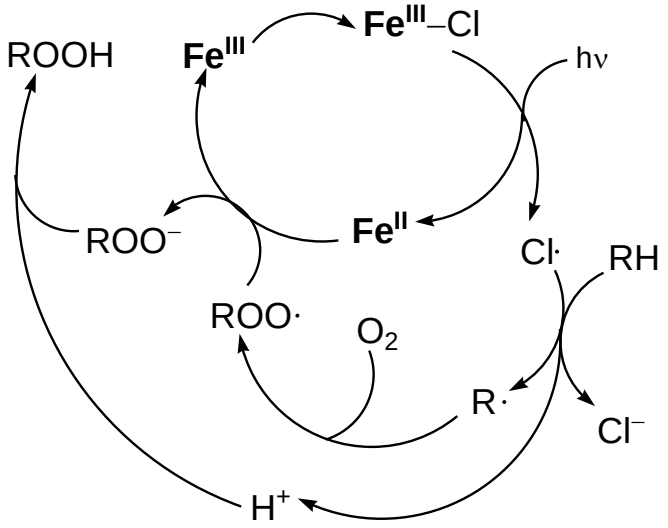

Scheme 2.1.3. The mechanism proposed for the $FeCl_3$-photocatalyzed oxygenation of alkanes, RH, into alkyl hydroperoxides, ROOH.

Following Scheme 2.1.3, the first step of this catalytic cycle is the photoexcitation of the iron(III) chloride yielding a chlorine radical and iron(II). The chlorine radical attacks then a C–H bond from the alkane yielding a carbon radical, R·, which reacts with molecular oxygen yielding the corresponding alkyl peroxo radical; this alkyl peroxo radical oxidizes Fe(II) to Fe(III) giving the corresponding alkyl hydroperoxide, thus restarting the catalytic cycle.

Also $FeBr_3$ was tested as catalyst instead of $FeCl_3$, but it cannot oxidize alkanes, only alkylbenzenes in the benzylic position to yield the corresponding alcohols and ketones [31]. Cyclopentadinyliron(II) and bis(arene)iron(II) complexes were used as catalysts in the photooxidation of cyclohexane by molecular oxygen from air in acetonitrile to yield cyclohexyl hydroperoxide [35-36].

$$Fe^{II} + O_2 \xrightarrow{h\nu} Fe^{III}\text{–}OO\cdot \quad (1)$$

$$Fe^{III}\text{–}OO\cdot + CyH \longrightarrow Fe^{III}\text{–}OOH + Cy\cdot \quad (2)$$

$$Cy\cdot + O_2 \longrightarrow CyOO\cdot \longrightarrow CyOOH \quad (3)$$

Scheme 2.1.4. Mechanistic outline for the photooxidation of cyclohexane in acetonitrile in the presence of cyclopentadienyliron(II) or bis(arene)iron(II) complexes as catalysts.

The mechanism is different from that of $FeCl_3$ as catalyst (Scheme 2.1.4). It involves the photoinduced formation of metal-peroxo radicals which attack the alkane, forming a carbon radical which reacts with oxygen yielding the alkyl hydroperoxide.

2.1.1.4 Gif Systems

Barton and co-workers discovered in 1983 a catalytic system for the oxidation of alkanes under mild conditions. This system is composed of iron powder and acetic acid, in pyridine as the solvent, and of air (atmospheric pressure). The first alkane used as a substrate was adamantane, and the product obtained was adamantan-2-one [37]. This reaction was the first of a family of reactions known under the name of

"Gif chemistry", because it was first discovered at the Natural Products Institute in Gif-sur-Yvette (France). The "Gif Chemistry" includes many catalytic systems which are variations of the first system discovered, and were studied by Barton's group [38, 39] and also in collaboration with other authors [40]. The different systems have geographically based names (Table 2.1.1).

Table 2.1.1. The nomenclature of Gif systems

System	Catalyst	Electron Source	Oxidant
[a] Gif^{III}	Fe(II)	Fe(metal)	O_2
Gif^{IV}	Fe(II)	Zn(metal)	O_2
[b] GO	Fe(II)	Cathode	O_2
[c] $GoAgg^{I}$	Fe(II)	KO_2/Ar	KO_2/Ar
$GoAgg^{II}$	Fe(III)	H_2O_2	H_2O_2
$GoAgg^{III}$	Fe(III)/Picolinic acid	H_2O_2	H_2O_2
[d] GoChAgg	Cu(II)	H_2O_2	H_2O_2
$Cu(0)/O_2$	Cu(I)	Cu(0)	O_2

[a] Gif comes from Gif-sur-Yvette (France), [b] GO means a collaboration between Gif-sur-Yvette and Orsay, [c] GoAgg comes from Aggieland (Texas-USA), and [d] GoChAgg means a collaboration between Chernogolovka (Russia) and Aggieland.

The Gif systems are always formed by a transition metal complex (mainly iron(II) or iron(III) complexes) as catalyst, pyridine as solvent, an organic acid as proton donor and oxygen from air or a peroxide as oxidant. When the oxidant is oxygen, a reducing agent as a metal powder or a cathode is needed to activate the oxygen molecule.

All Gif systems have the same chemical peculiarities:

1) The major products of the reaction are ketones; it is important that alcohols are not reaction intermediates.
2) The presence of an excess of some easily oxidizable compounds (e.g., alcohols, aldehydes) does not significantly suppress the alkane oxidation.
3) The selectivity of oxidation of branched hydrocarbons is secondary > tertiary > primary.
4) Secondary alkyl free radicals are not reaction intermediates.
5) Olefins are not epoxidized.
6) Addition of different trapping reagents diverts the formation of ketones to the appropriate monosubstituted alkyl derivatives. For example, in the presence of $CBrCl_3$ alkyl bromide is formed in quantitative yield.

Despite of the numerous studies devoted to the Gif systems, the mechanism of their action is not clear [38d, e]. The proposed catalytic cycle for the $GoAgg^{II}$ system [39a] is the most accepted one (Scheme 2.1.5), and it involves the oxidation of iron(III) to an iron(V)oxo species by a hydrogen peroxide molecule. This iron(V) oxo species attacks then the alkane, forming an alkyl-iron(V) hydroxo species, which acts in a similar way as the enzyme catalase, catalyzing the dismutation of hydrogen peroxide to molecular oxygen and water, to give an alkyl-iron(III) species [41]. This iron(III) species can insert an oxygen molecule in its carbon-metal bond, just as some Fe(III) porphyrinic derivatives do [42], and the decomposition of this species yields the corresponding ketone and restarts the Fe(III) catalyst.

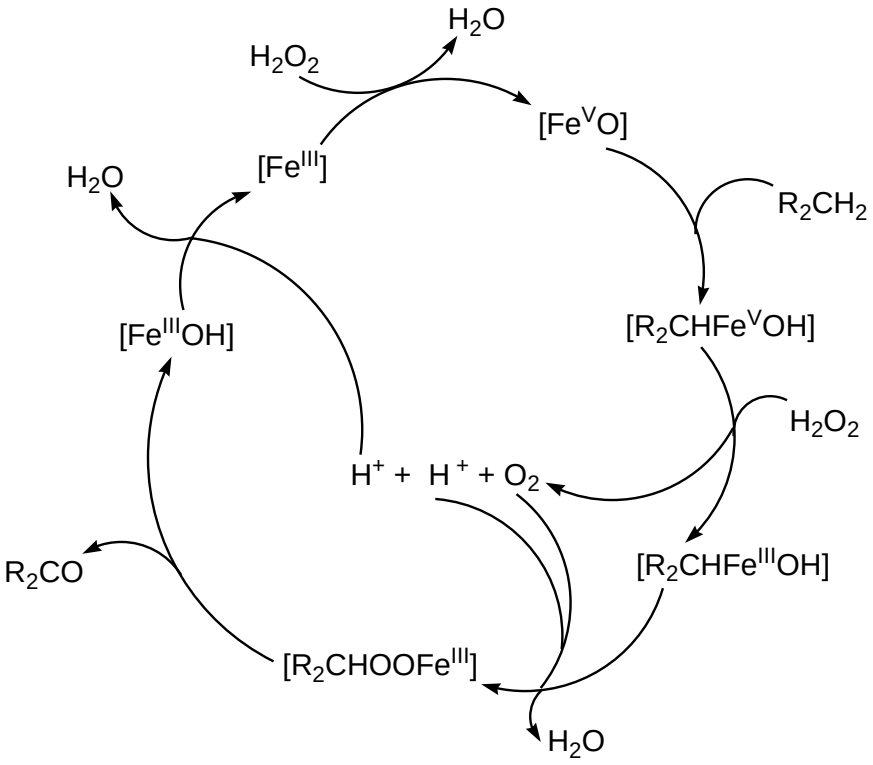

Scheme 2.1.5. Proposed mechanism for the alkane oxidation by the system $GoAgg^{II}$.

2.1.2 Oxidation by Peroxides and other Oxygen Atoms Donors

Next to the oxidation with molecular oxygen, the reactions of alkanes with peroxides, in particular with hydrogen peroxide, are of great importance for the synthesis of the corresponding oxygenates. These reactions may be a basis for a new technology for the transformation of alkanes into valuable oxygen-containing products. When the catalyst is an iron salt or an iron complex, we can differentiate oxidations promoted by hydrogen peroxide, alkyl peroxides or other oxygen atom donors.

2.1.2.1 Oxidation by Hydrogen Peroxide

In 1894, H. J. H. Fenton reported that iron(II) salts were able to oxidize maleic acid in the presence of hydrogen peroxide [43]. Later, F. Haber and J. Weiss proposed that a hydroxyl radical is formed in this system, and that it is actually the oxidizing species [44].

$$H_2O_2 + Fe^{2+} \longrightarrow Fe^{3+} + OH^- + HO\cdot \quad (1)$$

$$HO\cdot + RH \longrightarrow H_2O + R\cdot \quad (2)$$

$$R\cdot + O_2 \longrightarrow ROO\cdot \quad (3)$$

$$ROO\cdot + RH \longrightarrow ROOH + R\cdot \quad (4)$$

$$ROO\cdot + H_2O_2 \longrightarrow ROOH + HOO\cdot \quad (5)$$

$$ROO\cdot + HOO\cdot \longrightarrow ROOH + O_2 \quad (6)$$

Scheme 2.1.6. Proposed simplified mechanism for the oxidation of a substrate, RH, by the Fenton's reagent, Fe(II)/H_2O_2.

In 1940, J. H. Merz and W. A. Waters proposed a mechanistic model [45] which was revised in 1975 by C. Walling (Scheme 2.1.6): He proposed for a general substrate, R–H, that a hydroxyl radical, formed by the action of hydrogen peroxide and iron(II) (Eq. 1), can induce the formation of a carbon radical from the substrate (Eq. 2), which reacts further with molecular oxygen yielding an alkyl peroxo radical (Eq. 3). This radical yields the corresponding alkyl hydroperoxide by three different ways (Eqs. 4–7) [46]. In the early eighties, H. Mimoun developed an iron(II)-based system with a carboxylic acid as co-catalyst, which is able to hydroxylate alkanes [47]. In 1992, G. B. Shul'pin and G. V. Nizova discovered that a non-catalytic system

composed of $FeSO_4$, hydrogen peroxide and air in acetonitrile, can oxidize alkanes to the corresponding alkyl hydroperoxides as majoritary products [48]. Iron(III) complexes too, are efficient catalysts for the oxidation of alkanes with hydrogen peroxide, for example the μ-oxo diiron(III) complex $[Fe_2(\mu\text{-}O)(L)_4(H_2O)](ClO_4)_4$ (L = (–) 4, 5 pinenebipyridine), which oxidizes cyclohexane to give cyclohexanol and cyclohexanone [49].

2.1.2.2 Oxidation by Alkyl Hydroperoxides

The oxidation of alkanes by alkyl hydroperoxides catalyzed by iron(II) and (III) compounds yields alcohols, carbonyl compounds (ketones and aldehydes) and the corresponding alkyl hydroperoxides. For example, in the presence of *t*-butyl hydroperoxide and air, the iron(III) cation $[Fe(tpa)_2]^{3+}$, tpa = tris(2-pyridyl-methyl)amine, can oxidize cyclohexane to cyclohexanol, cyclohexanone and cyclohexyl-*t*-butyl peroxide [50].

$$^{t}BuOOH + Fe^{2+} \longrightarrow Fe^{3+} + OH^{-} + {}^{t}BuO\cdot \quad (1)$$

$$^{t}BuO\cdot + RH \longrightarrow {}^{t}BuOH + R\cdot \quad (2)$$

$$R\cdot + O_2 \longrightarrow ROO\cdot \quad (3)$$

$$ROO\cdot + RH \longrightarrow ROOH + R\cdot \quad (4)$$

$$ROO\cdot + {}^{t}BuOOH \longrightarrow ROO{}^{t}Bu + HOO\cdot \quad (5)$$

$$ROO\cdot + HOO\cdot \longrightarrow ROOH + O_2 \quad (6)$$

Scheme 2.1.7. Proposed mechanism for the oxidation of a substrate, RH, by an iron(II) cation as catalyst and *t*-butylhydroperoxide.

Many mechanistic investigations on these iron-catalyzed oxidations with *tert*-butyl hydroperoxide (or other alkyl (R') hydroperoxides) conclude that the processes involve free alkyl radicals from the substrate which are formed by ^{t}BuO· or R'O· radicals [51], as Scheme 2.1.7 shows, in a similar way as the mechanism proposed for the oxidation with hydrogen peroxide shown in Scheme 2.1.6.

2.1.2.3 Oxidation by Peroxyacids

Peroxyacids, directly introduced in the reaction mixture or formed *in situ* by H_2O_2 in strong acids as solvents, can oxidize alkanes with various iron complexes as catalysts. For example, in the presence of *m*-chloroperoxybenzoic acid, the diiron(III) complex $[Fe_2(\mu\text{-}O)(hexpy)(OAc)_2][ClO_4]_2$ (hexpy = 1,2-bis[2-di(2-pyridyl)-methyl-6-pyridyl]ethane) oxidizes cyclohexane, methylcyclohexane and adamantane to the corresponding alcohols and ketones [52]. In this case, the experiments indicate that the TON of the reaction is unaffected by the presence of O_2, suggesting a mechanism which does not involve radicals as in the case of oxidations by hydrogen peroxide and alkyl peroxides [52].

2.1.2.4 Oxidation by Other Oxygen Atom Donors

Cyclohexane can be oxidized using iodosylbenzene, PhIO, as oxygen donor, catalyzed by an iron porphyrin [53] or by a polyoxotungstenate containing iron(III), $[P_2W_{17}O_{61}FeBr]^{8-}$ [54]. Monopersulfate, HSO_5^-, is also a good oxygen donor, which oxidizes 2-methylnaphtalene at the benzylic position in the presence of an iron porphyrin as catalyst [55]. Other oxygen donors used are XeO_3 [56] and ozone [57].

$$A{=}O + M^{n+} \longrightarrow A + [MO]^{n+}$$

$$[MO]^{n+} + RH \longrightarrow [M{-}OH\ R\cdot]^{n+} \longrightarrow M^{n+} + ROH$$

Scheme 2.1.8. The oxygen rebound radical mechanism for the oxidation of an alkane, RH, by an oxygen atom donor, A=O, catalyzed by a metal atom, M^{n+}.

Usually, the oxygen atom transfer from the oxidizing reagent to the iron-catalyst gives rise to the formation of a high-valent oxo complex. This complex then is capable of oxidizing the alkane, RH, in a similar way as cytochrome P450 does, forming alkyl radicals by the oxygen rebound radical mechanism.

2.2 Iron-containing monooxygenases in living organisms

Alkanes, arenes and other organic compounds are easily oxidized by dioxygen in the cells of bacteria, fungi, plants, insects, fish, and mammals, including man (aerobic biological oxidation). According to the current views, aerobic biological oxidation of alkanes involves various enzymes called oxygenases. The term "monooxygenases" is generally applied to a group of enzymes that catalyze the hydroxylation of C–H compounds by molecular oxygen.

$$R{-}H + O_2 + AH_2 \xrightarrow{\text{monooxygenase}} R{-}OH + H_2O + A$$

Equation 2.2.1. Hydroxylation of a C–H bond catalyzed by a monooxygenase in the presence of molecular oxygen and a proton donor, AH_2.

Monooxygenases induce the insertion of only one oxygen atom from O_2 into the C–H bond, while the second oxygen atom is reduced with formation of water. Biological hydrogen donors, AH_2, are reductants such as NADH, NADPH and the ascorbate anion. The molecular oxygen does not react directly with the alkane, it has to be activated in order to react. This activation takes place thanks to the metal centre of the various monooxygenase enzymes mainly iron or copper. This metal centre is reduced by an electron-transfer from the biological reductant AH_2. Once the metal is reduced, it acquires the ability to react with molecular oxygen and can activate it for the interaction with the alkane [58]. The two most studied iron-containing monooxygenases in the last decade are cytochrome P450 and methane monooxygenase (MMO). The ways of action of these two enzymes are discussed below, as well as some of their chemical models.

2.2.1 Cytochrome P450

The enzyme cytochrome P450 is a representative of the family of heme-containing monooxygenases. These monooxygenases contain as active site a heme prosthetic group called protoheme IX.

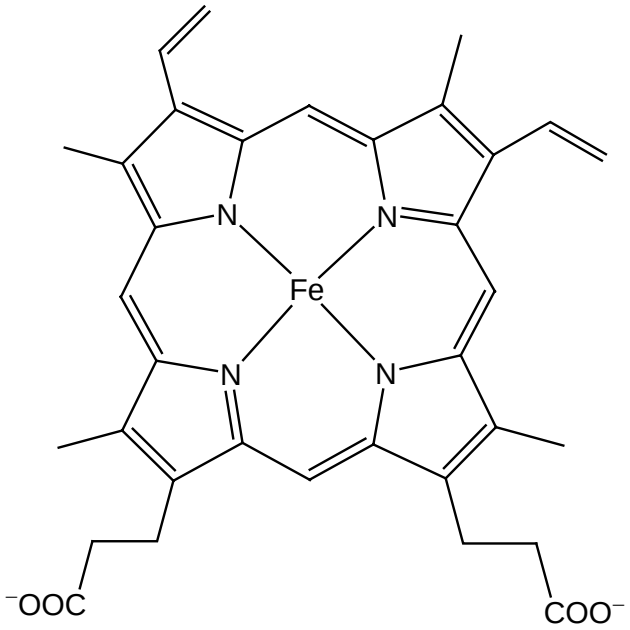

Figure 2.2.1. Structure of protoheme IX, [Fe^{III}(porph)]

As shown in Figure 2.2.1, Protoheme IX is formed by an iron atom coordinated to the four nitrogen atoms of a porphyrin molecule (porph). In cytochrome P450, the fifth coordination position of iron is occupied by a sulphur atom of a cystein molecule, and the sixth position is occupied by the substrate [59].

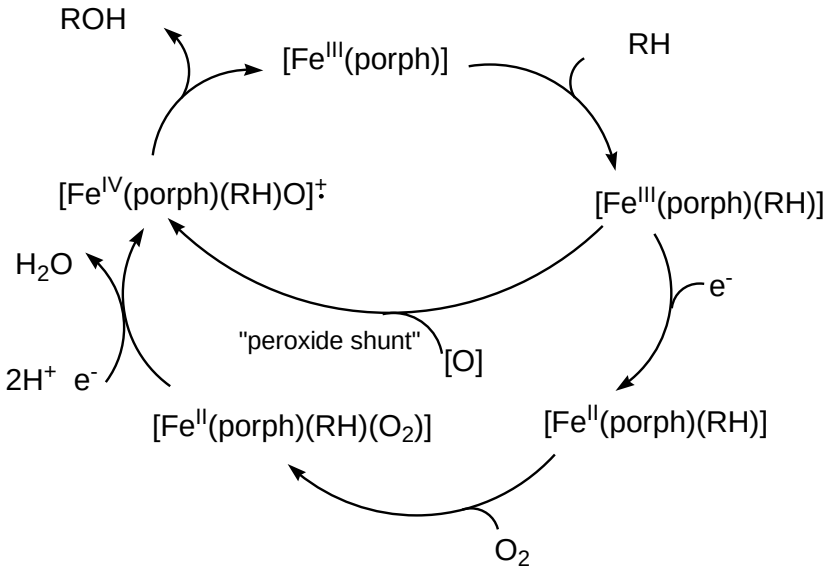

Scheme 2.2.1. The catalytic cycle proposed for the alkane oxidation by O_2 promoted by cytochrome P450.

The catalytic cycle proposed for the alkane oxidation by dioxygen catalyzed by cytochrome P450 is showed in Scheme 2.2.1 [60a]. This cycle starts from the coordination of the substrate, R–H, to the iron(III) centre of cytochrome P450. The reduction of the iron(III) centre takes place in the second step of the process. In the third step, an oxygen molecule is coordinated to the iron(II) atom, giving the iron(II)-peroxo species. This iron(II)-peroxo species is oxidized by the enzymatic system into an oxoiron(IV) radical cation species, $[O=Fe^{IV}(porph)(RH)]^{+\cdot}$. The last step consists in the cleavage of a C–H bond in the substrate molecule and extraction of the oxygen from the iron(V)oxo species, regenerating the cytochrome P450 and giving the corresponding alcohol R–OH. The existence of the proposed oxoiron(IV) radical cation species is supported by several observations; one of them is known as the "peroxide shunt", that is the pathway in which using oxygen atom donors like

peroxides, PhIO and NaOCl it is possible to generate species that give the same reactivity as in the O_2 system [60b].

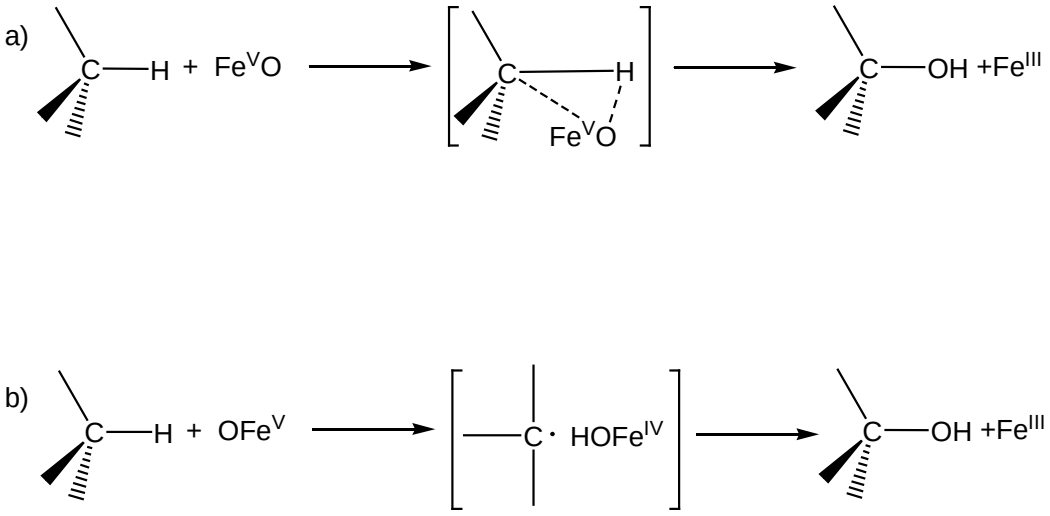

Scheme 2.2.2. The two alternative mechanisms proposed for the last step of the C–H bond activation by cytochrome P450: a) The oxenoid mechanism and b) the "rebound" radical mechanism.

The details of this last step are not very well understood in the catalytic cycle of the alkane oxidation by cytochrome P450. Two alternatives have been proposed for this crucial step: the "oxenoid" or "direct oxygen insertion" mechanism and the "rebound" radical mechanism. Both are shown in Scheme 2.2.2. The oxenoid mechanism was the only mechanism proposed until the late seventies. In 1978, Groves presented a series of experiments with deuterated norbornane derivatives which suggested that the "rebound" radical mechanism should be more reliable [61]. Therefore, the "rebound" radical mechanism has received the most ample recognition since the eighties. Today there are also some cytochrome systems whose results give rise to serious doubts about a radical mechanism [62]. Due to all these doubts and ambiguities, the conclusion is that a mechanistic generalization for all substrates

cannot be made. The predominance of one or another mechanism depends on the substrate studied and also on the origin of the cytochrome. Thus, the oxenoid mechanism is preferred if the substrate is a small molecule with strong C–H bonds, whereas the radical mechanism seems to take place predominantly in the reaction with higher hydrocarbons that are either sterically hindered and/or contain weaker C–H bonds[63].

The alkane hydroxylation catalyzed by cytochrome P450 can be modelled by using iron-porphyrin complexes as catalysts in aqueous or organic solution, a reducing agent as an electric current [64], thiosalycilic acid [65], molecular hydrogen [66], metallic zinc [67] or ferrocene [68], molecular oxygen as the oxidant, and also a proton source is required, such as a carboxylic acid. The hydroxylation reactions catalyzed by these systems occur at normal pressure and ambient temperature. Selectivity and rate of the reaction depend on the nature of the iron-porphyrins as well as on the electron and proton donors. The product yield with respect to the reducing agent is usually low. The yield of the reaction can be improved by replacing molecular oxygen by another oxygen atom donor as H_2O_2 [69], ROOH [70], PhIO [71], NaOCl [72], $KHSO_5$ [73], amine *N*-oxides [74], or magnesium monoperoxyphtalate [75]. Free alkyl radicals are the intermediates in some reactions, particularly for hydrocarbons with weak C–H bonds [76]. In some cases, the $[(porph)Fe^{IV}=O]^{+\cdot}$ intermediate was detected by low-temperature spectroscopy [77,78].

2.2.2 Methane monooxygenase

Methane monooxygenase (MMO) was the first oxygenase enzyme characterized [79]. It was found in methane-consuming bacteria, mainly *Methylococcus capsulatus*, and the cytoplasmic form of this enzyme has been studied in most detail. This cytoplasmic form contains three proteins: a hydroxylase, MMOH, which contains the active centre that hydroxylates methane, a reductase, MMOR, which takes two electrons from the oxidation of a NADH or NADPH molecule, and a coupling protein, MMOB, which activates the active centre in MMOH, transferring the two electrons from MMOR to MMOH.

$$CH_4 + O_2 + NAD(P)H + H^+ \xrightarrow{MMO} CH_3OH + NAD(P)^+ + H_2O$$

Equation 2.2.2. Methane oxidation catalyzed by the enzyme methane monooxygenase (MMO) in the presence of oxygen as oxidant and NADH or NADPH as the coupled-reductant.

MMO catalyzes the hydroxylation of alkanes exclusively, methane showing the highest yield [80]. This hydroxylation reaction is coupled to the oxidation of one NADH or NADPH molecule to give NAD^+ or $NADP^+$, respectively. The global reaction is shown in Equation 2.2.2.

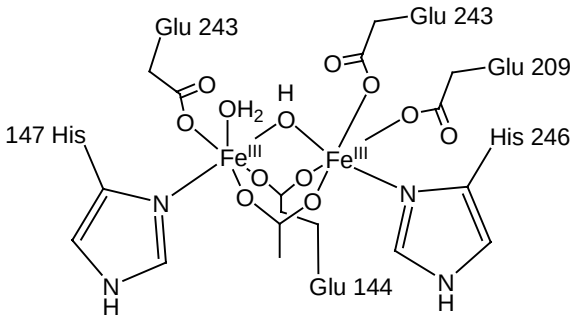

Figure 2.2.2. The active centre of MMOH.

The active centre of MMO is schematized in Figure 2.2.2. It is situated in the MMOH protein, and it contains a dinuclear iron(III) core with one μ-hydroxo bridge between both iron atoms and two μ-carboxylato ligands: one acetato ligand and one carboxylato ligand from glutamine 144. This structure was confirmed by X-ray structural analysis [81].

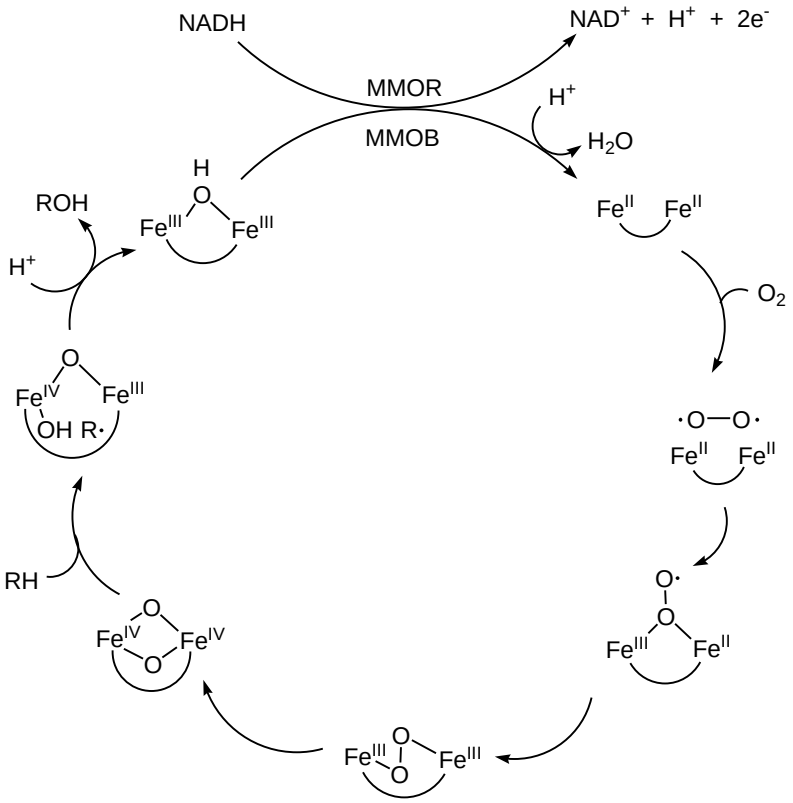

Scheme 2.2.3. Proposed mechanism for the alkane oxidation catalyzed by MMO.

Scheme 2.2.3 shows one of the mechanisms proposed for the oxygenation of methane by MMO. This mechanism involves in the first step the reduction of both iron(III) atoms to iron(II) by two-electron transfer from the MMOR protein through the MMOB protein [82]. The insertion of an oxygen molecule yields a peroxo-diiron(III) species. The activation of the substrate, methane or another alkane, takes place after the oxidation of both iron(III) atoms to iron(IV) in the peroxo species, yielding a bis(μ-oxo)-bis-iron(IV) species. The final step, the cleavage of the C–H bond in the substrate to yield the corresponding alcohol, proceeds through an alkyl radical, similar to the "rebound" radical mechanism for the hydroxylation of alkanes catalyzed by cytochrome P450.

The action of the active centre of MMO has been modelled using binuclear iron complexes. One of the most effective models was discovered recently by Panov *et al*, who found that the high-temperature reaction between nitrous oxide and iron compounds adsorbed in ZSM-5 zeolite, produces an high-valent iron oxo species that reacts with methane producing methanol in nearly quantitative yield [83]. So far, the reaction is not catalytic, since the product is bound to the zeolite and can be removed only by extraction with acetonitrile, destroying the system. Mononuclear iron derivatives have also been used as models for the active site of MMO: For example, a mononuclear iron carboxylato complex, immobilized on a modified silica surface, catalyzes the oxidation of hexane to hexanol and hexanone in the presence of mercaptane, acetic acid, triphenylphosphine and molecular oxygen at ambient temperature and atmospheric pressure [84].

2.3 Vanadium Compounds in Oxidation Catalysis

Many vanadium compounds are known to have interesting catalytic properties: Thus, vanadium(V) complexes are catalysts in the synthesis of polymers like polyethylene, and vanadium(V) oxide is one of the most important oxidation catalysts in industrial production, e.g. for the synthesis of sulphuric acid [85]. The first use of a vanadium compound for the catalytic oxidation of hydrocarbons was reported in 1937 by Milas, who studied the hydroxylation of alkenes by V_2O_5 and hydrogen peroxide [86]. Since this date, many vanadium(V) and vanadium(IV) compounds have been used to catalyze the oxidation of alcohols, alkenes, aromatics and thioethers with hydrogen peroxide [87]. In this paragraph we summarize the most important and recent results on alkane oxidation catalyzed by vanadium compounds using as oxidants hydrogen peroxide or oxygen from air.

2.3.1 Alkane Oxidation by Hydrogen Peroxide

Oxidation of cyclohexane using peroxo-vanadium complexes was first reported by Mimoun *et al.* in 1983, who had synthesized for this purpose a oxo-monoperoxo vanadium(V) complex containing a picolinato ligand (pic), $[VO(O_2)(pic)(H_2O)]$, which oxidizes cyclohexane and also aromatic compounds stoichiometrically [88]. In 1993, G. B. Shul'pin *et al*. reported a catalytic system composed of metavanadate and pyrazinic acid (pcaH) which catalyzes the oxidation of cycloalkanes and aromatics in acetonitrile in the presence of air and hydrogen peroxide [89]. In collaboration with G. B. Shul'pin, our group has shown that this system is even able to oxidize methane in acetonitrile using tetrabutylammonium

metavanadate and pcaH in a 1 : 4 ratio, and also in water using sodium metavanadate instead of the tetrabutylammonium salt [9] (Shcme 2.3.1.).

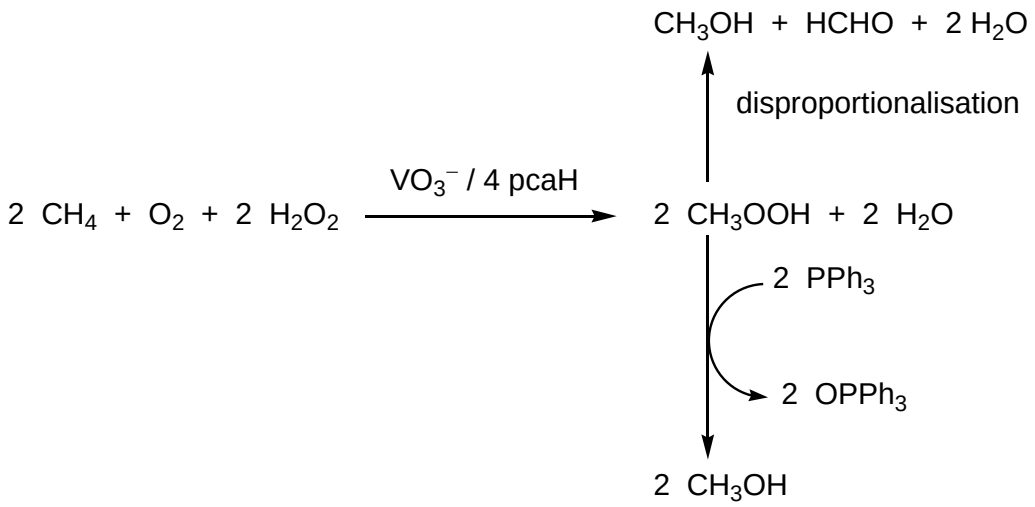

Scheme 2.3.1. Oxidation of methane in acetonitrile or water catalyzed by the system VO_3^- / 4 pcaH.

When the oxidation is carried out in acetonitrile, the products detected are methyl hydroperoxide, carbon monoxide, formaldehyde, formic acid and carbon dioxide. A blank experiment without the substrate (CH_4) reveals that formic acid and carbon dioxide as well as a small amount of formaldehyde come from the oxidation of the solvent, acetonitrile. The best yield of the methane functionalization reaction is obtained at 50°C, at higher temperatures, acetonitrile oxidation predominates. In aqueous solution, no solvent oxidation is possible, and only methyl hydroperoxide is detected up to 70°C. At higher temperatures, formaldehyde and formic acid obtained from the decomposition of methyl hydroperoxide are found. In water too, the maximum yield of CH_3OOH is found at T = 50°C.

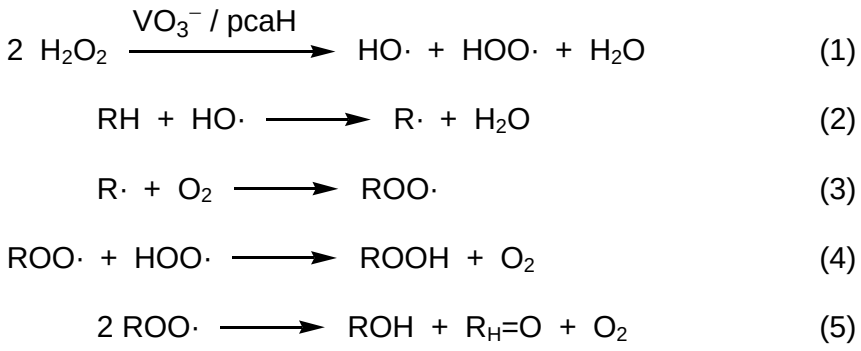

Scheme 2.3.2. The radical mechanism proposed for the alkane oxidation by the system VO_3^- / pcaH (R_H being an alkylidene fragment obtained by hydrogen abstraction from an alkyl fragment R).

After a detailed mechanistic study, involving kinetics and radical trapping, the conclusion is that the oxidation of alkanes by this system occurs via a radical mechanism [11], as shown in Scheme 2.3.2, in which the vanadium(V) species, with the help of the co-catalyst pcaH, generate OH· radicals from hydrogen peroxide (Eq. 1, Scheme 2.3.2). These radicals attack the alkane yielding the alkyl radical R·, which, after reaction with molecular oxygen gives the ROO· radical (Eq. 2-3, Scheme 2.3.2). This ROO· radical (when R = CH_3, Cy, at temperatures < 50 °C) cannot attack the alkane like in a classical radical chain mechanism, as the mechanistic studies show, and therefore, a formal interaction with an OOH· radical is proposed (Eq. 4, Scheme 2.3.2). Also a secondary reaction involving the interaction between two ROO· radicals which yields the corresponding alcohol and ketone is proposed (Eq. 5, Scheme 2.3.2).

In order to elucidate the role of the pcaH co-catalyst, the coordination chemistry of metavanadate with pcaH in acetonitrile was studied: The reaction yielded $[NBu_4][VO_2(pca)_2]$, which has the same catalytic properties as the system NBu_4VO_3 / 4 pcaH when used in the same conditions with two equivalents of pcaH as co-catalyst.

In the reaction of this system with H_2O_2, peroxo complexes were isolated in the form of the tetrabutylammonium or the ammonium salts [10]. The peroxo complex $[VO(O_2)(pca)_2]^-$ formed from $[VO_2(pca)_2]^-$ with hydrogen peroxide was originally thought to be the active species producing hydroxyl radicals [90]. However, the kinetic studies suggest vanadium(V) complexes with only one pca ligand to be the active catalytic species [11].

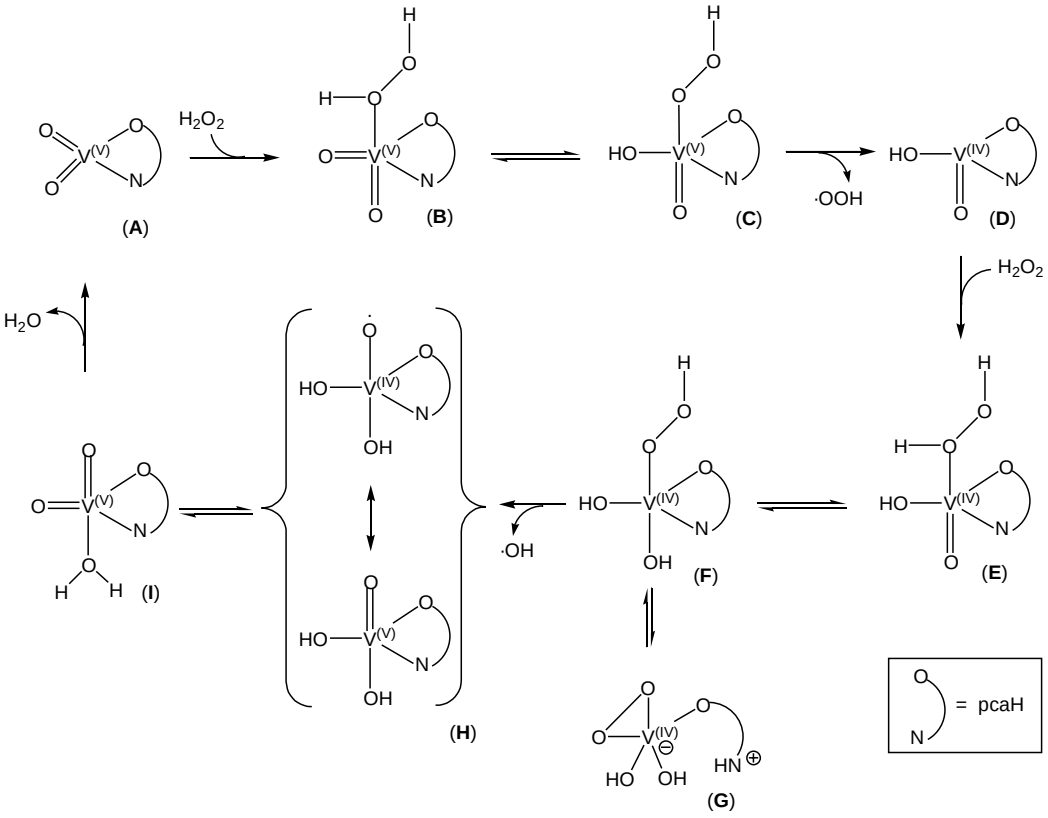

Scheme 2.3.3. Proposed catalytic cycle for hydroxyl radical generation.

The proposed mechanism for the catalytic formation of hydroxyl radicals from the system VO_3^-–pcaH–H_2O_2 is shown is Scheme 2.3.3. A dioxo vanadium(V) complex with only one pca ligand (**A**) coordinates a hydrogen peroxide molecule to give complex **B** which, after intramolecular proton transfer from the hydrogen

peroxide coordinated to an oxo ligand, yields complex **C**. The loss of one hydroperoxyl radical reduces vanadium(V) to vanadium(IV), giving complex **D**. The coordination of a second hydrogen peroxide molecule yields complex **E** which, after an intramolecular proton transfer from hydrogen peroxide to an oxo ligand, gives the hydroperoxo complex **F**, which is in equilibria with the zwitterionic species **G**. Complex **F** loses a hydroxyl radical, the species which will attack the substrate in the catalytic reaction, to give a vanadium(IV) radical species **H**. Complex **H** yields complex **I** after intramolecular proton transfer between two hydroxo ligands, and loss of a water molecule restores complex **A**.

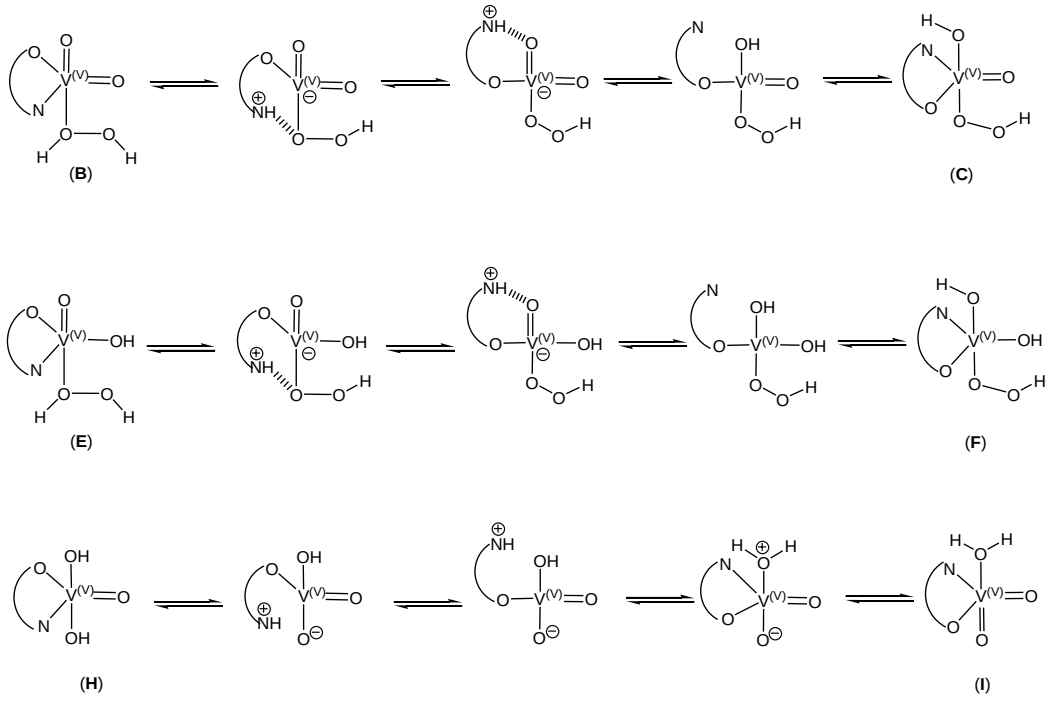

Scheme 2.3.4. Proposed "robot's arm mechanism" for the pcaH-assisted proton transfer in the H_2O_2 and OH complex intermediates.

The role of pcaH in this system is thought to be "a robot arm's" mechanism, facilitating the intramolecular proton transfer steps **B** to **C**, **E** to **F** and **H** to **I**. The co-

catalyst pcaH can also help this proton transfer steps without being coordinated to vanadium but in its zwitterionic form [11] (Scheme 2.3.4).

Without pcaH being present as a co-catalyst, vanadate alone does not catalyze the alkane oxidation, the maximun initial rate of the catalytic reaction is observed for a ratio V : pcaH of 1 : 4 when $[NBu_4VO_3] = 1 \times 10^{-4}$ mol dm^{-3}. This ratio can be explained by assuming competition between hydrogen peroxide and pcaH for the coordination at the vanadium(V) centre.

A very recent paper by A. Sen and co-workers describes the oxidation of benzene and of cyclohexane to give selectively the corresponding alcohols, using a vanadium(III) catalyst, VO(acac), and hydrogen peroxide generated "in situ" from a 1 : 1 mixture of hydrogen and oxygen in the presence of metallic palladium supported in Al_2O_3 in acetic or in propionic acid [91]. The careful analysis of the products obtained in this reaction shows that no alkyl hydroperoxide is formed, as opposed to the vanadium-catalyzed oxidation of hydrocarbons with hydrogen peroxide directly added to the reaction mixture. Mechanistic studies of the benzene reaction reveal that in this case the C–H functionalization of the hydrocarbon does not proceed *via* OH· radicals generating alkyl radicals (Scheme 2.3.5), but by an electron-transfer from the hydrocarbon to a dihydroxo-oxo vanadium(V) species, which gives rise to a hydrocarbon radical cation. This radical cation abstracts a further OH· radical from the vanadium(IV) complex, and after loss of a proton, it gives rise to the corresponding alcohol.

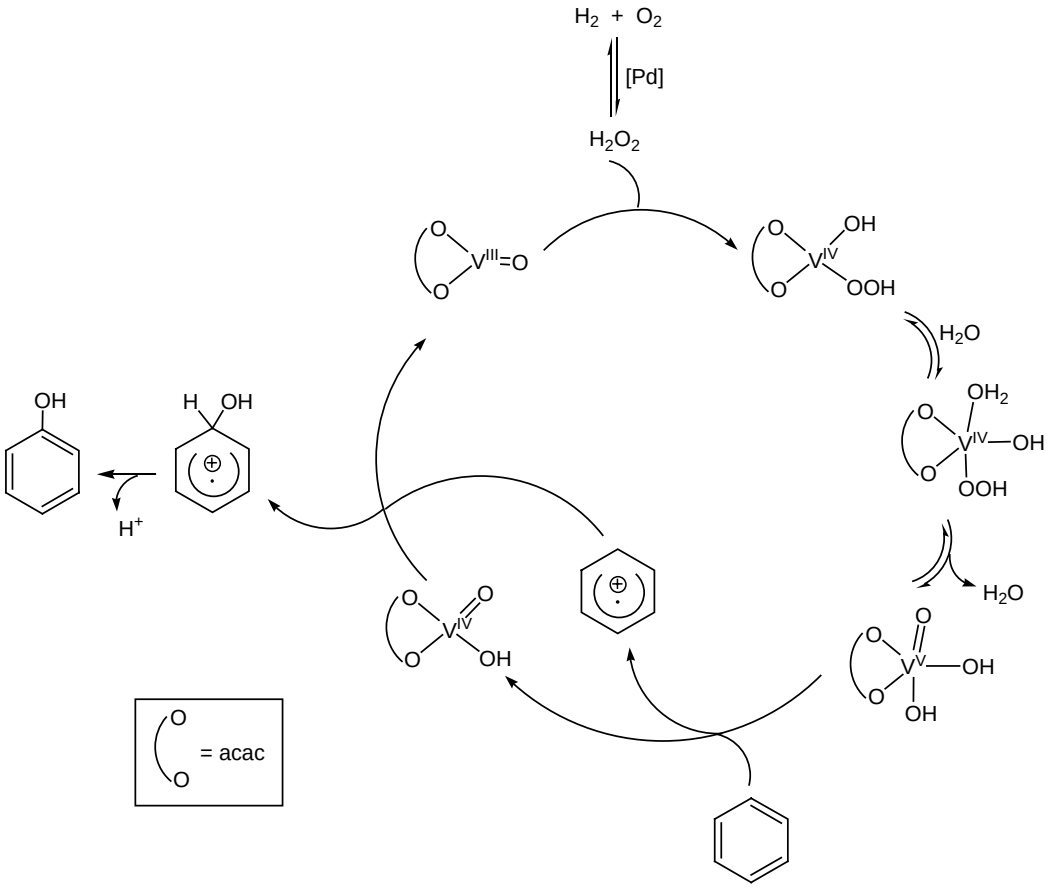

Scheme 2.3.5. Proposed mechanism for the benzene oxidation catalyzed by VO(acac) using "in situ" formed hydrogen peroxide.

2.3.2 Alkane Oxidation by Air

The system NBu_4VO_3 / pcaH in a ratio higher than 1 : 10 also catalyzes the oxidation of cyclohexane to cyclohexanol and cyclohexanone in acetonitrile at 30 °C without hydrogen peroxide present, using oxygen from air, if acetic acid, pyridine and zinc powder are present in the solution [92]. The mechanism proposed for this catalytic oxidation, shown in Scheme 2.3.6, involves a vanadium complex with only a pca ligand as in the case of the hydrogen peroxide catalytic oxidations. The vanadium(V) centre in this complex is reduced to vanadium(IV) by electron transfer

from Zn and a proton transfer from acetic acid, by means of a pyridine molecule which acts as an electron and proton transport reagent, as shown below. This vanadium(IV) species adds molecular oxygen from air, giving a hydroperoxo vanadium(V) complex, and after reduction it is converted to a hydroperoxo vanadium(IV) derivative, the actual catalytically active species, which gives rise to an oxo derivative and generates a hydroxyl radical. This hydroxyl radical will attack the substrate, RH, giving an alkyl radical which reacts further with oxygen giving the corresponding alkyl hydroperoxide, in the same way shown above. The role of pcaH in this system is to facilitate the intramolecular proton transfer in the different vanadium complexes by the "robot's arm mechanism" as shown above.

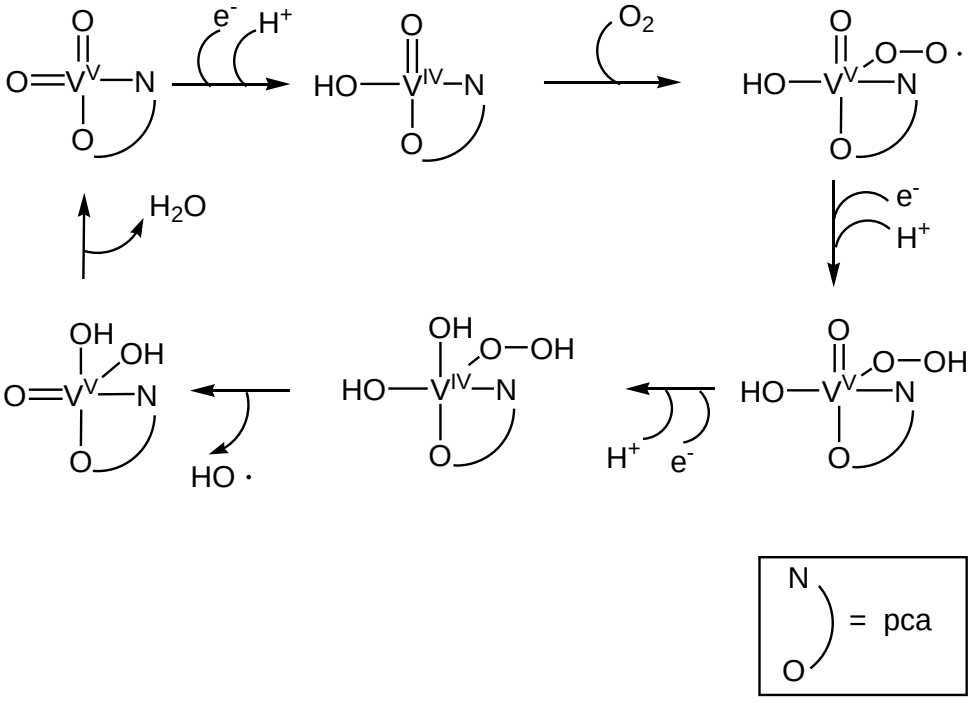

Scheme 2.3.6. Proposed mechanism for the catalytic generation of OH· radicals by the system NBu_4VO_3 / pcaH in the presence of a proton donor, acetic acid, an electron donor, zinc powder, and an electron transfer reagent, pyridine.

The role of pyridine, acetic acid and zinc together in this catalytic system can be compared to the role of NADH in biological systems as a proton and electron transfer reagent. Pyridine is protonated at the nitrogen atom by acetic acid, and this form is reduced by a one-electron transfer from zinc(0) and protonated by a second proton-transfer from acetic acid. This reduced form of pyridine is able to reduce one vanadium(V) atom into vanadium(IV) (Scheme 2.3.7).

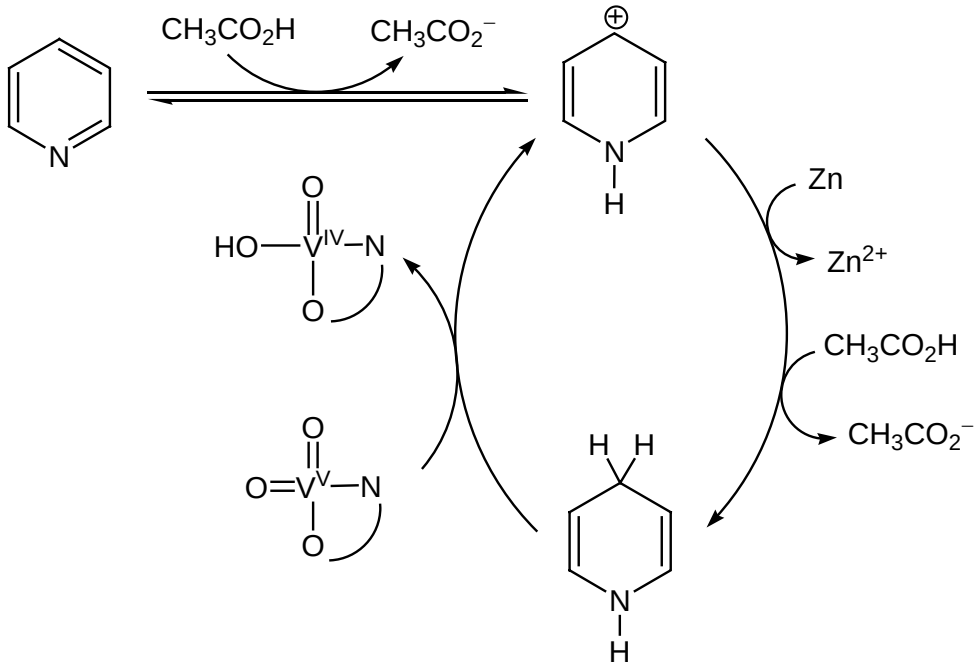

Scheme 2.3.7. Proposed role of pyridine as electron and proton transfer reagent.

The oxidation reaction of cyclohexane reaches the highest initial reaction rate, if a V : pcaH ratio of 1 : 10 or higher is used. This can be explained by taking into account a competition between pyridine and pcaH in the coordination to the vanadium(V) centre, preventing the formation of the active vanadium(V) complex with one pca ligand.

2.4 Vanadium in Biological Systems

Vanadium compounds play an important role in living organisms: They are present in the blood of some sea organisms and in the active centre of certain enzymes [93-100], and they are used in medicinal chemistry, as models for the antidiabetic action of insulin [101, 102], and as anti-tumor agents [103]. On the other hand, many vanadium derivatives are known to be potent toxicants and carcinogens [104, 110], which can act *via* generation of reactive oxygen species like hydroxyl radicals [111-113].

2.4.1 Vanadium-Containing Enzymes

Vanadium-containing enzymes which can transport oxygen and oxidize hydrocarbons are not known until this date. In 1911, Henze found vanadium in the blood of sea squirts, an organism of the family of ascidians, which looks like a sponge [93]. At that time, vanadium was thought to act as an oxygen carrier for the sea squirts and the vanadium-containing cells were called “haemovanadocytes” for this reason. Now it is clear that the oxygen transport is not the function of these vanadium-containing cells, their actual role still remains to be understood.

The two classes of well-identified vanadium-containing enzymes until now are the vanadium-nitrogenases and the vanadium-haloperoxidases. Vanadium-nitrogenases are found in the nitrogen-fixing bacterium *Azotobacter*, which consumes molecular nitrogen to produce ammonia [94] (Equation 2.4.1).

$$N_2 + 8\,H^+ + 8\,e^- + 16\,ATP \longrightarrow 2\,NH_3 + H_2 + 16\,ADP + 16\,P_i$$

Equation 2.4.1. The nitrogen reduction to ammonia catalyzed by vanadium-nitrogenase.

The mechanism of the nitrogen reduction to ammonia catalyzed by the vanadium-nitrogenase is still not unambiguously established to date, but it is believed to proceed in combination with the hydrolysis of ATP to ADP and inorganic phosphate (P_i) [95]. Vanadate-nitrogenase is composed of two metalloproteins: one iron-containing protein, which acts as an electron donor, and one vanadium-iron-containing protein, which contains the active centre for the nitrogen reduction.

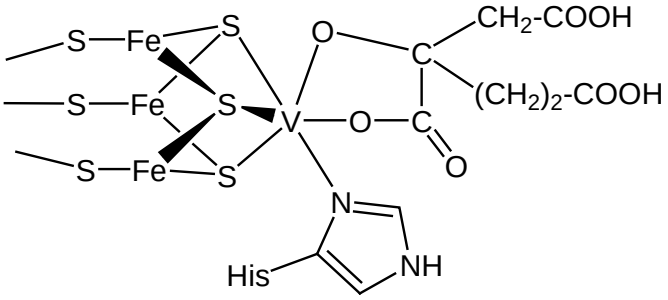

Figure 2.4.1. Active centre of the vanadium-nitrogenase.

The active centre on the vanadium-iron protein in vanadium-nitrogenase has not been structurally determined by X-ray analysis, but there is an analogous enzyme, molybdenum-nitrogenase, which also catalyzes the nitrogen reduction in some bacteria, and for which the structure of the active centre has been determined by X-ray analysis. By analogy, as shown in Figure 2.4.1, the vanadium centre in the vanadium-iron protein of vanadium-nitrogenase is believed to be bridge-linked by three sulfido ligands to three iron centres, and further coordinated to an imidazolyl nitrogen atom

of histidine and the vicinal carboxylato and alkoxo groups of homocitrate. The oxidation state of vanadium in this active centre is not well-defined, it is only clear that it is a low to medium oxidation state, certainly not vanadium(V) [96].

The second group of vanadium-containing enzymes, vanadium-haloperoxidases catalyzes the oxidation of inorganic halides by a hydrogen peroxide molecule to give the correspondent hypohalous acid, which can further react with an organic substrate, giving the corresponding alkyl halide, or with a second hydrogen peroxide molecule, giving molecular oxygen (Scheme 2.4.1).

$$H_2O_2 + X^- + H^+ \longrightarrow HXO + H_2O$$

$$HXO + RH \longrightarrow RX + H_2O$$

$$HXO + H_2O_2 \longrightarrow O_2 + H_2O + HX$$

Scheme 2.4.1. Halide oxidation by a vanadium haloperoxidase and its two possible further reaction pathways.

Depending on the halide oxidized, these vanadium-haloperoxidases are called chloro, bromo, or iodoperoxidases. The first enzyme of this family, a vanadium-bromoperoxidase (V-BPO), was isolated in 1983 from the brown algae *Ascophylum nodosum* [97], and its X-ray structure was elucidated seventeen years later [98]. Other vanadium-haloperoxidases have been isolated from red algae, lichens and fungus, such as the vanadium-chloroperoxidase (V-CPO) from the fungus *Curvularia inaequalis*, the molecular structure of which has been also determined [99]. Its active centre is shown in Figure 2.4.2

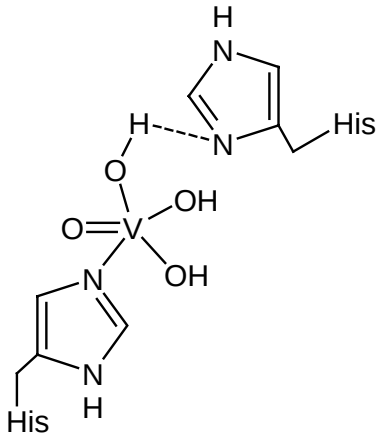

Figure 2.4.2. The active centre of the V-CPO enzyme from *Curvularia inaequalis*

The active sites in the V-BPO and V-CPO structures are very similar: a vanadium(V) atom coordinated to one oxo ligand, three hydroxo ligands and one imidazol substituent of a histidine; a hydrogen bond between one of the three hydroxo ligands of vanadium and another histidine, stabilizes the position of the active centre respect to the protein [96]. The X-ray analyses of vanadium-haloperoxidases as well as modelling studies suggest the active intermediate in the catalytic oxidation of halides to be a peroxovanadium(V) complex [100].

2.4.2 Vanadium Compounds in Medicine

Some vanadium complexes have been found to possess antitumor activity, as most of the studies focused on peroxovanadates(V) and bis(cyclopentadienyl) vanadium(IV) complexes show [114]. Recently, several oxovanadium(IV) complexes with one or two molecules of 1,10-phenantroline (phen) or 4,7-dimethylphenantroline (Me_2-phen) have been synthesized and tested *in vitro* as anti-leukemic agents, the bis(Me_2-phen) oxovanadium(IV) complex, $[VO(Me_2\text{-phen})_2]^{2+}$, being the most active

anti-leukemic agent of the complexes synthesized. The anti-leukemic action of these compounds is due to the production of reactive oxygen species under physiological conditions, which induce the destruction of the leukemic cells and prevent its further growth [103].

Vanadium compounds are also effective in the treatment of diabetes. A lowering of the glucose concentration in the blood of diabetic patients after treatment with sodium metavanadate has first been observed in 1899 [115]. But after the discovery of insulin in 1922, vanadium was not longer thought to be a potential therapeutic agent for diabetes until the 1980s, when the resistance to insulin of a many diabetic patients begun to be a serious medical problem, known as diabetes Type II [116]. The vanadium compounds investigated until now with success in the treatment of diabetes Type II are vanadium(IV) and vanadium(V) salts as sodium metavanadate or vanadyl sulphate [117-120] and also vanadium(IV) and vanadium(V) complexes with carboxylato ligands such as citrate [16] and maltolate [18]. The antidiabetic effect of vanadium compounds is related to the inhibition of the enzyme ATPase in the liver, which activates the glucose transport to the muscle, thus lowering the glucose concentration in blood [121]. The use of vanadium compounds in the treatment of diabetes on human remains without secondary effects until now, as the vanadium concentration is lower than 5 milligrams per kilogram of body weight and per day, the toxicity limit [122].

2.4.3 Toxicity of Vanadium Compounds

Some *in vivo* studies prove that ingestion of vanadium(V) and vanadium(IV) compounds in doses higher that 5 mg · kg^{-1} · day^{-1} produces peroxidation of the body tissues [123] and nucleotide oxidation with the consequent DNA damage [105]. These results suggest that, under physiological conditions, vanadium can produce some very reactive oxygen species, such as hydroxyl radicals. Mechanistic studies to investigate the formation of hydroxyl radicals in the presence of vanadium(V) have been carried out *in vitro* at physiological pH in the presence of ascorbate and hydrogen peroxide. The studies used ESR spectroscopic analysis to detect the formation of vanadium(IV) species and radical traps such as 5,5-dimethyl-1-pyrroline N-oxide (DMPO) to detect hydroxyl radicals. The results suggest that vanadium(V) is reduced by ascorbate to vanadium(IV), which reacts with hydrogen peroxide yielding a hydroxyl radical *via* a Fenton-like reaction [111] (Equation 2.4.2).

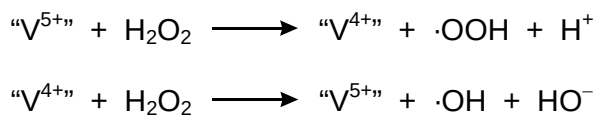

Equation 2.4.2. Generation of a hydroxyl radical by a vanadium(V) atom in the presence of hydrogen peroxide

ESR studies *in vivo*, too, suggest that vanadium(V) is reduced to vanadium(IV) by NADH, which produces hydroxyl radicals from hydrogen peroxide which originates from oxygen [124].

Oxidations of Alkanes Catalyzed by Iron and Vanadium Complexes - Results

The present chapter reports on our results about alkane oxidation catalyzed by iron and vanadium complexes. In addition to known compounds, new vanadium(IV) and vanadium(V) complexes have been synthesized and studied as catalysts for alkane oxidation.

3.1 Catalysis by Vanadium(V)-Containing Polyoxomolybdates

Polyoxometalates are known to catalyze various oxidation reactions [125], in particular, the oxygenation of aromatic hydrocarbons with hydrogen peroxide and *tert*-butyl hydroperoxide [126-135]. Only a few examples for oxidations of saturated hydrocarbons using polyoxomolybdates and polyoxotungstates containing transition metal ions (Co, Mn, Cu, Fe, Ru, Rh, Ni, and Cr) have been reported [136-144]. Herein we present our results on the homogeneous oxidation of alkanes with hydrogen peroxide and air, catalyzed by two known vanadium-containing polyphospho-molybdates: the non-lacunary anion $[PMo_{11}VO_{40}]^{4-}$ (**1**) and the lacunary anion $[PMo_6V_5O_{39}]^{12-}$ (**2**) [145]. The non-lacunary anion **1** is structurally characterized and it presents a Keggin-type structure, consisting in eleven MoO_6 and one VO_6 octahedral moieties assembled around a central PO_4 tetrahedron [133], (Figure 3.1.1). The lacunary anion **2** is not structurally characterized.

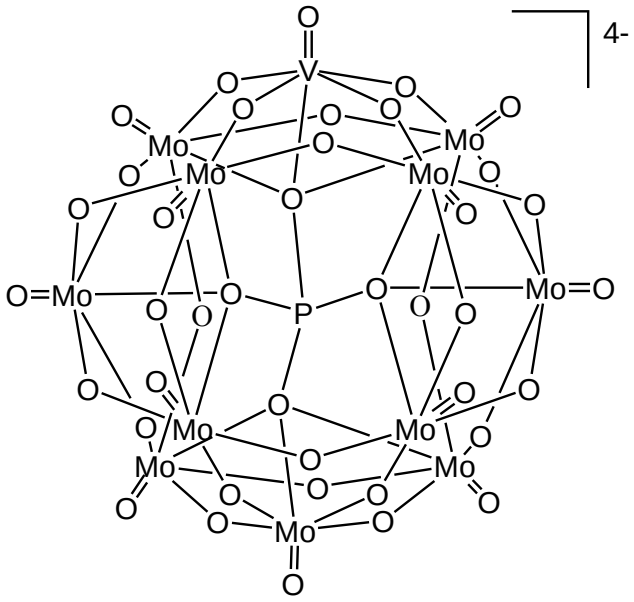

Figure 3.1.1. Structure of the non-lacunary Keggin anion **1**.

3.1.1 Oxidation of Cyclooctane

The oxidation of cyclooctane in acetonitrile at 60°C catalyzed by the *n*-tetrabutylammonium salt of anion **1** gives cyclooctyl hydroperoxide as the main product, as well as small amounts of cyclooctanol and cyclooctanone (Scheme 3.3.1). The profile of this oxidation reaction is shown in Figure 3.1.2. The total concentration of all products divided by the catalyst concentration, representing the total catalytic turnover number, (TON), is 1180 after 9 hours. After this time, there is no longer an accumulation of oxygenates, but only a slow decomposition of cyclooctyl hydroperoxide to give additional amounts of both cyclooctanol and cyclooctanone. The concentrations of the products in this reaction and in the rest in this work are established by GC analysis, using an internal reference and applying a method developed earlier by Shul'pin *et al.* which allows to determine the real concentration of alkyl hydroperoxide, the alcohol and the ketone in the reaction mixture, taking into

account the alkyl hydroperoxide decomposition in the GC column [9a, 33, 34, 48, 136-137, 146-150, 153-154]. This method is explained in chapter 4.

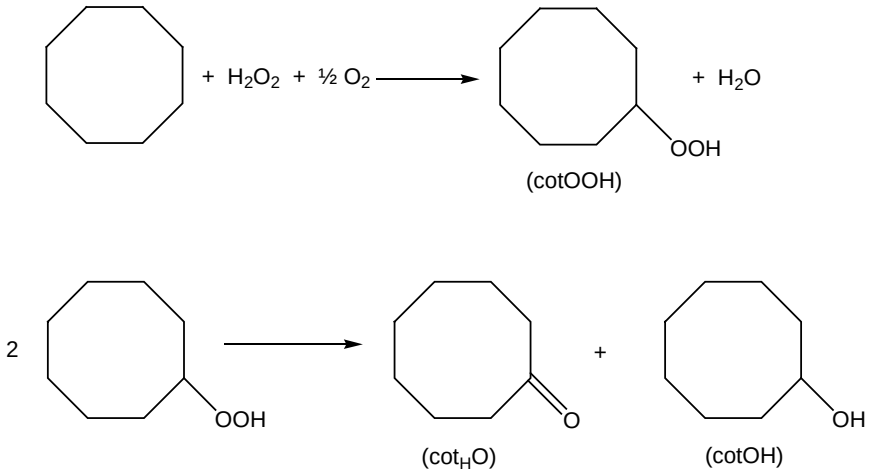

Scheme 3.1.1. The oxidation of cyclooctane catalyzed by **1** and **2**.

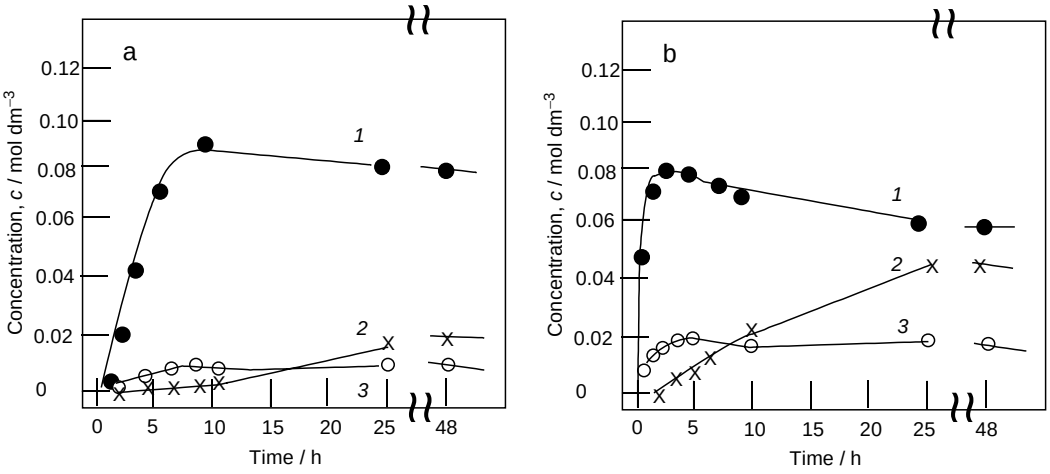

Figure 3.1.2. Reaction profile of the oxidation of cyclooctane in acetonitrile catalyzed by **1** in the absence of pcaH (a) and in the presence of V : pcaH 1 : 10 (b). Conditions: $[\text{cyclooctane}]_0 = 0.37$ mol dm^{-3}; $[H_2O_2]_0 = 0.59$ mol dm^{-3}; [catalyst] = 1.0×10^{-4} mol dm^{-3}; [pcaH] = 1.0×10^{-3} mol dm^{-3}; 60°C, 10 ml total volume. Products: cyclooctyl hydroperoxide (*1*), cyclooctanone (*2*), cyclooctanol (*3*).

It has been demostrated that, in the case of alkane oxidation catalyzed by NBu_4VO_3, the presence of pcaH is indispensable [9-11, 89, 146, 147]. Therefore, it was interesting to study the effect of pcaH in the case of the cyclooctane oxidation catalyzed by **1** and **2**, using a V : pcaH ratio of 10. The maximum TON for the reaction catalyzed by **1** is 1200, and it is attained after 5 hours, so we can conclude that the total reaction yield is not affected by the presence of pcaH. However, the initial reaction rate is higher in this case, and the highest cyclooctyl hydroperoxide concentration is attained after 5 hours versus 9 hours for the oxidation in the absence of pcaH.

The oxidation of cyclooctane catalyzed by **2** attains the maximun TON (470) after 2 hours, and the addition of pcaH (V : pcaH ratio 1 : 10) does not significantly enhance the maximum TON (620); moreover, it does not affect the initial reaction rate. In the case of **2**, however, the major product is cyclooctanone, which can be explained by assuming that cyclooctyl hydroperoxide is decomposed from the beginning of the reaction (Table 3.1.1).

Table 3.1.1. Concentrations (mol × dm^{-3}) of the products formed from the oxidation of *n-oc*tane catalyzed by **1** and **2** with H_2O_2 and air.

Catalyst		**[cotOOH], × 10^2**	**[cot_HO], ×10^2**	**[cotOH], × 10^2**	**TON_{max}**	**Time, hours**
1	Without pcaH	9.3	1.9	0.6	1180	9
	With pcaH	8.0	2.1	1.9	1200	5
2	Without pcaH	1.3	2.7	0.7	470	2
	With pcaH	1.2	3.5	1.5	620	2

Conditions: $[cyclooctane]_o$ = 0.37 mol dm^{-3}; $[H_2O_2]_0$ = 0.59 mol dm^{-3}; [catalyst] = 1.0×10^{-4} mol dm^{-3}; [pcaH] = 1.0×10^{-3} mol dm^{-3}; 60°C, 10 ml total volume.

In conclusion, the presence of pcaH as a co-catalyst is not necessary for the efficient alkane oxidation catalyzed by **1** and **2**. This is the fundamental difference between these vanadium-containing polyoxometalates and the simple vanadate anion.

We also tested acetic acid as a solvent for the oxidation of cyclooctane catalyzed by **1**. Acetic acid turned out to be much less efficient as solvent in comparison with acetonitrile; the TON being only 30 after 48 hours. The profile of this reaction in acetic acid is shown is Figure 3.1.3.

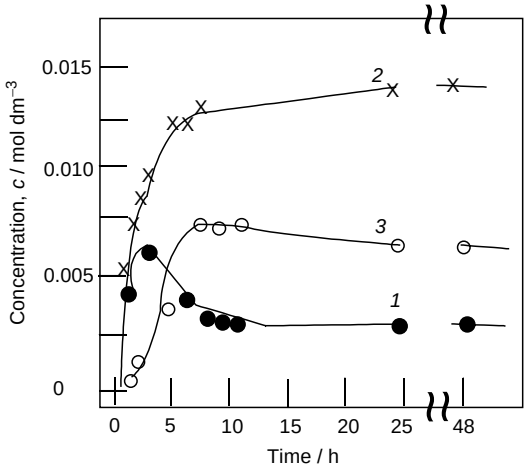

Figure 3.1.3. Reaction profile of the oxidation of cyclooctane in acetic acid catalyzed by **1**. Conditions: $[\text{cyclooctane}]_0 = 0.37$ mol dm^{-3}; $[H_2O_2]_0 = 0.59$ mol dm^{-3}; [catalyst] = 1.0×10^{-4} mol dm^{-3}; 60°C, 10 ml total volume. Products: cyclooctyl hydroperoxide (*1*), cyclooctanone (*2*), cyclooctanol (*3*).

3.1.2 Oxidation of *n*-Octane and Adamantane: Regioselectivity

The oxidation of a linear alkane like *n*-octane allows us to determine which carbon atom is preferentially attacked to give the corresponding alkyl hydroperoxide, along with traces of alcohols and ketones(aldehydes) originating from its partial

decomposition. Scheme 3.1.2 shows the possible oxidation products of *n*-octane. In order to facilitate the analysis, we measured the concentration of the products by GC only after reduction of the sample with PPh_3, which converts the hydroperoxides quantitatively into the corresponding alcohol, so, that only alcohols and ketones are detected in the sample.

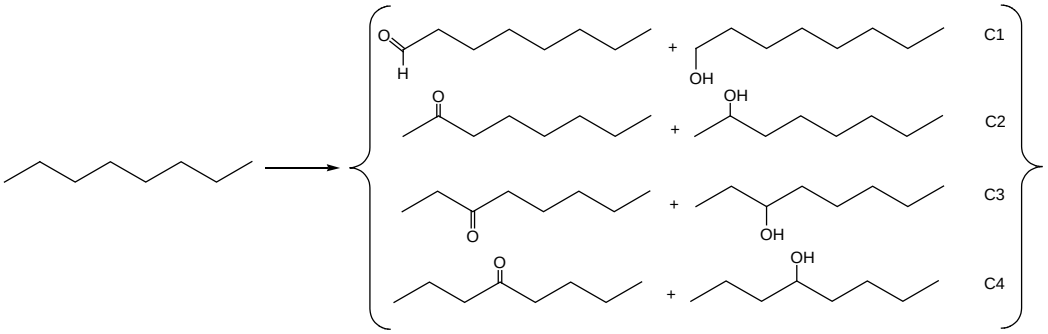

Scheme 3.1.2. Reaction products of the *n*-octane oxidation with H_2O_2 and air catalyzed by the anions **1** and **2** after treatment with PPh_3.

Table 3.1.2. Concentrations (mol × dm^{-3}) of the products formed from the oxidation of *n-oc*tane catalyzed by **1** and **2** with H_2O_2 and air.

Catalyst	**[alcohols], × 10^3**				**[ketones(aldehydes)], × 10^3**				**TON**
	C1	C2	C3	C4	C1	C2	C3	C4	
1	4.2	14	13	12	0.2	0.6	0.7	0.6	453
2	0.7	3	4	3	3	12	10	9	447

Conditions: $[n\text{-octane}]_0$ = 0.29 mol dm^{-3}; $[H_2O_2]_0$ = 1.1 mol dm^{-3}; [catalyst] = 1.0×10^{-4} mol dm^{-3}; 60 °C, 7 hours, 10 ml total volume.

The results shown above (Table 3.1.2) indicate that both catalysts have comparable activity. However, the product distribution is different: **2** leads to higher

ketone/aldehyde concentrations than **1**. This is possibly due to a more extensive decomposition of the hydroperoxide intermediates in the course of the reaction. The most important observation is that with both, **1** and **2**, secondary C–H bonds (C2 to C4) are preferably oxidized over the primary C-H bonds (C1).

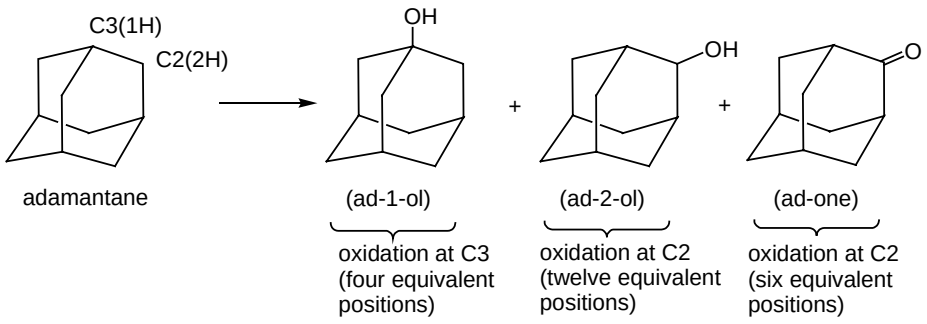

Scheme 3.1.3. Reaction products of the adamantane oxidation with H_2O_2 and air catalyzed by the anions **1** and **2** after treatment with PPh_3.

We also studied the oxidation of adamantane with both catalytic systems. The products from the oxidation of adamantane are shown in Scheme 3.1.3. Adamantane has 6 equivalent secondary carbon atoms (C2), each one with 2 hydrogen atoms, and four equivalent tertiary carbon atoms (C3), each one with 1 hydrogen atom. The oxidation at C2 gives adamantan-2-ol and adamantanone, while the oxidation at C3 gives adamantan-1-ol. We calculated the normalized reactivity ratio (C2:C3) as the proportion of the products on C2 positions (adamantan-2-ol and adamantanone) obtained in relation to those on C3 positions (adamantan-1-ol). For this purpose, we divided the area obtained by GC corresponding to a product by the number of its isomers (equivalent positions), that is, 4 for adamantan-1-ol, 12 for adamantan-2-ol and 6 for adamantanone. As in the case of *n*-octane oxidation, we analyzed the adamantane oxidation products after treatment with PPh_3 in order to convert the alkyl

hydroperoxides into the corresponding alcohol, so that only alcohols and ketone remain in the sample.

Table 3.1.3. Concentrations (mol dm^{-3}) of the products formed from the oxidation of adamantane catalyzed by **1** and **2** with H_2O_2 and air and C2:C3 ratio.

Catalyst	[ad-1-ol]	[ad-2-ol]	[ad-one]	C2:C3
1	0.006	0.008	0.0008	0.6
2	0.0083	0.006	0.0024	0.7

Conditions: $[adamantane]_o$ = 0.037 mol dm^{-3}; $[H_2O_2]_0$ = 1.1 mol dm^{-3}; [catalyst] = 1.0×10^{-4} mol dm^{-3}; 60 °C, 7 hours, 10 ml total volume.

Table 3.1.3 shows the concentrations of the products from adamantane oxidation, and the relative ratios C2:C3. The C2 : C3 ratios obtained for both catalysts are very close to those determined for the oxidations by catalytic systems which proceed *via* hydroxyl radical formation, such as O_2-H_2O_2-hν (C2 : C3 = 0.7) and O_2-H_2O_2-NBu_4VO_3-pcaH (C2 : C3 = 0.75).

3.1.3 Oxidation of *cis*- and *trans*-Decalin

After we had studied the regioselectivity of the alkane oxidation catalyzed by **1** and **2**, we investigated the stereoselectivity of this reaction, using the *cis*- and *trans*-isomers of decalin and the anion **1** as catalyst. The oxidation of one of the two tertiary C–H bonds in these compounds gives rise to the corresponding alkyl hydroperoxide, which can be reduced to the corresponding tertiary alcohol by PPh_3 in order to

facilitate the GC analyses and calculations. The oxidation of the secondary C–H bonds of both decalin isomers gives rise to secondary alcohols and ketones after treatment with PPh_3, and their concentrations are not included, because they are not relevant to our study of the stereoselectivity. The oxidation of both *cis*- and *trans*-isomers of decalin at the tertiary position proceeds with epimerization at the tertiary carbon atom, as it is demonstrated by the fact that both *trans*- and *cis*-alcohols are obtained from both *trans*- and *cis*-isomers of decalin (Scheme 3.1.4).

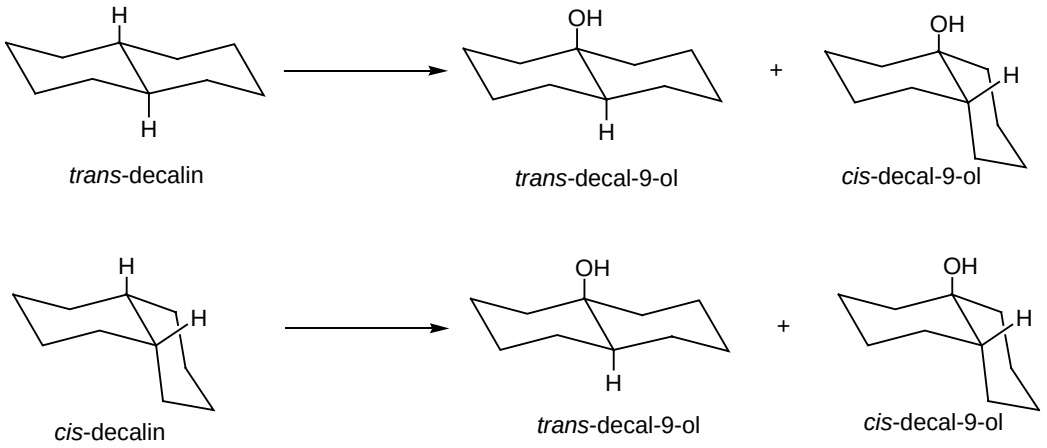

Scheme 3.1.4. Reaction products of the *trans*- and *cis*-decalin oxidation with H_2O_2 and air catalyzed by anion **1** after treatment with PPh_3.

In order to establish the stereoselectivity quantitatively, we used a simple *trans*/*cis* parameter which represents the ratio [*trans*-decal-9-ol] / [*cis*-decal-9-ol]. The lower the value of this *trans*/*cis* parameter in the oxidation of *cis*-decalin, the higher is the steroselectivity of the reaction. On the other hand, if the oxidation of *trans*-decalin exhibits a high value of this *trans*/*cis* parameter, this testifies that the reaction is stereoselective. The oxidation of the decalin isomers by non-

stereoselective reagents gives approximately equal *trans*/*cis* values for both *cis*- and *trans*-isomers, these parameters being usually different from unity. Stereoselective reactions lead to the predominant formation of the most thermodynamically stable or less strained isomer (usually *trans*-decal-9-ol).

Table 3.1.4. *Trans/cis* ratio for the tertiary alcohols obtained from the oxidation of *cis*- and *trans*-decalin catalyzed by **1** with H_2O_2 and air in acetonitrile.

Substrate	***trans*/*cis* ratio**
Trans-decalin	4.4
Cis-decalin	4.7

Conditions: $[decalin]_0 = 0.31$ mol dm^{-3}; $[H_2O_2]_0 = 0.6$ mol dm^{-3}; [catalyst] = 1.0×10^{-4} mol dm^{-3}; 60 °C, 2 hours, 10 ml total volume.

We can conclude, from the *trans/cis* ratio values obtained for both *cis*- and *trans*-decalin isomers (Table 3.1.4), that the oxidation by anion **1** does not occur with retention of configuration, being in line with a radical mechanism. Both *trans/cis* ratio values are higher than unity, meaning that *trans*-decalol is the major product from both substrates. Comparable values were also observed in hydroxyl radical-generating systems earlier: O_2–H_2O_2–hν (1.3 and 2.7 for *cis*- and *trans*-decalin respectively) and O_2–H_2O_2–NBu_4VO_3 (2.1 and 2.4 for *cis*- and *trans*-decalin respectively) [11].

3.1.4 Oxidation of Light Alkanes

The *n*-tetrabutylammonium salt of the anion **1** also catalyzes the oxidation of ethane to give ethyl hydroperoxide, ethanol and acetaldehyde in acetonitrile solution with hydrogen peroxide and 1 atm of air. The TON obtained after 10 hours is 14 (Table 3.1.5 and Figure 3.1.4). Methane is also oxidized under the same conditions to give a small amount of formaldehyde (Table 3.1.5). Blank experiments (in the absence of substrate) showed that acetonitrile is also oxidized and hydrolyzed, but the product concentrations are sufficiently lower (Table 3.1.6). The oxidation of ethane in aqueous solution afforded only a small concentration of ethanol. Thus, it may be concluded that acetonitrile is the solvent of choice for this reaction.

Table 3.1.5. Concentrations (mol dm^{-3}) of the products from the oxidation of methane and ethane catalyzed by **1** with H_2O_2 and air in acetonitrile (the concentration of products from the acetonitrile oxidation is already subtracted).

Substrate	**$[CH_3CH_2OOH]$, $\times 10^3$**	**$[CH_3CH_2OH]$, $\times 10^3$**	**$[CH_3CHO]$, $\times 10^3$**	**TON**
Ethane	0.5	0.3	0.6	14
Substrate	**$[CH_2O]$, $\times 10^3$**			**TON**
Methane	0.1			1

Conditions: Methane pressure = 40 bar; Ethane pressure = 30 bar; air pressure = 1 bar; $[H_2O_2]_0$ = 0.6 mol dm^{-3}; [catalyst] = 1.0×10^{-4} mol dm^{-3}; 60 °C, 10 hours, 10 ml total volume.

Table 3.1.6. Concentrations (mol dm^{-3}) of the products from the oxidation of acetonitrile (blank experiment) catalyzed by **1** with H_2O_2 and air.

Substrate	**$[CH_2O]$,× 10^3**	**$[CH_3COOH]$,× 10^3**
Acetonitrile	0.012	0.012

Conditions: Air pressure = 1 bar; $[H_2O_2]_0$ = 0.6 mol dm^{-3}; [catalyst] = 1.0×10^{-4} mol dm^{-3}; 60 °C, 10 hours, 10 ml total volume.

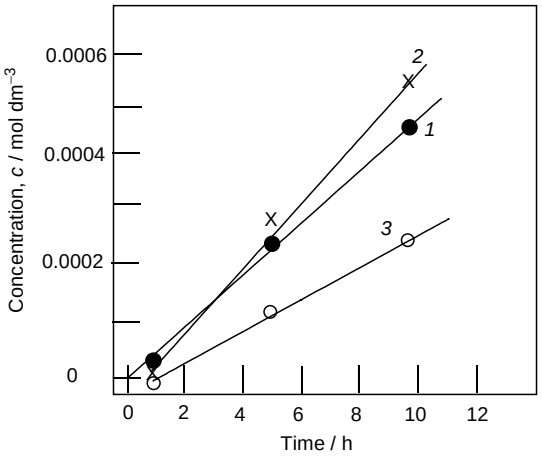

Figure 3.1.4. Reaction profile of the oxidation of ethane in acetonitrile catalyzed by **1**. Conditions: Ethane pressure = 30 bar; air pressure = 1 bar; $[H_2O_2]_0$ = 0.59 mol dm^{-3}; [catalyst] = 1.0×10^{-4} mol dm^{-3}; 60°C, 10 ml total volume. Products: ethyl hydroperoxide (*1*), acetaldehyde (*2*), ethanol (*3*).

3.1.5 Conclusions

Taking into account the low bond selectivity and the lack of stereoselectivity, we assume that this reaction proceeds via formation of hydroxyl radicals from hydrogen peroxide. Polyoxometalates that do not contain vanadium ions are poor catalysts [126, 127] and, consequently, the most reasonable route for the formation of

hydroxyl radicals is the interaction of a V(IV) species with H_2O_2. It was shown that vanadium-containing polyoxomolybdates decompose in solution giving Mo-O-V fragments that must be the real catalytic species [210]. Since in the alkane hydroperoxidation catalyzed by the simple VO_3^- anion [9a, 9c, 10, 90, 48, 146-152], the rate-limiting step is the monomolecular decomposition of the V(V) complex containing one coordinated H_2O_2 molecule, it is probable that, in the case of the vanadium-polyoxometalate catalysis, the first slow step is also the coordination of a hydrogen peroxide molecule to vanadium, the homolytic decomposition of this complex producing a vanadium(IV) complex and a hydroperoxyl radical.

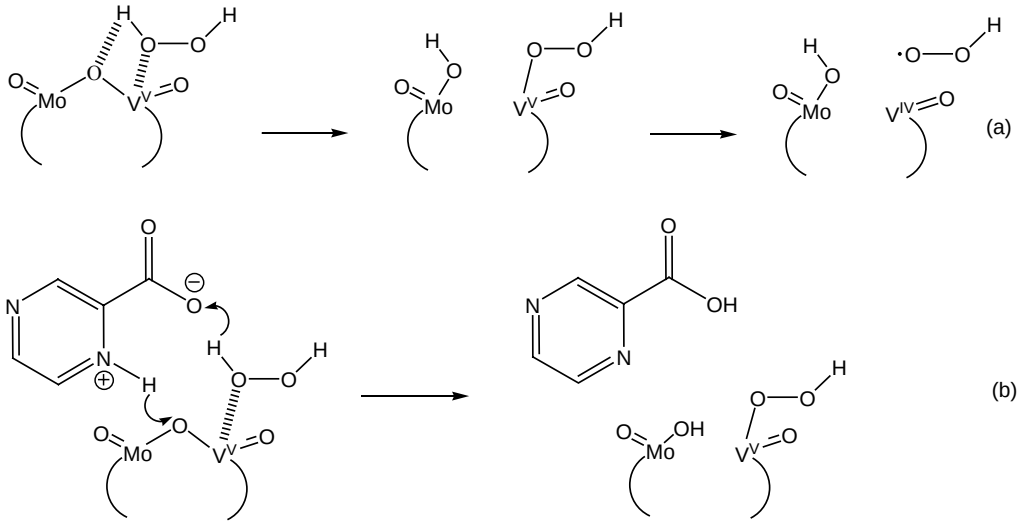

Scheme 3.1.5. Proposed mechanism for the decomposition of one hydrogen peroxide molecule by a Mo-O-V moiety in anions **1** and **2** to produce a V(IV) active species (a) and the possible role of a pcaH molecule as a proton transfer reagent (b).

The environment of the oxovanadium ion which consists of many oxomolybdenum fragments definitely facilitates this process, because the VO_3^- anion

itself does not catalyze the alkane oxidation in acetonitrile in the absence of pcaH or other acids. Two explanations for this assistance are possible: first, the Mo=O fragments enhance the oxidizing ability of V(V) toward H_2O_2, which is a reducing agent in the first step of the process. Second, the oxygen atoms of the Mo-O-V moieties in the polyoxometalate can accept a hydrogen atom from H_2O_2, as it is shown in Scheme 3.1.5. A pcaH molecule coordinated to vanadium(V) or in the zwitterionic form possibly facilitates this proton transfer from H_2O_2 to the oxygen atom of a Mo-O-V moiety (Scheme 3.1.5). The lost of a hydroperoxyl radical from the vanadium(V) complex yields a V(IV) species. The V(IV) species thus formed can then react with a second H_2O_2 molecule to generate a hydroxyl radical (*cf.* Scheme 2.3.3) which will attack the alkane yielding the corresponding oxidation products (*cf.* Scheme 2.3.2).

3.2 Synthesis and Characterization of New Vanadium(IV) and (V) Complexes

Very recently, catalytic systems mimicking the generation of hydroxyl radicals in certain vanadium-dependent biological processes have been reported: Thus, the vanadate anion was found to catalyze the aerobic hydroxylation of hydrocarbons in the presence of solid ascorbic acid or zinc and with the obligatory participation of pyridine, pcaH and acetic acid as mediators of proton and electron transfer [91].

Therefore, it was interesting to extend our studies to a set of vanadium complexes bearing various *N,O*-, N_3- and O_2- chelating ligands as potential biomimetic systems which may be capable of generating hydroxyl radicals from hydrogen peroxide. For this purpose we used in particular *N,O*- chelating ligands, anions of pyrazine-2-carboxylic acid (pcaH) and pyrazine-2,5-dicarboxylic acid (pdcaH) for the synthesis of vanadium(V) oxo derivatives.

In a previous paper, our group had reported the synthesis of anionic complexes $[VO_2(pca)_2]^-$ which contain two pca ligands in the molecule [10]. Inspired by the pioneering work of Mimoun *et al.* [88], we decided to block a vanadium(V) coordination site by the bulky hexamethylphosphoramide $(Me_2N)_3PO$ (hmpa), in order to prevent the coordination of a second pca ligand. The same strategy was applied to the synthesis of a dinuclear dioxovanadium(V) complex containing a *N,O*-chelating ligand derived from pyrazine-2,5-dicarboxylic acid. It was interesting to compare the latter ligand with that derived from pyridine-2,5-dicarboxylic acid

($pycaH_2$) which can give rise to the formation of a similar mononuclear vanadium derivative.

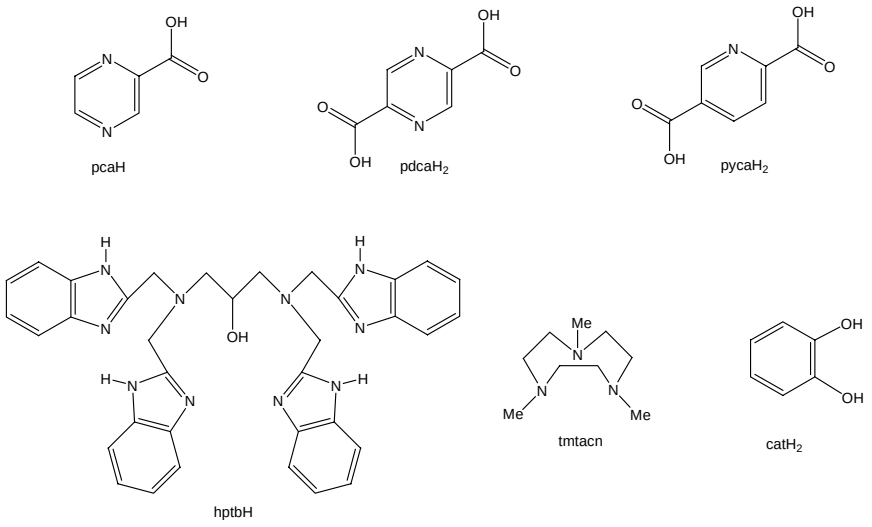

Scheme 3.2.1. *N,O*-, N_3-, and O_2- containing molecules used as ligands or ligand precursors for the coordination to vanadium(V) or vanadium(IV).

Furthermore, it was important to compare the catalytic properties of these vanadium complexes containing *N,O*- chelating ligands as well as the weakly coordinating hmpa ligands with vanadium complexes containing strongly coordinating chelating ligands. For this purpose we prepared complexes containing 1,4,7-trimethyl-1,4,7-triazacyclononane (tmtacn) as a ligand, and complexes containing ligands derived from *N,N,N',N'*-tetrakis(2-benzimidazolylmethyl)-2-hydroxo-1,3-diaminopropane (hptb) and from *pyro*-catechol ($catH_2$). Scheme 3.2.1 shows the ligands or ligand precursors used.

3.2.1 Synthesis

The reaction of pyrazine-2-carboxylic acid, pyrazine-2,5-dicarboxylic or pyridine-2,5-dicarboxylic acid with ammonium vanadate in the correct metal to ligand

ratio gives, in the presence of excessive hexamethylphosphoramide, rise to the formation of the neutral complexes **3**, **4** and **5** according to Eq. 1 - 3. The use of an excess of hmpa helps to avoid the coordination of a second *N,O*-chelating ligand to the vanadium(V) centre. Complexes **3**, **4** and **5** are easily extracted in dichloromethane and recrystallized from a mixture of dichloromethane and diethyl ether.

$$VO_3^- + pcaH + hmpa \longrightarrow [VO_2(pca)(hmpa)] + OH^- \quad \text{(Eq. 1)}$$

(**3**)

$$2\ VO_3^- + pdcaH_2 + 2\ hmpa \longrightarrow [(VO_2)_2(pdca)(hmpa)_2] + 2\ OH^- \quad \text{(Eq. 2)}$$

(**4**)

$$VO_3^- + pycaH_2 + hmpa \longrightarrow [VO_2(pycaH)(hmpa)] + OH^- \quad \text{(Eq. 3)}$$

(**5**)

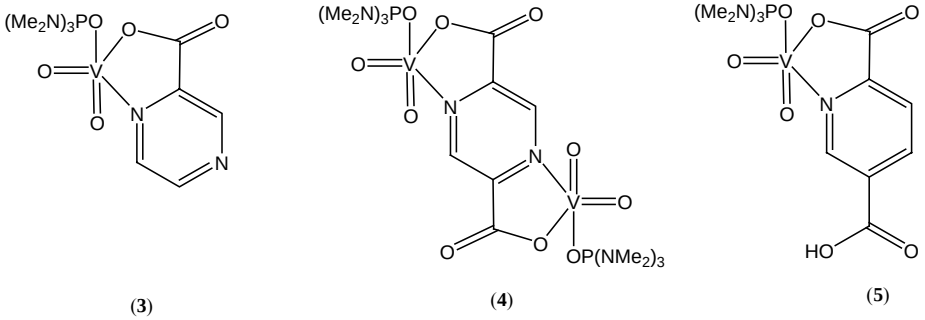

(**3**) (**4**) (**5**)

Scheme 3.2.2. Mono- and dinuclear vanadium(V) complexes containing *N,O*-chelating ligands.

The reaction of $VOSO_4$ with hptbH in methanol, the metal to ligand ratio being 2 : 1, yields, in the presence of $NaClO_4 \cdot n\ H_2O$ after some weeks at room temperature green crystals of $[(VO)_4(hptb)_2(H_2O)_2(\mu\text{-}O)][ClO_4]_4$ (cation **6**), according

to Eq. 4. Complex **6** has a tetrameric structure composed of two dinuclear vanadium(IV) moieties held together by a μ-oxo bridge. Each dinuclear moiety is formed by two vanadyl moieties chelated through two imidazol-nitrogen atoms, one amino nitrogen and the oxygen atom of the alkoxo function of the hptb ligands.

$$4\,[VO]^{2+} + 2\,hptbH + 3\,H_2O \longrightarrow [(VO)_4(hptb)_2(H_2O)_2(\mu\text{-}O)]^{4+} + 4\,H^+ \quad \text{(Eq. 4)}$$

(**6**)

$$2\,VCl_3 + 2\,tmtacn + H_2O + \tfrac{1}{2}\,O_2 \longrightarrow 2\,[VOCl_2(tmtacn)] + 2\,HCl \quad \text{(Eq. 5)}$$

(**7**)

$$[VO_3]^- + 3\,catH_2 \longrightarrow [V(cat)_3]^- + 3\,H_2O \quad \text{(Eq. 6)}$$

(**8**)

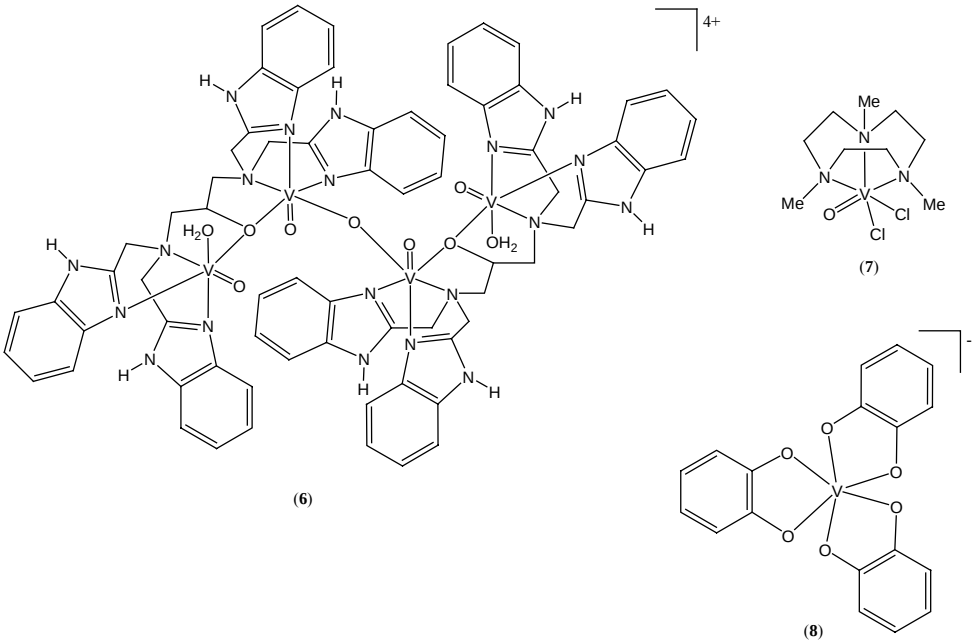

Scheme 3.3.3. The tetranuclear vanadium(IV) complex **6** and the known mononuclear vanadium complexes **7** and **8**.

The known [155,157] vanadium(IV) 1,4,7-trimethyl-1,4,7-triazacyclononane complex $[VOCl_2(tmtacn)]$ (**7**) is synthesized by a slightly modified procedure with respect to that of the original paper [155]: Vanadium (III) chloride is reacted in wet acetonitrile at 0°C with tmtacn, after the colour change from violet to black, the reaction solution is refluxed in air to allow the oxidation of vanadium (III) to vanadium (IV) according to Eq. 5. Blue crystals of **7** are obtained by recrystallization from acetonitrile. The known [156] vanadium(V) catecholate complex $[V(cat)_3]^-$ (**8**) is accessible as the tetrabutylammonium salt from $[n\text{-}Bu_4N][VO_3]$ and catechol (1 : 3) in acetonitrile, in the presence of triethylamine to facilitate the deprotonation of catechol, according to Eq. 6.

3.2.2 Molecular Structures

The molecular structures of compounds **3**, **4**, **5**, **6**$[ClO_4]_4$ and **7** have been determined by single-crystal X-ray structure analysis. Due to poor crystal quality, the structure analysis for **4** is not good enough for a precise structure determination; nevertheless it was possible to elucidate the molecular constitution and configuration.

The X-ray crystal structure analysis of **3** (Figure 3.2.1) reveals a trigonal-bipyramidal environment of the vanadium atom, which agrees with that of the analogous picolinato complex [88]. In the dioxovanadium moiety, the two terminal oxo ligands are *cis* positioned with respect to each other. The V=O distances are 1.606 Å and 1.600 Å, and the O=V=O angle is 109.2°. The pca ligand is coordinated to the dioxovanadium moiety by an oxygen atom of the carboxylato function and by the nitrogen atom of the aromatic cycle in the α position with respect

to the carboxylato substituent; this coordination gives an almost planar five-membered metallacyclic moiety. The V-O bond is 2.001 Å and the V-N bond is 2.173 Å, and the O-V-N angle is 75.34°. The hmpa ligand is bonded to the vanadium atom through the oxygen atom, with a distance of 1.967 Å and a V-O-P angle of 139.5°.

Table 3.2.1. Selected bond distances (Å) and angles (°) of complexes **3**, **4**, **5**.

Bond distances				
	3	**4**		**5**
V(1)-O(1)	1.606(4)	1.670(15)	V(1)-O(5)	1.617(4)
V(1)-O(2)	1.600(4)	1.607(16)	V(1)-O(6)	1.628(4)
V(1)-O(3)	2.001(4)	2.065(15)	V(1)-O(9)	1.987(5)
V(1)-O(5)	1.967(4)	1.968(17)	V(1)-O(1)	1.976(3)
V(1)-N(1)	2.173(4)	2.17(2)	V(1)-N(1)	2.137(4)
V(2)-N(2)		2.132(2)	O(11)-H(11)	0.840
V(2)-O(2)		1.966(17)	H(11)-O(3)	1.670
V(2)-O(7)		1.622(16)		
V(2)-O(8)		1.633(15)		
V(2)-O(13)		2.004(15)		
Bond angles				
	3	**4**		**5**
O(1)-V(1)-O(2)	109.2(2)	104.6(8)	O(5)-V(1)-O(6)	109.3(2)
N(1)-V(1)-O(3)	75.34(16)	74.8(7)	N(1)-V(1)-O(9)	75.27(18)
O(3)-V(1)-O(5)	80.59(16)	85.2(7)	O(1)-V(1)-O(9)	82.45(17)
V(1)-O(5)-P(1)	139.5(3)	135.6(11)	V(1)-O(1)-P(1)	137.3(3)
V(2)-O(2)-P(2)		140.0(11)	O(11)-H(11)-O(3)	169.87

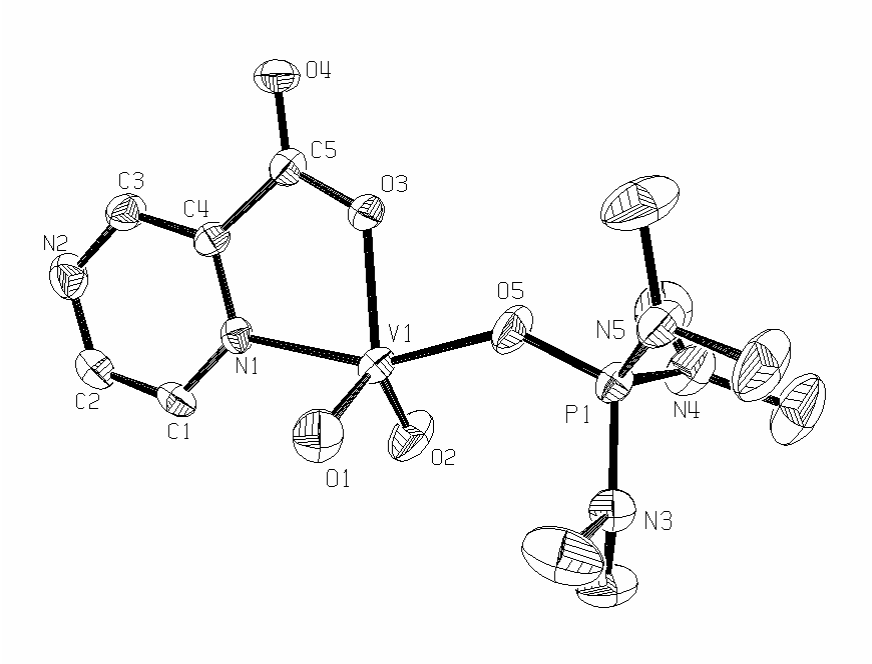

Figure 3.2.1. Molecular structure of **3**.

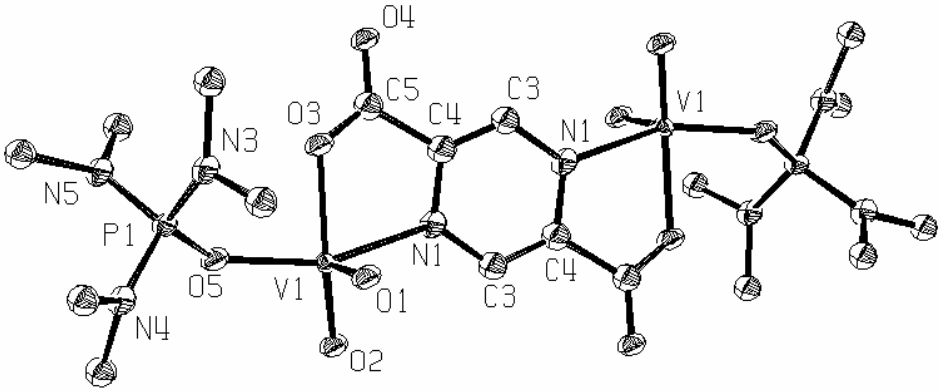

Figure 3.2.2. Molecular structure of **4**.

In **4** (Figure 3.2.2), both vanadium atoms also have a trigonal bipyramidal environment, both being coordinatively equivalent due to the symmetry of the molecule. The pdca ligand is chelated to both VO_2 moieties by one oxygen atom of the carboxylato function and by the nitrogen atom of the aromatic ring in the α-position. The carboxylato function and the aromatic nitrogen form with the vanadium atom an almost planar five-membered metallacyclic moiety. One hmpa ligand is bonded to each vanadium atom by its oxygen atom, the coordination geometry of both vanadium atoms in **4** is similar to that found in **3**. As the final R_{int} value is only 15%, the bond angles and distances are not reliable enough for precise values.

The molecular structure of **5** (Figure 3.2.3) is similar to that of **3**. The vanadium centre is bonded to two terminal oxo ligands, the V-O bond distances being 1.617 and 1.628 Å, respectively, and the O-V-O angle 109.3. The vanadium atom is coordinated to the pycaH ligand through the oxygen atom of the α-carboxylato function, the bond distance being 1.087 Å, and through the nitrogen atom of the aromatic cycle, with a V-N distance of 2.137 Å. The N-V-O angle is 75.27°. The vanadium centre is also bonded to the oxygen atom of the hmpa ligand with a bond distance of 1.976 Å and a V-O-P angle of 137.3°. As in **5** only one of the carboxylic functions is coordinated, while the other one is present as a free carboxylic function, the crystal structure reveals an adduct of **5** with an additional hmpa molecule linked by hydrogen bonding: The H atom is bonded to the oxygen of the carboxylic function with a bond distance of 0.840 Å and to the oxygen of the additional hmpa ligand with a bond distance of 1.670 Å. The O-H-O angle is 169.87°.

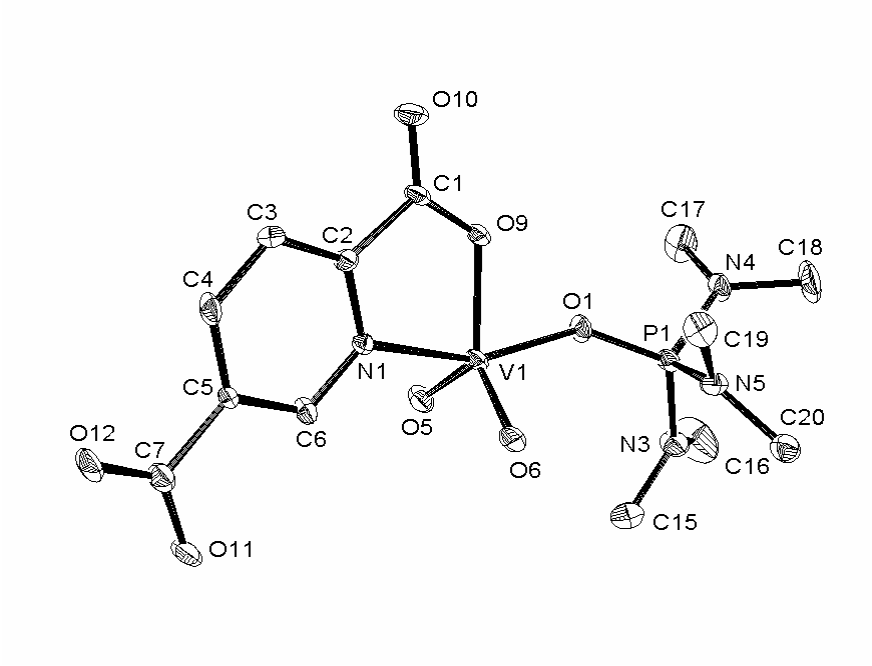

Figure 3.2.3. Molecular structure of **5**.

Complex **6** (Figure 3.2.4) was found to contain four vanadium atoms and two N_3O-ligands, two $V_2(hptb)(O)_2(H_2O)$ moieties being connected by an μ-oxo bridge situated at the centre of symmetry of the molecule. The four vanadium atoms are six-coordinated in a distorted octahedral geometry, two of which being pairwise equivalent. Both V(2) atoms are bonded to the μ-O bridge with a vanadium-oxygen distance of 1.8102 Å and an V-O-V angle of 180°. The environment of these two vanadium atoms is formed by three nitrogen atoms and one oxygen atom of the hptb ligand, a terminal oxo ligand and the bridging oxo ligand. The hptb ligand chelates these V(2) atoms through two imidazol nitrogen atoms with a V-N distances of 2.054 and 2.057 Å, one amino nitrogen atom with a V-N distance of 2.359 and one alkoxo oxygen atom, with a V-O distance of 2.052; the terminal oxo ligand is bonded to each V(2) with a V-O distance of 1.603 Å, and forms an angle of 162.34° with the μ-oxo bridge. The other two equivalent vanadium atoms V(1) also have an octahedral

coordination geometry, formed by three nitrogen atoms and one oxygen atom of the hptb ligand, a terminal oxo ligand, and a water ligand. Each hptb ligand bonds one V(1) by two imidazol nitrogen atoms with the V-N distances of 2.040 and 2.054 Å, one nitrogen amino ligand with the V-N distance of 2.361 Å and one alkoxo oxygen atom with the V-O distance of 2.017 Å. The oxo ligand in each V(1) centre bonds to vanadium with a V-O distance of 1.609 Å, and a water molecule is bonded to each V(1) with a V-O distance of 2.045 Å. The angle between the oxo ligand, the V(1) centre and the oxygen atom of the water molecule is 99.5°. In each $V_2(hptb)(O)_2(H_2O)$ moiety, the two terminal oxo ligands are *syn* and they are *anti* with respect to the corresponding oxo ligands in the other moiety, comparable to the structure of $[(VO)_4(btppnol)_2(\mu\text{-}O)_2](ClO_4)_2 \cdot 2\ DMF \cdot 2\ H_2O$ published very recently [158].

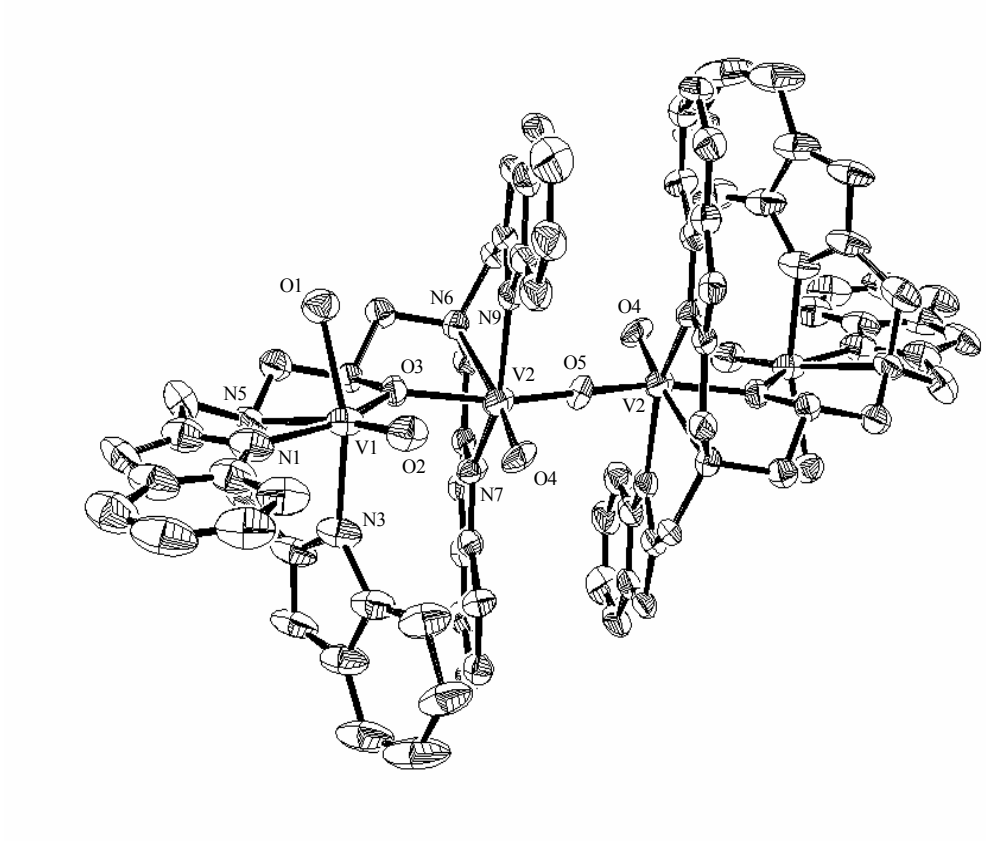

Figure 3.2.4. Molecular structure of **6**.

Table 3.2.2. Selected bond distances (Å) and angles (°) of complex **6**[ClO_4].

Bond distances			
V(1)-N(1)	2.040(9)	V(1)-O(1)	2.045(5)
V(1)-N(3)	2.054(6)	V(1)-O(2)	1.609(5)
V(1)-N(5)	2.361(7)	V(1)-O(3)	2.017(6)
V(2)-N(7)	2.057(6)	V(2)-O(3)	2.052(5)
V(2)-N(9)	2.065(6)	V(2)-O(4)	1.603(5)
V(2)-N(6)	2.359(6)	V(2)-O(5)	1.810(16)
Bond angles			
O(2)-V(1)-O(3)	108.9(3)	V(2)-O(5)-V(2)#1	180.0
O(2)-V(1)-N(1)	98.6(3)	O(4)-V(2)-O(3)	95.6(3)
O(3)-V(1)-N(1)	152.5(3)	O(5)-V(2)-O(3)	162.34(17)
O(2)-V(1)-O(1)	99.5(2)	O(4)-V(2)-N(7)	104.4(2)
O(3)-V(1)-O(1)	88.3(2)	O(5)-V(2)-N(7)	85.6(2)
N(1)-V(1)-O(1)	85.9(3)	O(3)-V(2)-N(7)	89.8(2)
O(2)-V(1)-N(3)	98.1(3)	O(4)-V(2)-N(9)	105.0(3)
O(3)-V(1)-N(3)	90.6(2)	O(5)-V(2)-N(9)	89.60(19)
N(1)-V(1)-N(3)	86.8(3)	O(3)-V(2)-N(9)	86.0(2)
O(1)-V(1)-N(3)	161.7(3)	N(7)-V(2)-N(9)	150.5(3)
O(2)-V(1)-N(6)	171.7(3)	O(4)-V(2)-N(6)	172.3(3)
O(3)-V(1)-N(6)	77.1(2)	O(5)-V(2)-N(6)	85.55(17)
N(1)-V(1)-N(6)	75.7(3)	O(3)-V(2)-N(6)	76.8(2)
O(1)-V(1)-N(6)	86.2(2)	N(7)-V(2)-N(6)	75.7(2)
N(3)-V(1)-N(6)	75.8(3)	N(9)-V(2)-N(6)	75.0(3)
O(4)-V(2)-O(5)	102.1(2)		

The molecular structure of compound **7** was published by Fiedler *et al* during the preparation of our analysis and our data are comparable to theirs [157]. In compound **7** (Figure 3.2.5) the vanadium atom has a distorted octahedral environment and it is coordinated by the three nitrogen atoms of the tmtacn ligand, two chlorides ligands and one oxo ligand. The nitrogen in *trans* to the oxo ligand has a V-N bond distance of 2.353 Å which is significantly longer than the other two V-N distances (2.187 and 2.184 Å), which is consistent with the data for other analogous vanadium-oxo complexes containing triazacyclononane ligand [155, 159] the angle between this *trans*-nitrogen atom , the vanadium center and the oxo ligand is 165.38° similar to values observed in analogous Ti^{IV} (162.54°) [159] and Mo^{IV} (160.55°) [161] complexes. The oxo ligand is bonded to vanadium with a bond length of 1.590 Å, which is a typical distance for terminal oxo ligand in vanadyl moieties [155].

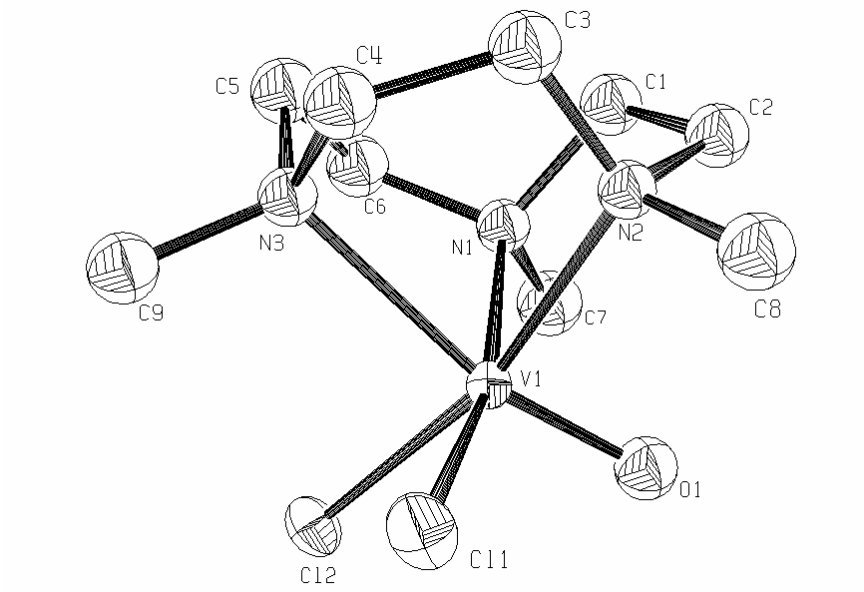

Figure 3.2.5. Molecular structure of **7**.

Table 3.2.3. Selected bond distances (Å) and angles (°) of complex **7**.

Bond distances			
N(1)-V(1)	2.187(3)	O(1)-V(1)	1.590(3)
N(2)-V(1)	2.184(3)	Cl(1)-V(1)	2.3502(12)
N(3)-V(1)	2.353(3)	Cl(2)-V(1)	2.3590(11)
Bond angles			
O(1)-V(1)-N(2)	90.62(14)	N(2)-V(1)-N(3)	77.33(12)
O(1)-V(1)-N(1)	93.19(15)	N(1)-V(1)-N(3)	76.45(12)
N(2)-V(1)-N(1)	80.36(13)	Cl(1)-V(1)-N(3)	88.15(9)
O(1)-V(1)-Cl(1)	101.28(13)	O(1)-V(1)-Cl(2)	101.27(11)
N(2)-V(1)-Cl(1)	93.20(9)	N(2)-V(1)-Cl(2)	165.85(9)
N(1)-V(1)-Cl(1)	164.26(10)	N(1)-V(1)-Cl(2)	91.24(9)
O(1)-V(1)-N(3)	165.17(13)	Cl(1)-V(1)-Cl(2)	91.97(5)
		N(3)-V(1)-Cl(2)	89.69(9)

3.3 Catalytic Potential of the Vanadium(IV) and (V) Complexes Synthesized

We studied the catalytic activity of all compounds synthesized (*cf.* Section 3.2) for the oxidation of cyclohexane with hydrogen peroxide and air in acetonitrile. Based on the experience of our previous publication [11], we carried out the reactions at 40ºC. In accordance with our previous findings [9c, 10, 11, 89, 91, 146, 147, 149, 151, 162, 163], we added pcaH as a co-catalyst (V/pcaH ratio 1 : 4) which accelerates the reaction, even in the cases where the vanadium complexes contain already one or two pca ligands. We normally followed the course of the reaction for 24 h. The results are shown in Table 3.3.1 and the products obtained are shown in Scheme 3.3.1.

Table 3.3.1. Concentrations for the products of the oxidation of cyclohexane.

Catalyst	**[pcaH added]**	**Initial rate**	**TOF**[a]	**TON**[b]	**Products, M (after 24 h)**		
(× 10^4)	**× 10^4**	**× 10^6 mol dm^{-3} s^{-1}**	**h^{-1}**		Cy_HO	CyOH	CyOOH (%)[c]
3 (1.0)	3.0	3.9	256	1370	0.017	0.080	0.040 (29)
4 (0.5)	3.5[d]	3.5	98	550	0.005	0.040	0.010 (18)
5 (1.0)	3.0	6.6	121	1440	0.014	0.014	0.116 (80)
6 (0.25)	4.0	0.8	14	570	0.002	0.002	0.053 (93)
7 (1.0)	4.0	1.8	23	290	0.001	0.001	0.027 (94)
8 (1.0)	4.0	6.7	224	980	0.087	0.087	0.001 (1)

Conditions: $[cyclohexane]_0 = 0.46$ mol dm^{-3}; $[H_2O_2]_0 = 0.50$ mol dm^{-3}; 40 °C; total volume 10 ml. [a] Turnover frequency, i. e., number of moles of all products per one mol of vanadium during the first hour. [b] Turnover number, i. e., number of moles of all products per one mol of vanadium after 24 h. [c] Relative content of cyclohexyl hydroperoxide in the mixture after 24 h. [d] $pdcaH_2$ was used instead of pcaH.

The samples were analyzed twice, i.e. before and after the addition of the excess of solid PPh_3, a method which allows to measure the concentrations of all three products, cyclohexyl hydrperoxide (CyOOH), cyclohexanone (Cy_HO) and cyclohexanol (CyOH) (*cf.*chapter 4).

$$C_6H_{12} + H_2O_2 + \tfrac{1}{2} O_2 \longrightarrow C_6H_{11}OOH + H_2O$$

$$2\ C_6H_{11}OOH \longrightarrow C_6H_{11}OH + C_6H_{10}O$$

Scheme 3.3.1. Reaction products of the oxidation of cyclohexane with H_2O_2 and air catalyzed by complexes **3** to **8.**

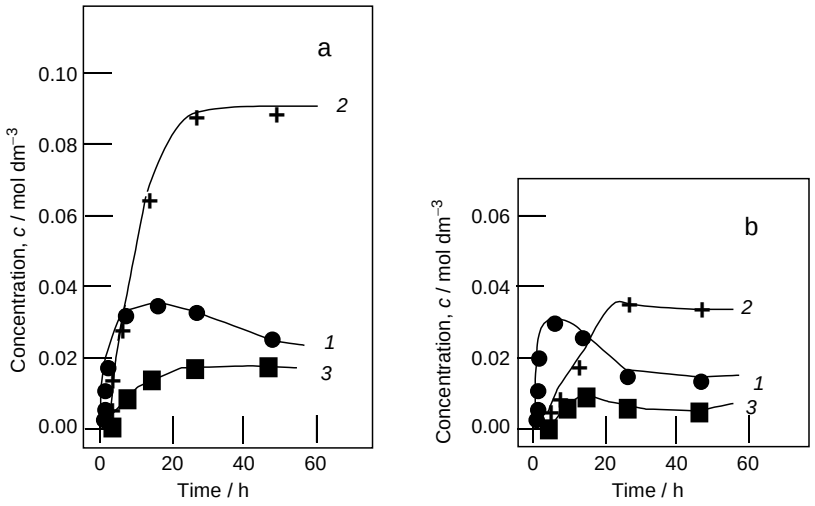

Figure 3.3.1. Reaction profile of the cyclohexane oxidation catalyzed by **3** in the presence of pcaH (a) and **4** in the presence of $pdcaH_2$ (b). Conditions: (*cf.* table 3.3.1). Products: cyclohexyl hydroperoxide (*1*), cyclohexanol (*2*), cyclohexanone (*3*).

The vanadium complexes differ significantly in their catalytic behaviour, the most efficient catalyst (per vanadium) being complex **3**. It oxidizes cyclohexane with high initial rate and high TON after 24 h. The reaction gives initially cyclohexyl

hydroperoxide which decomposes in the course of the reaction to give cyclohexanone and cyclohexanol, the decomposition being catalysed by **3**. After 24 h the content of CyOOH is only 29%. The dinuclear complex **4** catalyses the reaction with approximately the same activity, but the efficiency per vanadium is only half of that of **3** (Figure 3.3.1).

Complex **5** exhibits a high activity in combination with only 3 equivalents of pcaH; one can assume that the free carboxylic group in the pycaH ligand takes part in the proton transfer processes and thus replaces 1 eq of pcaH (Figure 3.3.2).

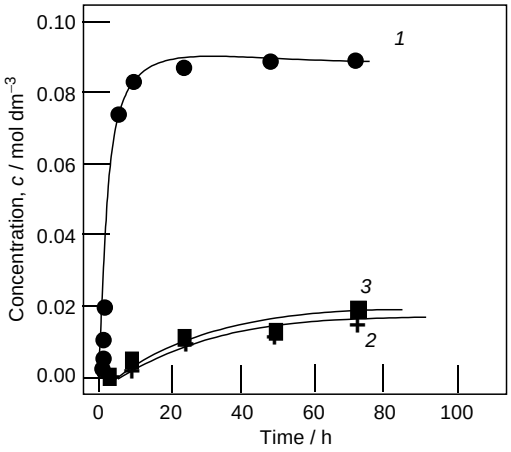

Figure 3.3.2. Reaction profile of the cyclohexane oxidation catalyzed by **5** in the presence of pcaH. Conditions: (*cf.* table 3.3.1). Products: cyclohexyl hydroperoxide (*1*), cyclohexanol (*2*), cyclohexanone (*3*).

The behaviour of complexes **6** and **7** containing strongly complexing chelating and voluminous ligands is remarkable, because they give rise to the formation of almost pure cyclohexyl hydroperoxide, although their activity is not as high. The accumulation of oxidation products occurs with auto-acceleration (Fig. 3.3.3), which is

apparently due to a gradual destruction of **6** in the course of the reaction leading to more efficient catalytically species. These species presumably contain weaker ligands (for example, acetonitrile, water and fragments of hptb) which provide easier access of H_2O_2 to the vanadium center.

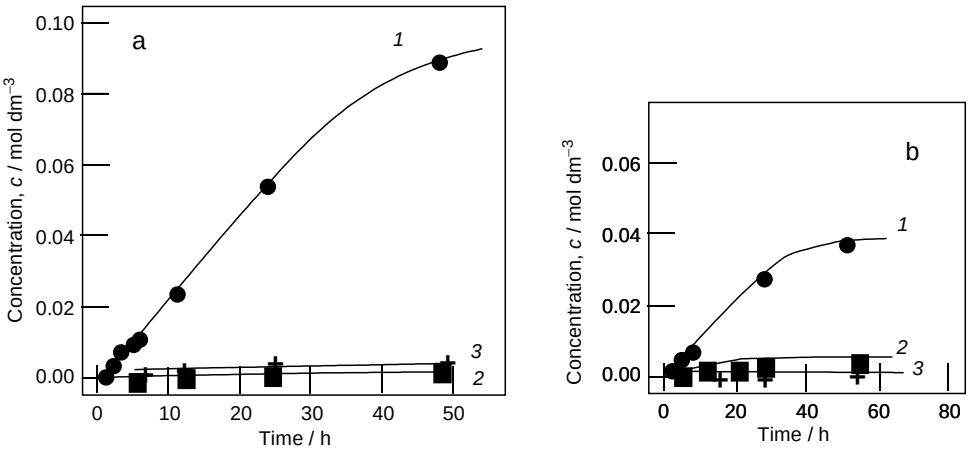

Figure 3.3.3. Reaction profile of the cyclohexane oxidation catalyzed by **6** (a) and **7** (b) in the presence of pcaH. Conditions: (*cf.* table 3.3.1). Products: cyclohexyl hydroperoxide (*1*), cyclohexanol (*2*), cyclohexanone (*3*).

Complex **8** surprisingly catalyzes the oxidation with the highest initial rate (6.7 $\times 10^{-6}$ mol dm^{-3} s^{-1} *versus* 3.9 $\times 10^{-6}$ mol dm^{-3} s^{-1} in the case of **3**). This behaviour suggests that the catecholate ligands can be easily removed in the beginning of the reaction, and that this detachment proceeds *via* the reduction of V(V) to (IV) by the strongly reducing catecholate ions. It has been shown previously that the reduction of vanadium by H_2O_2 is the first step of the catalytic cycle [11, 163]. Electron transfer from one of the catecholate ligands (which can be transformed into semiquinone) may allow hydrogen peroxide to coordinate to a vacant site thus formed at V(IV). It is noteworthy that **8** catalyzes also the complete decomposition of cyclohexyl hydroperoxide into cyclohexanol and cyclohexanone (Figure 3.3.4).

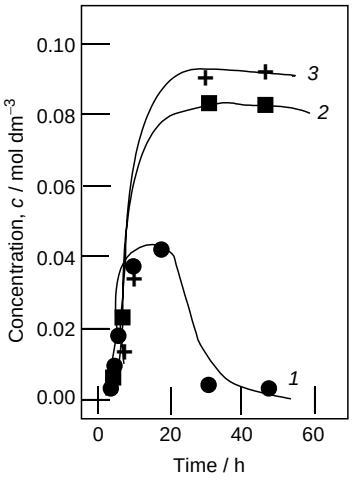

Figure 3.3.4. Reaction profile of the cyclohexane oxidation catalyzed by **8** in the presence of pcaH. Conditions: (*cf.* table 3.3.1). Products: cyclohexyl hydroperoxide (*1*), cyclohexanol (*2*), cyclohexanone (*3*).

3.4 Alkane Oxidation with Peroxyacetic Acid Catalyzed by Vanadium Complexes

Peroxy acids (*e.g*. peroxyacetic, *m*-chloroperbenzoic acids) including those generated *in situ* have been widely used in the oxidation of various hydrocarbons [137, 200, 203, 212-217]. Earlier it has been demonstrated that the "NBu_4VO_3–pcaH–*tert*-butyl hydroperoxide" system in air oxidizes alkanes in acetonitrile solution to give alkyl hydroperoxides as main products which decompose during the course of the reaction to produce the more stable corresponding alcohols and ketones [211].

In the present section we report our kinetic studies on alkane oxidation by peroxyacetic acid using tetrabutylammonium vanadate as catalyst, and our studies on the catalytic potential of complexes **1** (*cf.* Section 3.1), **4**, **7**, **8** (*cf.* Section 3.2), $[NBu_4][VO_2(pca)_2]$ [10] and $VO(acac)_2$ (acac = acetylacetonate) for this oxidation reaction.

3.4.1 Oxidation of Cyclohexane Catalyzed by NBu_4VO_3

The reaction of cyclohexane (CyH) with peroxyacetic acid (paaH) and air in acetonitrile at 30 ºC, catalyzed by NBu_4VO_3, gives rise to the relatively slow formation of cyclohexyl hydroperoxide, CyOOH, which decomposes in the course of the reaction to produce cyclohexanone and cyclohexanol (Figure 3.4.1). The reaction occurs with auto-acceleration and reaches the maximum rate after approximately 3 h (curve *4*). The total concentration of the oxidation products is 0.8×10^{-2} mol dm^{-3} which corresponds to a turnover number (TON) of 80. The reaction proceeds much

more rapidly at 60 ºC and the TON is 90 in this case (Figure 3.4.2). The kinetic curve for the accumulation of the sum of all products also exhibits an S-shape. We found that the addition of pcaH does not accelerate the reaction.

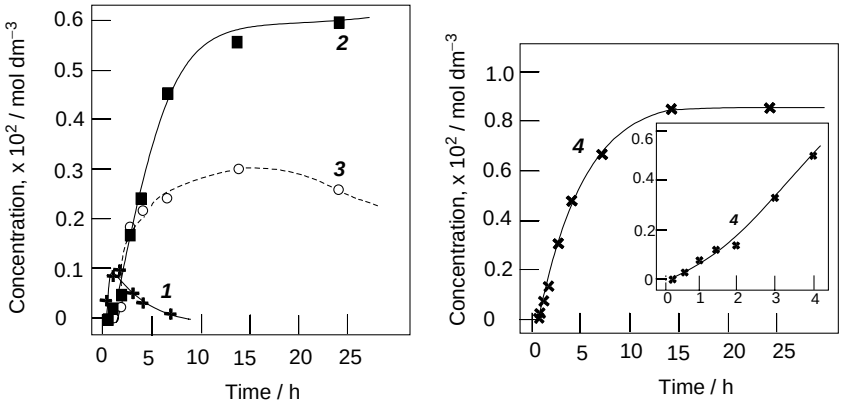

Figure 3.4.1. Accumulation of cyclohexyl hydroperoxide (*1*), cyclohexanone (*2*), cyclohexanol (*3*) and the sum of all products (*4*) in the oxidation of cyclohexane with paaH and air catalyzed by NBu_4VO_3 in acetonitrile at 30 °C. Conditions: [CyH] = 0.46 mol dm^{-3}; [catalyst] = 1 × 10^{-4} mol dm^{-3}; [paaH] = 0.30 mol dm^{-3}; 30°C; 10 ml total volume; 1 atm air.

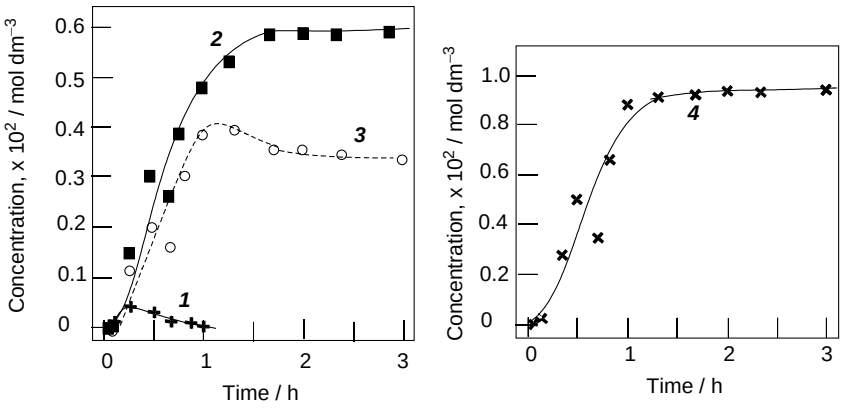

Figure 3.4.2. Accumulation of cyclohexyl hydroperoxide (*1*), cyclohexanone (*2*), cyclohexanol (*3*) and the sum of all products (*4*) in the oxidation reaction of cyclohexane with paaH and air catalyzed by NBu_4VO_3 in acetonitrile at 60 °C. Conditions: [CyH] = 0.46 mol dm^{-3}; [catalyst] = 1 × 10^{-4} mol dm^{-3}; [paaH] = 0.30 mol dm^{-3}; 60°C; 10 ml total volume; 1 atm air.

We found that paaH is completely consumed after approximately 2 h, because at this time, the addition of a new amount equal to that added at the beginning of the reaction, rises the yield on cyclohexanone and cyclohexanol (Figure 3.4.3, curves *1b* and *2b*). The addition of a new amount of NBu_4VO_3 after 4 hours does not enhance the yield of the products (curves *1c* and *2c*). In all our kinetic studies, we measured the concentrations of cyclohexanone and cyclohexanol after reduction of the reaction mixture with PPh_3, in order to reduce all cyclohexyl hydroperoxide to cyclohexanol.

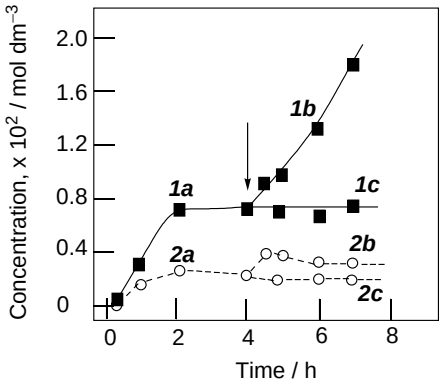

Figure 3.4.3. Accumulation of cyclohexanone (*1a*) and cyclohexanol (*2a*) in the oxidation of cyclohexane with paaH and air catalyzed by NBu_4VO_3 in acetonitrile at 60 ºC. After 4 hours of reaction (arrow) either paaH (0.30 mol dm^{-3}, curves *1b* and *2b*) or NBu_4VO_3 (1×10^{-4} mol dm^{-3}, curves *1c* and *2c*) was added to the reaction mixture. Conditions: [CyH] = 0.46 mol dm^{-3}; $[catalyst]_0 = 1 \times 10^{-4}$ mol dm^{-3}; [paaH] = 0.30 mol dm^{-3}; 60°C; 10 ml total volume; 1 atm air.

We might assume that paaH can be generated *in situ* by mixing acetic acid and hydrogen peroxide. To check this proposal we studied the cyclohexane oxidation with H_2O_2 catalyzed by NBu_4VO_3 in a CH_3CN–CH_3CO_2H (19 : 1) mixture and in pure acetic acid. It turned out that although the oxidation in both cases is comparable with

that for the NBu_4VO_3–paaH system, the selectivities of both reactions are different: the predominant products are cyclohexanol in CH_3CN–CH_3CO_2H and cyclohexyl hydroperoxide in CH_3CO_2H (Fig. 3.4.4). Thus we can conclude that, apparently, paaH is not produced in sufficient concentration by a simple mixture of acetic acid and hydrogen peroxide.

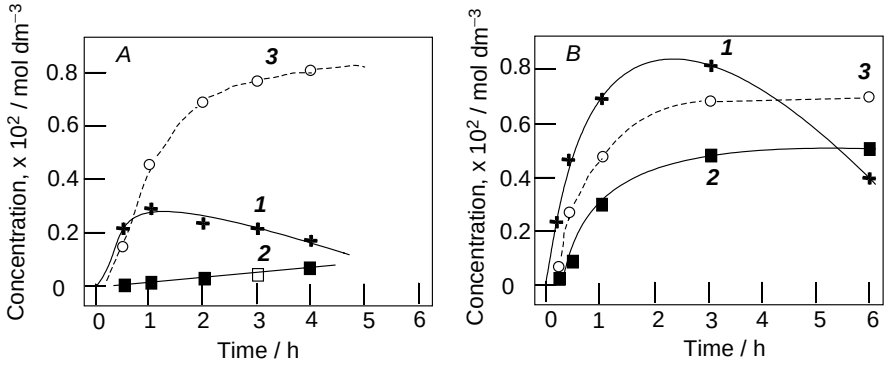

Figure 3.4.4. Accumulation of cyclohexyl hydroperoxide (*1*), cyclohexanone (*2*) and cyclohexanol (*3*) in the oxidation reaction of cyclohexane with H_2O_2 and air at 60 ºC catalyzed by NBu_4VO_3 (1×10^{-4} mol dm^{-3}) in an 19 : 1 acetonitrile : acetic acid mixture (graph A) and in acetic acid (graph *B*). Conditions: [CyH] = 0.46 mol dm^{-3}; [catalyst] = 1×10^{-4} mol dm^{-3}; [H_2O_2] = 0.30 mol dm^{-3}; 60°C; 10 ml total volume; 1 atm air.

Studies of the dependence of the initial rate of the cyclohexane oxidation with paaH upon the initial catalyst concentration under different conditions have shown that the curves for this dependence correspond to first order with respect to the catalyst (Fig. 3.4.5).

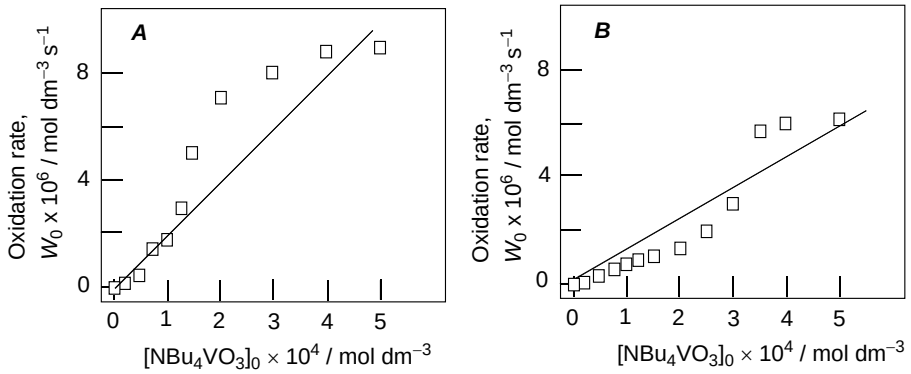

Figure 3.4.5. Initial rate of cyclohexane oxidation with paaH and air catalyzed by NBu_4VO_3 in acetonitrile *vs* initial concentration of NBu_4VO_3. Conditions: [CyH] = 0.46 mol dm^{-3}; 10 ml total volume; 1 atm air; $[paaH]_0$ = 0.30 mol dm^{-3} and 60°C (graph A); $[paaH]_0$ = 0.45 mol dm^{-3} and 40°C (graph B).

The initial rate of the cyclohexane oxidation by the system NBu_4VO_3–paaH exhibits a first order dependence upon paaH concentration at $[paaH]_0 < 0.2$ mol dm^{-3} and the rate is independent of paaH concentration at $[paaH]_0 > 0.4$ mol dm^{-3} (Fig. 3.4.6).

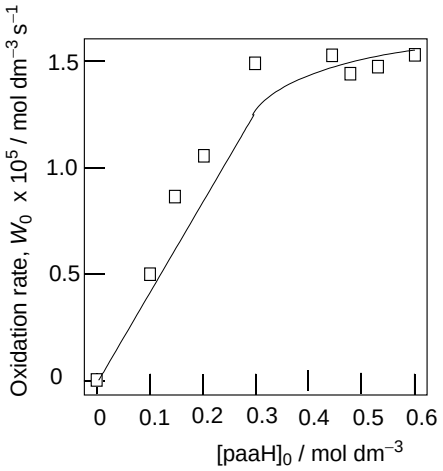

Figure 3.4.6. Initial rate of cyclohexane oxidation with paaH and air catalyzed by NBu_4VO_3 in acetonitrile at 60 ºC *vs* initial concentration of paaH. Conditions: [CyH] = 0.46 mol dm^{-3}; [catalyst] = 1 × 10^{-4} mol dm^{-3}; 60°C; 10 ml total volume; 1 atm air.

The curve for the dependence of the initial rate upon the initial cyclohexane concentration also exhibits saturation (at $[CyH]_0 > 1$ mol dm^{-3}) (Fig.3.4.7). Addition of acetic acid accelerates the reaction (Fig.3.4.8).

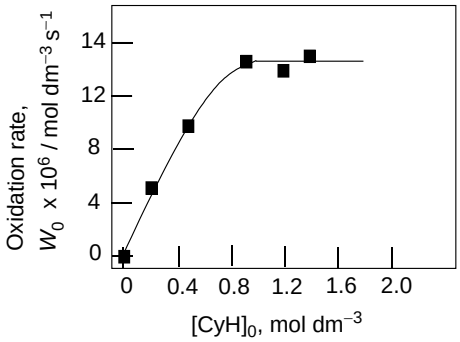

Figure 3.4.7. Initial rate of cyclohexane oxidation with paaH and air catalyzed by NBu_4VO_3 in acetonitrile at 60 ºC *vs* initial concentration of cyclohexane. Conditions: [catalyst] = 4×10^{-4} mol dm^{-3}; [paaH] = 0.30 mol dm^{-3}; 60°C; 10 ml total volume; 1 atm air.

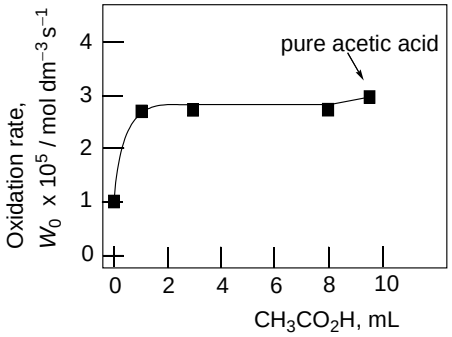

Figure 3.4.8. Initial rate of cyclohexane oxidation with paaH and air catalyzed by NBu_4VO_3 in acetonitrile at 60 ºC *vs* volume of added acetic acid. Conditions: [CyH] = 0.46 mol dm^{-3}; [catalyst] = 4×10^{-4} mol dm^{-3}; [paaH] = 0.30 mol dm^{-3}; 60°C; 10 ml total volume; 1 atm air.

The oxidation of cyclohexane by the NBu_4VO_3–paaH system in pure acetic acid as solvent gives only cyclohexanone and cyclohexanol with a total TON of 50 after 0.5 h (Fig. 3.4.9). The catalyst is stable under the reaction conditions and after addition of a new paaH portion the oxidation continues with the same initial rate.

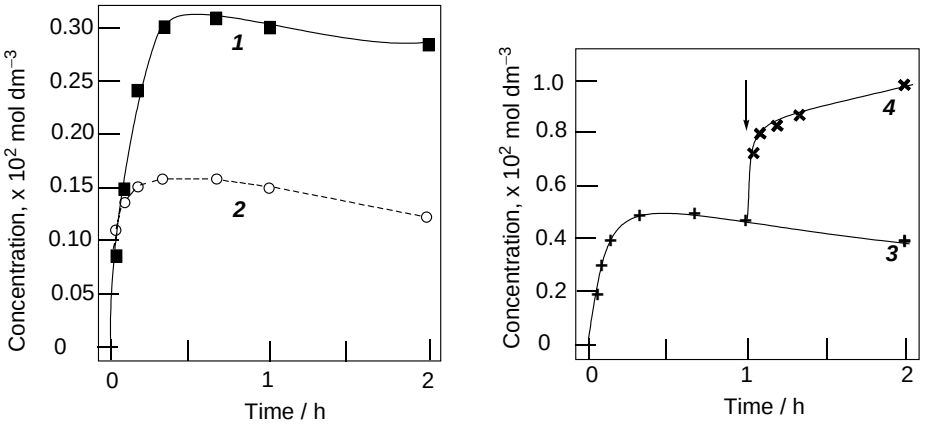

Figure 3.4.9. Accumulation of cyclohexanone (*1*), cyclohexanol (*2*) and the sum of all products (*3*) in the oxidation reaction of cyclohexane with paaH and air catalysed by NBu_4VO_3 in acetic acid at 60 ºC. At the moment marked by an arrow an additional amount of paaH (0.30 mol dm^{-3}) was added (further accumulation of products is shown by curve *4*). Conditions: [CyH] = 0.46 mol dm^{-3}; [catalyst] = 1×10^{-4} mol dm^{-3}; [paaH] = 0.30 mol dm^{-3}; 60°C; 10 ml total volume; 1 atm air.

The dependences of the initial oxidation rate upon the initial concentrations of vanadate, paaH and cyclohexane in acetic acid showed a behaviour similar to that found for the reaction in acetonitrile: At low concentrations of one of the components, the reaction rate exhibits a linear dependence, whereas at relatively high concentrations the reaction rate does not depend on the component concentrations.

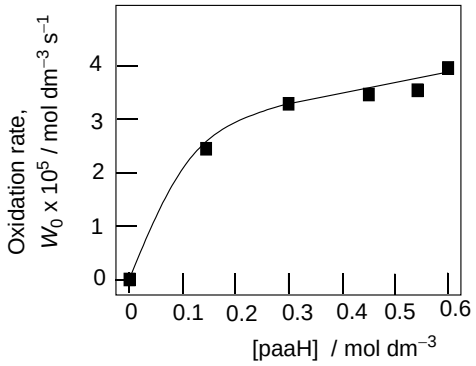

Figure 3.4.10. Initial rate of cyclohexane oxidation with paaH and air catalyzed by NBu_4VO_3 in acetic acid at 60 ºC *vs* initial concentration of paaH. Conditions: [CyH] = 0.46 mol dm^{-3}; [catalyst] = 1×10^{-4} mol dm^{-3}; 60°C; 10 ml total volume; 1 atm air.

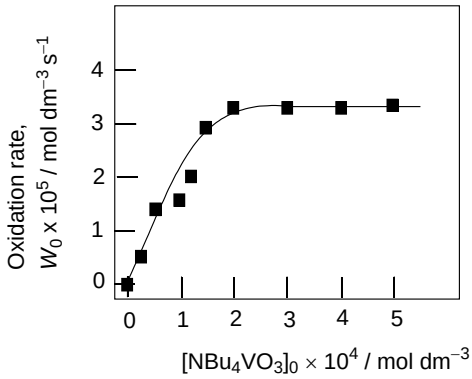

Figure 3.4.11. Initial rate of cyclohexane oxidation with paaH and air catalyzed by NBu_4VO_3 in acetic acid at 60 ºC *vs* initial concentration of NBu_4VO_3. Conditions: [CyH] = 0.46 mol dm^{-3}; [paaH] = 0.30 mol dm^{-3}; 60°C; 10 ml total volume; 1 atm air.

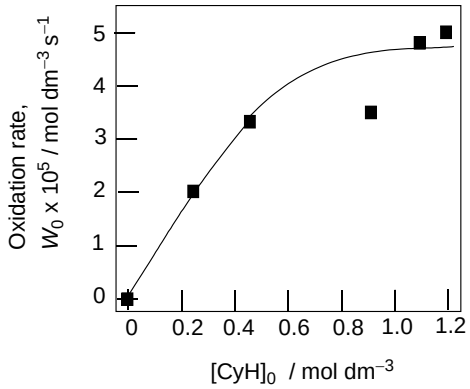

Figure 3.4.12. Initial rate of cyclohexane oxidation with paaH and air catalyzed by NBu_4VO_3 in acetic acid at 60 ºC *vs* initial concentration of cyclohexane. Conditions: [catalyst] = 4×10^{-4} mol dm^{-3}; [paaH] = 0.30 mol dm^{-3}; 60°C; 10 ml total volume; 1 atm air.

3.4.2 Oxidation of Cyclohexane Catalyzed by Vanadium(IV) and (V) Complexes

We studied the catalytic behaviour of the vanadium complexes **1**, **4**, **7**, **8**, $[NBu_4][VO_2(pca)_2]$ and $VO(acac)_2$ in the cyclohexane oxidation with paaH and air in acetonitrile for comparison.

The data obtained for $VO(acac)_2$ are comparable to those for NBu_4VO_3 (Fig. 3.4.13). At the same time, the efficiency of complex **7** is very low (Fig. 3.4.16, curves *b*), possibly due to a great sterical hindrance of the tmtacn ligand. The less voluminous *N*,*O*-chelating ligands coordinated to vanadium(V) in complexes $[NBu_4][VO_2(pca)_2]$ (Fig. 3.4.14, curves *a*) and **4** (Fig. 3.4.16, curves *a*) gives an efficiency in the cyclohexane oxidation comparable to that of simple vanadate. The activity of the vanadium(V)-containing polyoxometalate **1**, in which the vanadium ion

is surrounded by a few molybdenum ions, is very low (Fig. 3.4.14, curves *b*). In this case the oxidation proceeds with auto-acceleration, which is possibly due to a gradual decomposition of the polyoxometalate ion to smaller fragments, the real catalytic species [210]. The high activity of complex **8** containing three cathecolate ligands (Fig. 3.4.15) can be explained by its possible decomposition *via* oxidation of the catecholate ligand. Thus, it can be concluded that complexes of vanadium(V) and vanadium(IV) are active in the alkane oxidation with paaH only if these complexes do not contain strongly bound bulky ligands.

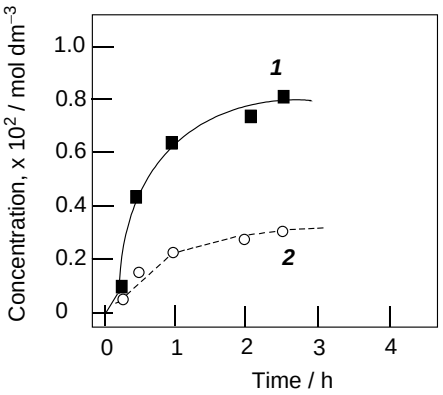

Figure 3.4.13. Accumulation of cyclohexanone (*1*) and cyclohexanol (*2*) in the oxidation reaction of cyclohexane (0.46 mol dm^{-3}) with paaH catalyzed by $VO(acac)_2$ in acetonitrile at 60 ºC. Conditions: [CyH] = 0.46 mol dm^{-3}; [catalyst] = 1×10^{-4} mol dm^{-3}; [paaH] = 0.30 mol dm^{-3}; 60°C; 10 ml total volume; 1 atm air.

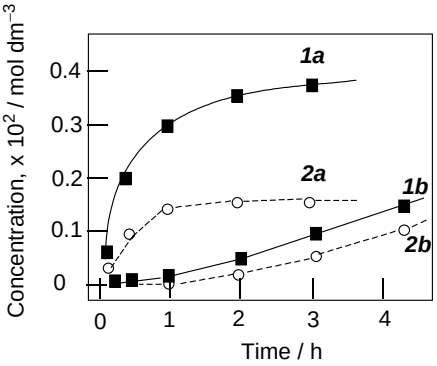

Figure 3.4.14. Accumulation of cyclohexanone (*1*) and cyclohexanol (*2*) in the oxidation reaction of cyclohexane (0.46 mol dm^{-3}) with paaH and air catalyzed by $[NBu_4][VO_2(pca)_2]$ (*1a* and *2a*) and by the tetraacid of anion **1** (*1b* and *2a*) in acetonitrile at 60 °C. Conditions: [CyH] = 0.46 mol dm^{-3}; [catalyst] = 1×10^{-4} mol dm^{-3}; [paaH] = 0.30 mol dm^{-3}; 60°C; 10 ml total volume; 1 atm air.

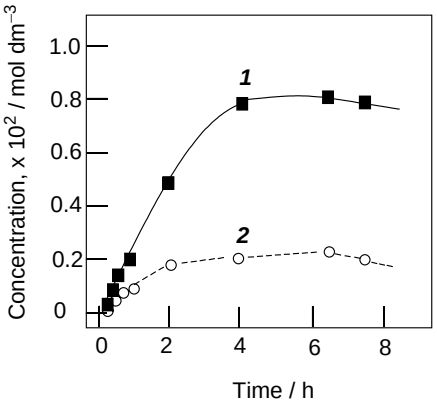

Figure 3.4.15. Accumulation of cyclohexanone (*1*) and cyclohexanol (*2*) in the oxidation reaction of cyclohexane (0.46 mol dm^{-3}) with paaH (0.30 mol dm^{-3}) in MeCN at 60 ºC catalyzed by the tetrabutylammonium salt of anion **8**. Conditions: [CyH] = 0.46 mol dm^{-3}; [catalyst] = 1×10^{-4} mol dm^{-3}; [paaH] = 0.30 mol dm^{-3}; 30°C; 10 ml total volume; 1 atm air.

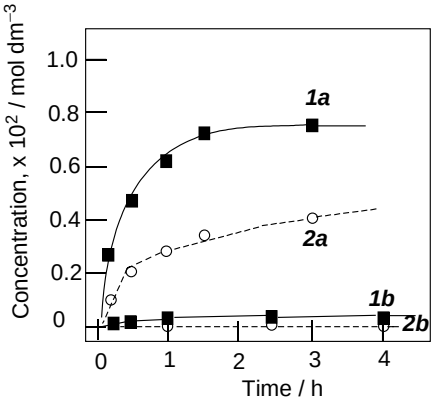

Figure 3.4.16. Accumulation of cyclohexanone (*1*) and cyclohexanol (*2*) in the reaction of cyclohexane (0.46 mol dm^{-3}) with paaH (0.30 mol dm^{-3}) in acetonitrile at 60 ºC catalyzed by **3** (*1a* and *2b*) and by **7** (*1b* and *2b*). Conditions: [CyH] = 0.46 mol dm^{-3}; [catalyst] = 1×10^{-4} mol dm^{-3}; [paaH] = 0.30 mol dm^{-3}; 60°C; 10 ml total volume; 1 atm air.

3.4.3 Oxidation of Higher Alkanes Catalyzed by NBu_4VO_3

We studied the regioselectivity of the alkane oxidation by the system NBu_4VO_3–paaH using as substrates higher alkanes as isooctane (2,2,4-trimethylpentane, *cf.* Scheme 3.6.2), *n*-hexane and 1,2-dimethylcyclohexane (*cf.* Scheme 3.4.1).

The selectivity parameters determined for the oxidations of these higher alkanes are close to those found for oxidations by the "H_2O_2–NBu_4VO_3–pcaH" reagent, which has been shown to operate *via* a radical mechanism [11, 162, 163].

Table 3.4.1. Selectivity parameters in alkane oxidations by various systems.

Substrate	System	Selectivity
n-hexane		C(1) : C(2) : C(3)
	VO_3^-–paaH in MeCN[a]	1 : 2.8 : 2.5
	VO_3^-–H_2O_2 in MeCN–$MeCO_2H$[b]	1 : 4.2 : 4.1
	VO_3^-–H_2O_2 in $MeCO_2H$[c]	1 : 5.8 : 4.8
	VO_3^-–pcaH–H_2O_2 in MeCN[d]	1 : 8 : 7
Isooctane		1° : 2° . 3°
	VO_3^-–paaH in MeCN	1 : 7 : 38
	VO_3^-–H_2O_2 in MeCN–$MeCO_2H$	1 : 3.8 : 7.3
	VO_3^-–H_2O_2 in $MeCO_2H$	1 : 1.4 : 5.2
	VO_3^-–pcaH–H_2O_2 in MeCN	1 : 4 : 9
Cis-1,2-dmch		*trans / cis*
	VO_3^-–paaH in MeCN	0.46
	VO_3^-–pcaH–H_2O_2 in MeCN	0.70
	H_2O_2–Mn_2^{IV}–$MeCO_2H$[e]	0.34
Trans-1,2-dmch		*trans / cis*
	VO_3^-–paaH in MeCN	1.2
	VO_3^-–pcaH–H_2O_2 in MeCN	0.8
	H_2O_2–Mn_2^{IV}–$MeCO_2H$	4.1

Common conditions for *a, b, c*: [*n*-hexane] = 0.34 mol dm^{-3}; [isooctane] = 0.30 mol dm^{-3}; [*cis*-1,2-dmch] = 0.39 mol dm^{-3}; [catalyst] = 1×10^{-4} mol dm^{-3}; 60°C; 6 hours; total volume 10 ml. [a] [paaH] = 0.30 mol dm^{-3}; [b] [H_2O_2] = 0.30 mol dm^{-3}; solvent: 19 : 1 MeCN–$MeCO_2H$ mixture. [c] [H_2O_2] = 0.30 mol dm^{-3}. [d] Refs: [11, 162, 163]. [e] Mn_2^{IV} is $[LMn^{IV}(O)_3Mn^{IV}L](PF_6)_2$, where L is 1,4,7-trimethyl-1,4,7-triazacyclononane [176, 200–203].

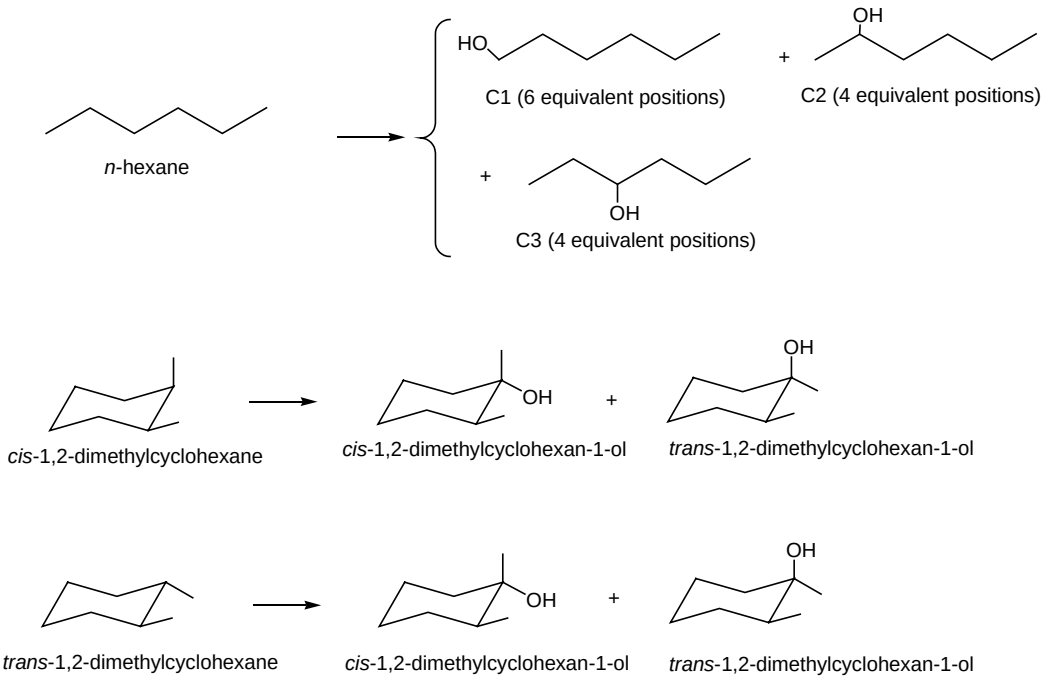

Scheme 3.4.1. Reaction products of the *n*-hexane, *cis*-1,2-dimethylcyclohexane and *trans*-1,2-dimethylcyclohexane oxidations with paaH and air catalyzed by NBu_4VO_3 after treatment with PPh_3.

3.4.4 Oxidation of Light Alkanes Catalyzed by NBu_4VO_3

Light alkanes (methane, ethane and propane) can be also oxidized by paaH, both in acetonitrile and acetic acid (Table 3.4.1). The propane oxidation in acetonitrile gives predominantly acetone with a total TON up to 165.

Table 3.4.2. Oxidation of light alkanes by peroxyacetic acid.

Alkane (P, bar)	**Solvent**	**Products (× 10^3, mol dm^{-3})**	**TON**
Methane (30)[a]	MeCN	Formaldehyde (0.1)	35
		Methanol (0.4)	
		Methyl acetate (3.0)	
	$MeCO_2H$	Formaldehyde (2.0)	21
		Methanol (0.17)	
Ethane (25)	MeCN	Acetaldehyde (2.3)	34
		Ethanol (1.0)	
		Ethyl acetate (0.43)	
	$MeCO_2H$	Acetaldehyde (1.0)	12
		Ethyl acetate (0.2)	
Propane (5)	MeCN	Acetone (10)	165
		Isopropanol (3)	
		Isopropyl acetate (3)	
		n-Propanol (0.5)	

Conditions: $[NBu_4VO_3] = 1 \times 10^{-4}$ mol dm^{-3}; [paaH] = 0.30 mol dm^{-3}; 60 °C; 10 ml total volume; 3 hours. [a]All products concentrations are given after substraction of corresponding concentrations obtained in blank (without methane) experiments.

3.4.5 Conclusions

The observed dependencies of the initial reaction rates upon the initial concentrations of cyclohexane and paaH (Figures 3.4.5–3.4.7, 3.4.10–3.4.12) are similar to those found previously for the cyclohexane oxidation by the "H_2O_2–NBu_4VO_3–pcaH" system [11, 162, 163] and by the "*tert*-BuOOH–NBu_4VO_3" system

[211]. The dependence type of the reaction rate upon the initial paaH concentration indicates that a complex between vanadium and peroxyacetic acid takes part in the generation of the $CH_3C(O)O\cdot$ species which induces the CyH oxidation (Scheme 3.4.2, Eqs. 1-3). This complex could be a cationic complex, "$[V^V–OOC(O)CH_3]^{4+}$" (Equation 1), but we cannot say anything definitive about its nature and for kinetic purposes we consider it as an "adduct", "V^V-$CH_3C(O)OOH$". In order to calculate the equilibrium constants for the formation of the complex in acetonitrile and acetic acid as solvents, Equation 1 was simplified to "V^V" + $CH_3C(O)OOH$ ⟶ "V^V-$CH_3C(O)OOH$", so, the equilibrium constants are not dimensionless as it could be concluded from Equation 1.

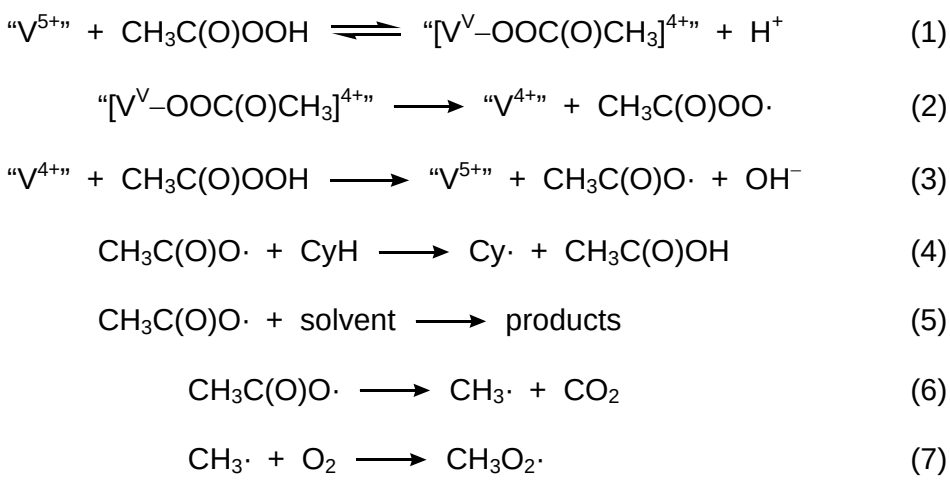

Scheme 3.4.2. Proposed mechanism for the cyclohexane oxidation with paaH and air catalyzed by NBu_4VO_3.

The dependence mode for the oxidation rate upon the cyclohexane concentration suggests a competition between the productive interaction of $CH_3C(O)O\cdot$ with cyclohexane to give the cyclohexyl radical (Scheme 3.4.2, Eq. 4)

and its non-productive decomposition to give the methylperoxyl radical (Scheme 3.4.2, Eqs. 5-7).

The analysis of the experimental data presented in Figures 3.4.6 and 3.4.11 using the kinetic scheme derived from Equations 1 to 3 (Scheme 3.4.2) allowed to determine the equilibrium constants for the formation of the "V^{V}-$CH_3C(O)OOH$" complex. They turned out to be equal to 3.3 and 6.8 $dm^3\ mol^{-1}$ for acetonitrile and acetic acid as solvents, respectively.

Using the kinetic scheme derived from Equations 4 to 7 and the experimental parameters given in Figures 3.4.7 and 3.4.12, we found that the ratio between the rate constant for the interaction of the $CH_3C(O)O\cdot$ radical with CyH and the first order constant rate for its decomposition is approximately 1 for the two solvents. This value is 5 times lower than the corresponding parameter calculated for the reaction between cyclohexane and hydroxyl radicals, suggesting that the oxidizing species in the NBu_4VO_3–paaH system, $CH_3C(O)O^{\cdot}$, is less reactive than the hydroxyl radical, and therefore, more selective. Finally, the dependence of the initial oxidation rate upon the vanadate concentration (Figs. 3.4.5 and 3.4.10) turned out to be more complex than for the systems studied previously [11,162,163,167]. This is possibly due to equilibrium between the vanadate anion and the different vanadium species that can exist in an acid medium (acetic acid).

3.5 Catalysis by Simple Iron Salts

Soluble iron salts play a very important role as initiators and catalysts in the oxidation of alkanes with hydrogen peroxide (*cf.* Section 2.1.2 and references therein).

In this Section we present our results on alkane oxidation with hydrogen peroxide in acetonitrile catalyzed by the following iron(III) salts: iron(III) perchlorate, $Fe(ClO_4)_3$; iron(III) chloride, $FeCl_3$; and iron(III) hydroxoacetate, $Fe(OAc)_2(OH)$.

3.5.1 Oxidation of Cyclohexane

First of all we studied the oxidation of cyclohexane with hydrogen peroxide and air in acetonitrile at room temperature catalyzed by the simplest iron(III) salt, *i.e.* iron(III) perchlorate, which does not contain any ligand strongly bound to iron. The accumulation of oxygenates (the sum of cyclohexyl hydroperoxide, cyclohexanol and cyclohexanone) with time in the cyclohexane oxidation catalyzed by $Fe(ClO_4)_3$ show that the catalyst efficiency is not high, and the turnover number (TON) attains only 10 after approximately 3 min (Figure 3.5.1, graph *A*). The rate dependence of the oxidation is of first order with respect to the initial hydrogen peroxide concentration (Fig. 3.5.1, graph *B*). We observed an oxygen evolution in the oxidation reaction of cyclohexane, indicating a "catalase activity" of $Fe(ClO_4)_3$, that is to say, the ability to decompose hydrogen peroxide to oxygen and water (cf. Section 3.6). The initial rate of this molecular oxygen evolution is proportional to the initial concentration of hydrogen peroxide.

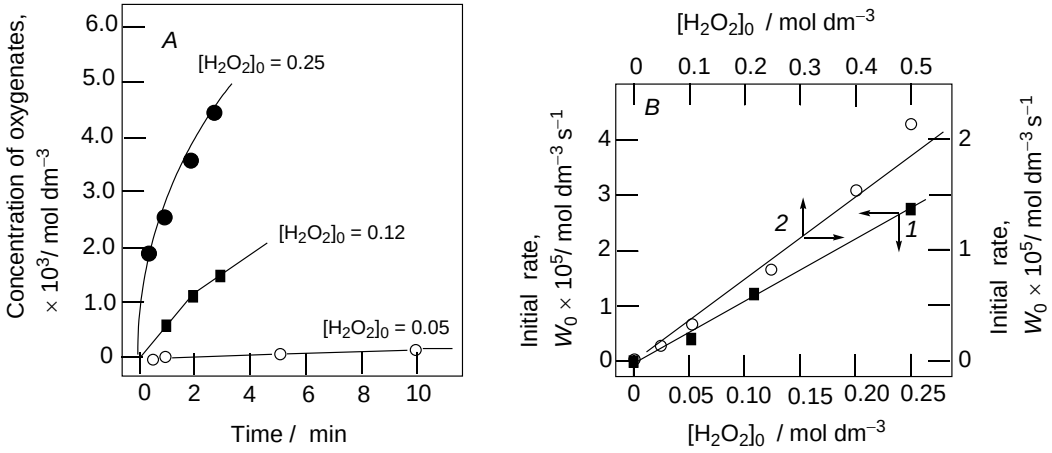

Figure 3.5.1. Graph *A*: accumulation of oxidation products with time at various initial concentrations of H_2O_2 (mol dm^{-3}) in the cyclohexane oxidation by H_2O_2 and air catalyzed by $Fe(ClO_4)_3$ in acetonitrile at 25 ºC. Graph *B*: initial rates of oxidation products accumulation measured from data of graph *A* (*1*) and O_2 evolution (*2*) *vs* initial concentration of H_2O_2. Conditions: [CyH] = 0.46 mol dm^{-3}; [catalyst] = 5×10^{-4} mol dm^{-3}; 25°C; 10 ml total volume; 1 atm air.

We studied the effect of adding pcaH on the oxidation reaction of cyclohexane, and we found that the initial cyclohexane oxidation rate decreases (Fig. 3.5.2). The dependence of the initial cyclohexane oxidation rate upon the initial cyclohexane concentration shows a plateau at $[cyclohexane]_0 > 0.4$ mol dm^{-3} (Fig. 3.5.3). This is in accordance with the assumption of a competition between cyclohexane and the solvent for the interaction with an active oxidizing species (*cf.* Section 3.5.4).

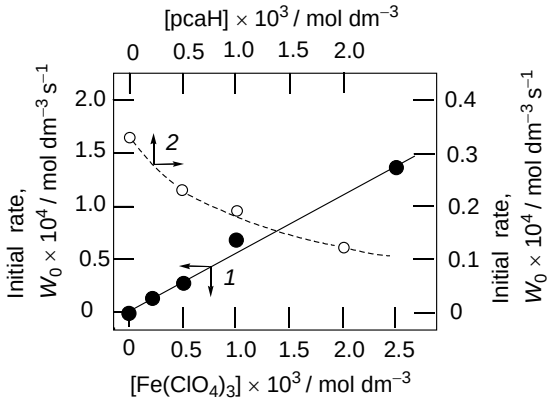

Figure 3.5.2. Initial rate of the oxidation products formed *vs* concentration of $Fe(ClO_4)_3$ (*1*) and *vs* concentration of added pcaH (*2*) in the cyclohexane oxidation with H_2O_2 and air catalyzed by $Fe(ClO_4)_3$ in acetonitrile at 25 ºC. Conditions: [CyH] = 0.46 mol dm^{-3}; [H_2O_2] = 0.25 mol dm^{-3}; for curve *2*, [catalyst] = 5×10^{-4} mol dm^{-3}.

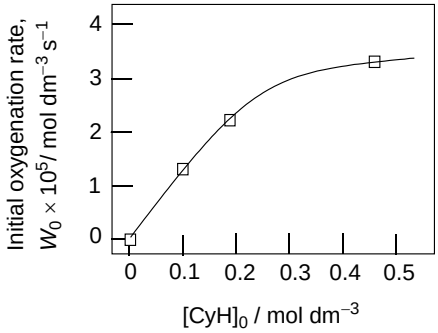

Figure 3.5.3. Initial rate of oxidation products formed *vs* initial concentration of cyclohexane in the oxidation of cyclohexane with hydrogen peroxide and air catalyzed by $Fe(ClO_4)_3$ in acetonitrile at 25 ºC. Conditions: [catalyst] = 5×10^{-4} mol dm^{-3}; [H_2O_2] = 0.25 mol dm^{-3}; 25°C; 10 ml total volume; 1 atm air.

It is noteworthy that lithium chloride (LiCl) added to the reaction solution accelerates both, hydroperoxide consumption and oxygen evolution (Fig.3.5.4). Another remarkable feature of this effect is a bell-shaped dependence of the initial oxidation rate and the initial oxygen evolution rate on the concentration of LiCl

added. It is reasonable to assume that, in the presence of LiCl in solution, iron(III) cations can coordinate the chloride anions to afford the same species that are present when the catalyst is $FeCl_3$, which is a more efficient catalyst, as shown below.

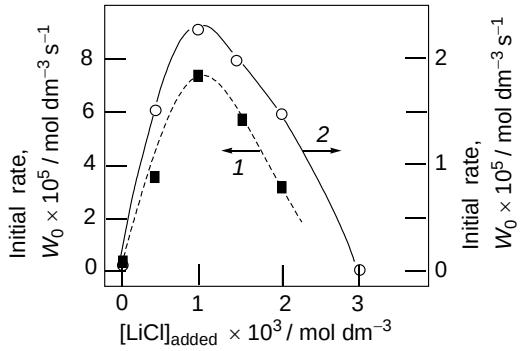

Figure 3.5.4. Initial rate of the hydrogen peroxide consumption (*1*) and O_2 evolution (*2*) *vs* initial concentration of added LiCl in the hydrogen peroxide decomposition catalyzed by $Fe(ClO_4)_3$ in acetonitrile at 25 ºC. Conditions: [catalyst] = 5×10^{-4} mol dm^{-3}; [H_2O_2] = 0.05 mol dm^{-3}; 25°C; 10 ml total volume; 1 atm air.

After $Fe(ClO_4)_3$ we studied $FeCl_3$ as a catalyst for the cyclohexane oxidation with hydrogen peroxide and air in acetonitrile. The rate dependence of the oxidation is of first order with respect to the $FeCl_3$ concentration at [$FeCl_3$] < 2×10^{-3} mol dm^{-3} (Fig. 3.5.5). In contrast to the situation found for $Fe(ClO_4)_3$, in the case of the $FeCl_3$–catalyzed reaction, the oxidation rate dependence is of first order for cyclohexane concentration, and a plateau is not observed (Fig. 3.5.6). The initial rate dependence is depicted with a bell-shape curves for oxygenate accumulation, hydrogen peroxide consumption and O_2 evolution upon the concentration of hydrogen peroxide (Fig. 3.5.7, graph B).

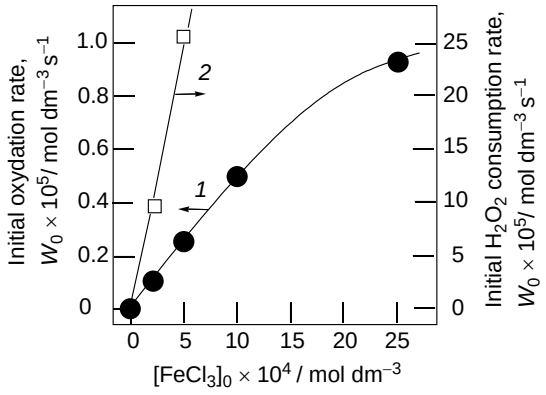

Figure 3.5.5. Initial rate of products formed (*1*) and initial rate on H_2O_2 consumption (*2*) *vs* initial catalyst concentration in the oxidation of cyclohexane with H_2O_2 and air catalyzed by $FeCl_3 \cdot 6\ H_2O$ in acetonitrile at 25 °C. Conditions: [CyH] = 0.46 mol dm^{-3}; [H_2O_2] = 0.05 mol dm^{-3}; 25°C; 10 ml total volume; 1 atm air.

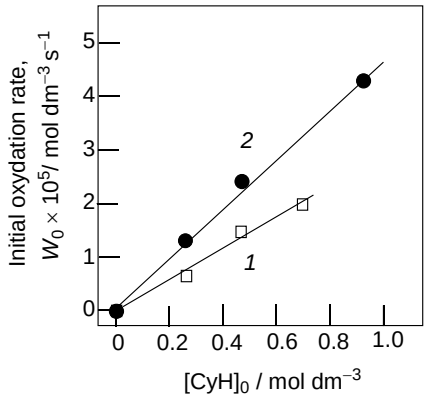

Figure 3.5.6. Initial rate of products formed *vs* initial concentration of cyclohexane in the cyclohexane oxidation with air and H_2O_2 catalyzed by $FeCl_3 \cdot 6\ H_2O$ in acetonitrile at 25 ºC. Conditions: [catalyst] = 5×10^{-4} mol dm^{-3}; [H_2O_2] = 0.02 mol dm^{-3} (*1*); [H_2O_2] = 0.05 mol dm^{-3} (*2*); 25°C; 10 ml total volume; 1 atm air.

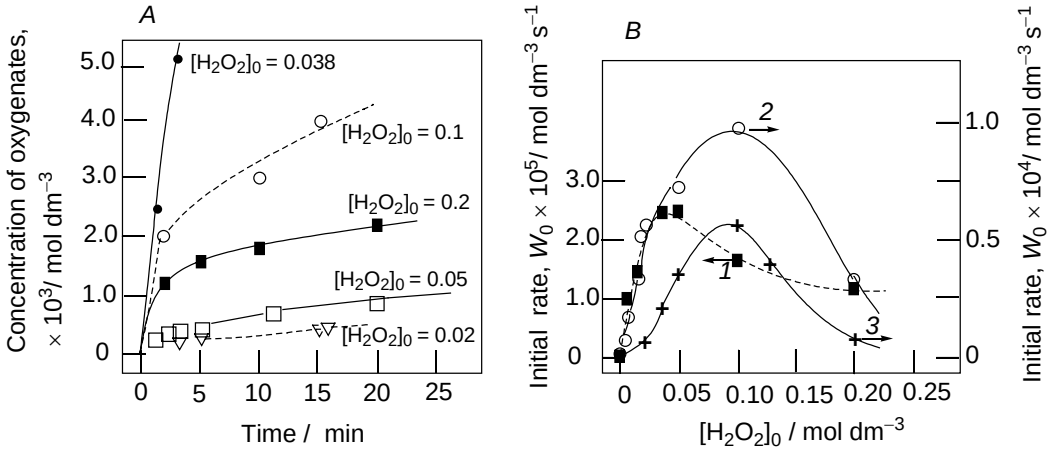

Figure 3.5.7. Graph *A*: Accumulation of products for the cyclohexane oxidation with H_2O_2 and air catalyzed by $FeCl_3 \cdot 6\ H_2O$ in acetonitrile at 25 °C at various hydrogen peroxide concentrations. Conditions: [CyH] = 0.23 mol dm^{-3}; [catalyst] = 5×10^{-4} mol dm^{-3}; 25°C; 10 ml total volume; 1 atm air. Graph *B*: Initial rates of: oxygenates formed (*1*), H_2O_2 consumption in the absence of cyclohexane (*2*) and O_2 evolution (*3*) *vs* initial concentration of H_2O_2 in the oxidation of cyclohexane with H_2O_2 and air catalyzed by $FeCl_3 \cdot 6\ H_2O$ in acetonitrile at 25 °C. Conditions: [CyH] = 0.23 mol dm^{-3}; [catalyst] = 5×10^{-4} mol dm^{-3}; 25°C; 10 ml total volume; 1 atm air.

The efficient activation energy for the cyclohexane oxidation catalyzed by $FeCl_3$ was estimated to be 14 kcal mol^{-1} (Fig. 3.5.8). As it could be predicted, the addition of lithium perchlorate, $LiClO_4$, to the reaction mixture decreases the initial reaction rate for the oxygen evolution only slightly (Fig. 3.5.9).

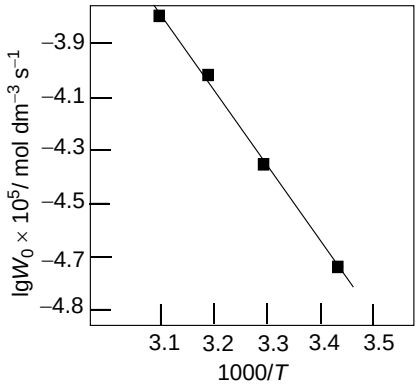

Figure 3.5.8. The Arrhenius plot for the cyclohexane oxidation by H_2O_2 and air catalyzed by $FeCl_3 \cdot 6\ H_2O$ in acetonitrile at 25 °C which corresponds to the activation energy E_a = 14 kcal mol^{-1}. Conditions: [CyH] = 0.23 mol dm^{-3}; [catalyst] = 5×10^{-4} mol dm^{-3}; [H $_2O_2$] = 0.02 mol dm^{-3}; 25°C; 10 ml total volume; 1 atm air.

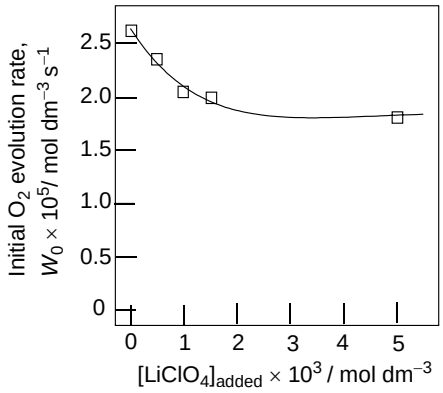

Figure 3.5.9. Initial rate of the O_2 evolution *vs* concentration of added $LiClO_4$ in the hydrogen peroxide decomposition catalyzed by $FeCl_3 \cdot 6\ H_2O$ in acetonitrile at 25 ºC. Conditions: [catalyst] = 5×10^{-4} mol dm^{-3}; [H_2O_2] = 0.05 mol dm^{-3}; 25°C; 10 ml total volume; 1 atm air.

As in the case of $FeCl_3$, the oxidation catalyzed by $Fe(ClO_4)_3$ is also depressed by addition of pcaH, and this effect is even more strongly pronounced (Fig. 3.5.10).

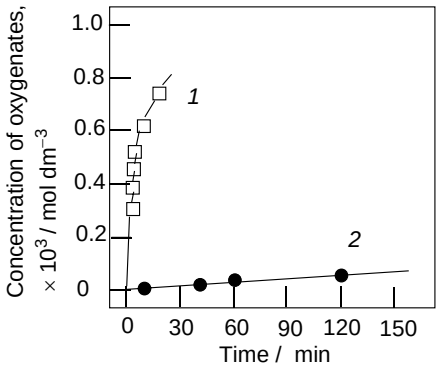

Figure 3.5.10. Accumulation of oxygenates formed in the cyclohexane oxidation with H_2O_2 and air catalyzed by $FeCl_3$ in acetonitrile at 25 ºC. in the absence (*1*) and in the presence of pcaH (*2*). Conditions: [CyH] = 0.23 mol dm^{-3}; [H_2O_2] = 0.05 mol dm^{-3}; [catalyst] = 5×10^{-4} mol dm^{-3}; [pcaH] = 5×10^{-4} mol dm^{-3}; 25°C; 10 ml total volume; 1 atm air.

We obtained some preliminary results for the catalysis by iron(III) acetate existing in the form of $Fe(OAc)_2(OH)$. Surprisingly, it turned out that $Fe(OAc)_2(OH)$ catalyzes the alkane oxidation only if pcaH is added as a co-catalyst (Fig. 3.5.11). The initial reaction rate and the final yield of products grow with increase of the pcaH concentration.

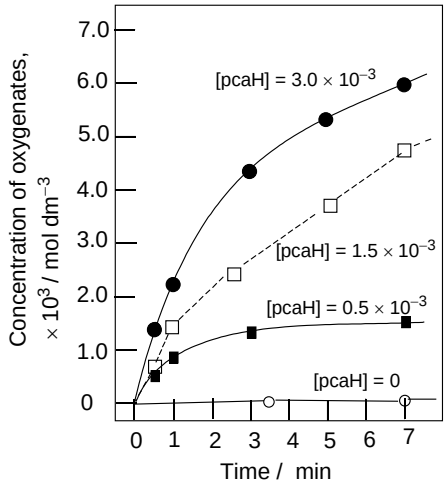

Figure 3.5.11. Accumulation of the products formed in the cyclohexane oxidation with H_2O_2 and air catalyzed by $Fe(OAc)_2(OH)$, at various concentrations of added pcaH, in acetonitrile at 25 ºC. Conditions: [CyH] = 0.46 mol dm^{-3}; [catalyst] = 5 × 10^{-4} mol dm^{-3}; [H_2O_2] = 0.1 mol dm^{-3}; 25°C; 10 ml total volume; 1 atm air.

3.5.2 Oxidation of Higher Alkanes and Benzene

We determined the regio-selectivity parameters for the oxidations of certain higher branched alkanes. In Table 3.5.1, the parameters are summarized for the oxidations catalyzed by the simple iron salts presented in this Section as well as, for comparison, by certain other systems for which the mechanism is clear. It can be concluded that the selectivity parameters for $Fe(ClO_4)_3$ and $Fe(OAc)_2(OH)$–pcaH are similar to those found previously for the systems operating with generation of free hydroxyl radicals (the "H_2O_2–VO_3^-–pcaH", "H_2O_2–hv" and "H_2O_2–$FeSO_4$" systems). The selectivity parameters for the oxidation of branched alkanes catalyzed by $FeCl_3$ are, however, higher, and therefore we cannot conclude that the oxidizing species are hydroxyl radicals.

Table 3.5.1. Selectivities of 3-methylhexane, methyl-cyclohexane, 2,2,4-trimethylpentane, *cis*- and *trans*-decalin oxidations by various systems in acetonitrile.

System	Hydrocarbon oxidized / selectivity parameter				
	3-methyl-hexane	2,2,4-trimethyl-pentane	Methyl-cyclohexane	*Cis*-decalin	*Trans*-decalin
	1°:2°:3°	1°:2°:3°	1°:2°:3°	*t:c*	*t:c*
$Fe(ClO_4)_3$–O_2–H_2O_2	1:4:30	1:5:13	1:7:43		
$FeCl_3$–O_2–H_2O_2		1:7:57		1	1
$Fe(OAc)_2(OH)$–pcaH–O_2–H_2O_2		1:5:13		3	4.5
$FeSO_4$–O_2–H_2O_2 [a]		1:3:6		3.5	9
O_2–H_2O_2–hv [a]	1:4:12	1:2:6		1.3	2.7
H_2O_2–VO_3^-–pcaH [a]	1:5.7:22	1:4:9	1:6:18	2.1	2.4
H_2O_2–Mn(IV)–CH_3COOH [b]	1:22:200	1:5:55	1:26:200	0.12	33

Conditions for $Fe(ClO_4)_3$–O_2–H_2O_2, $FeCl_3$–O_2–H_2O_2, $Fe(OAc)_2(OH)$–pcaH–O_2–H_2O_2: [3-methylhexane] = 0.34 mol dm^{-3}; [2,4,4-trimethylpentane] = 0.30 mol dm^{-3}; [methylcyclohexane] = 0.39 mol dm^{-3}; [*cis*-decalin] = [*trans*-decalin] = 0.31 mol dm^{-3} [H_2O_2] = 0.4 mol dm^{-3}; [catalyst] = 5×10^{-3} mol dm^{-3}; [pcaH] = 5×10^{-4} mol dm^{-3}; 25°C; 6 hours; total volume 10 ml. Products concentration measured after treatment with PPh_3. [a] Refs. [11, 48, 137, 146, 147, 151, 163, 176]. [b] Refs. [176, 200–203].

The oxidation of benzene was studied using $FeCl_3$ as catalyst. The major product was phenol, and the initial rate of its accumulation upon the initial benzene concentration showed a plateau at $[C_6H_6] > 0.3$ mol dm^{-3} (Fig. 3.5.12).

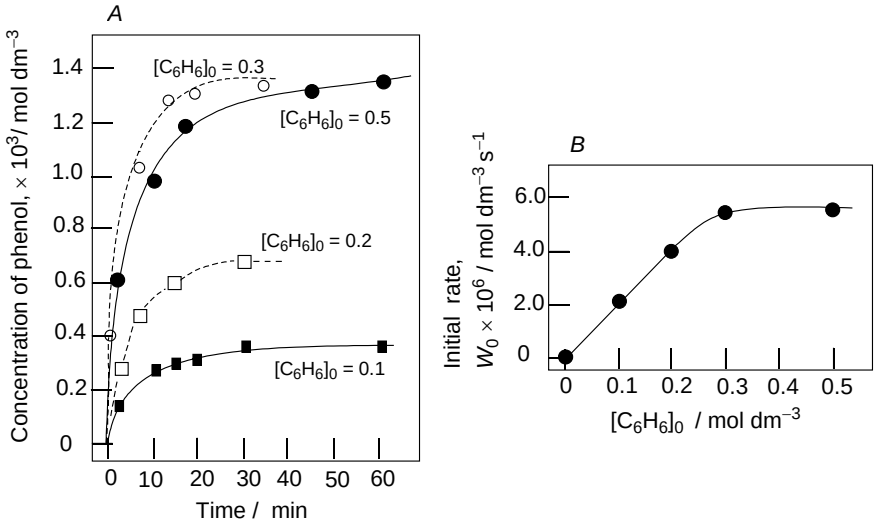

Figure 3.5.12. Accumulation of phenol (graph A) from the oxidation of different benzene concentrations with hydrogen peroxide and air catalyzed by $FeCl_3$ in acetonitrile and initial rate of phenol accumulation *vs* initial benzene concentration (graph B). Conditions: $[H_2O_2]$ = 0.04 mol dm^{-3}; [catalyst] = 5 × 10^{-4} mol dm^{-3}; 25°C; 10 ml total volume; 1 atm air.

3.5.3 Oxidation of Light Alkanes

The data on methane and ethane oxidation with hydrogen peroxide catalyzed by $Fe(ClO_4)_3$ and $Fe(OAc)_2(OH)$ are summarized in Tables 3.5.2 and 3.5.3. The highest TON, 68, is obtained for the oxidation of ethane catalyzed by $Fe(ClO_4)_3$.

Table 3.5.2. Oxidation products of methane with hydrogen peroxide and air catalyzed by $Fe(ClO_4)_3$ and $Fe(OAc)_2(OH)$–pcaH in acetonitrile.

Catalyst (mol dm^{-3})	**Time, h**	**Products, × 10^3 mol dm^{-3}**			**TON**
		CH_3OOH	CH_3OH	HCHO	
$Fe(ClO_4)_3$ (1×10^{-3})	1	5.6	2.3	2.2	
	3[a]	3.5	2.4	2.4	7
$Fe(OAc)_2(OH)$ (1×10^{-3})–pcaH (5×10^{-3})	2	0.0	9.6	1.0	
	4	0.0	19.3	1.1	
	6	0.0	24.0	4.2	
	7	0.0	25.0	5.6	31
$Fe(OAc)_2(OH)$ (1×10^{-4})–pcaH (3.5×10^{-4})	6[a]	8.0	0.0	2.5	10

Conditions: methane pressure = 90 bar; air pressure = 1 bar; $[H_2O_2]$ = 0.6 mol dm^{-3}; 25 °C; 10 ml total volume. [a] In the absence of methane, formaldehyde (formed from acetonitrile) was detected (1.3 mol dm^{-3}).

Table 3.5.3. Oxidation products of ethane with hydrogen peroxide and air catalyzed by $Fe(ClO_4)_3$ and $Fe(OAc)_2(OH)$–pcaH in acetonitrile.

Catalyst (mol dm^{-3})	**Time, h**	**Products, × 10^3 mol dm^{-3}**			**TON**
		CH_3CH_2OOH	CH_3CH_2OH	CH_3CHO	
$Fe(ClO_4)_3$ (5×10^{-4})	3	30.0	1.0	3.2	68
$Fe(OAc)_2(OH)$ (1×10^{-3})–pcaH (5×10^{-3})	2[a]	0.4	7.8	3.3	12
$Fe(OAc)_2(OH)$ (1×10^{-4})–pcaH (3.5×10^{-4})	4	2.5	4.0	1.8	8

Conditions: ethane pressure = 27 bar; air pressure = 1 bar; $[H_2O_2]$ = 0.6 mol dm^{-3}; 25 °C; 10 ml total volume. [a] In the absence of ethane, acetaldehyde and ethanol were not detected after 3 hours.

The oxidation of methane by $FeCl_3$ gave methyl hydroperoxide as main product and a small amount of formaldehyde (Fig. 3.5.13). Propane and isobutane can also be oxidized by $FeCl_3$ to afford mainly the corresponding alkyl hydroperoxides (Table 3.5.4).

Table 3.5.4. Oxidation products of propane and isobutane with hydrogen peroxide and air catalyzed by $Fe(ClO_4)_3$ and $Fe(OAc)_2(OH)$–pcaH in acetonitrile.

Alkane	**Products, (× 10^3 mol dm^{-3})**	**TON**
Propane	$CH_3CH(OOH)CH_3$ (5.5), CH_3CH_2CHO (1.0), $CH_3CH_2CH_2OOH$ (1.4), CH_3COCH_3 (1.1), $CH_3CH_2CO_2H$ (0.3)	17
Isobutane	$(CH_3)_3COOH$ (0.24), $(CH_3)_3COH$ (5.0), $(CH_3)_2CCHO$ (5.0), $(CH_3)_2CCO_2H$ (0.25)	21

Conditions: propane pressure = 7 bar; isobutene pressure = 5 bar; air pressure = 1 bar; [catalyst] = 5×10^{-4} mol dm^{-3}; $[H_2O_2] = 0.05$ mol dm^{-3}; 25 °C; 1 hour; 10 ml total volume.

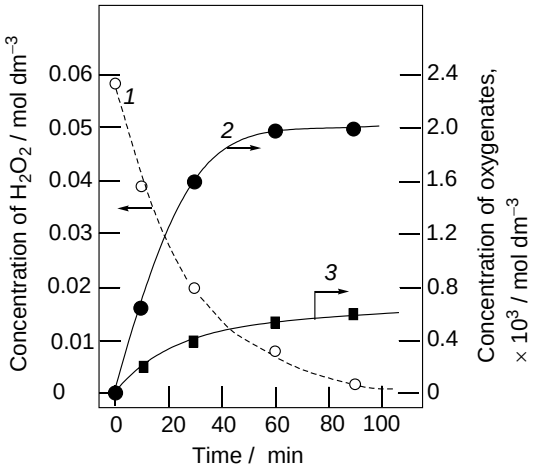

Figure 3.5.13. Hydrogen peroxide consumption (*1*), accumulation of methyl hydroperoxide (*2*) and formaldehyde (*3*) in the oxidation of methane by H_2O_2 and air catalyzed by $FeCl_3 \cdot 6\ H_2O$ in acetonitrile at 40 ºC. Conditions: Methane pressure = 55 bar; [catalyst] = 5×10^{-4} mol dm^{-3}; [H_2O_2] = 0.06 mol dm^{-3}; 40°C; 10 ml total volume; 1 atm air.

3.5.4 Comparison of $FeCl_3$ and $Fe(ClO_4)_3$ as Catalysts

It has been shown that neither hydrogen peroxide alone nor iron salts alone induce the alkane oxidation under mild conditions, and also that saturated hydrocarbons are not known to form strong complexes with iron ions. Therefore the observed alkane oxidation induced by the iron-catalyzed hydrogen peroxide decomposition is due to the oxidizing action of an intermediate species generated in the course of H_2O_2 decomposition. In accordance with modern knowledge about iron-induced hydrogen peroxide decomposition, the most probable oxidizing species is the hydroxyl radical generated by the Fe^{2+} cation (formed from Fe^{3+}) after the interaction with hydrogen peroxide (Fenton's mechanism, *cf.* Scheme 2.1.6). The radical HO· can react both with the alkane, RH, and with the solvent, CH_3CN, *via* routes (1) and (2):

$$HO\cdot + RH \xrightarrow{k_1} R\cdot + H_2O \qquad (1)$$

$$HO\cdot + CH_3CN \xrightarrow{k_2} \text{products} \qquad (2)$$

The observed alkane oxidation rate should depend on the RH concentration as depicted by the equation 3.5.1:

$$-\frac{\mathrm{d}[\mathrm{RH}]}{\mathrm{d}t}=\frac{\mathrm{d}[\mathrm{ROOH}]}{\mathrm{d}t}=\frac{W_\mathrm{i}}{1+\dfrac{k_2[\mathrm{CH_3CN}]}{k_1[\mathrm{RH}]}}$$

Equation 3.5.1. Kinetic expression for the reaction rate of the alkane oxidation in acetonitrile.

W_i is the rate of the hydroxyl radical generation in this system. The alkane oxidation rate approaches W_i when $[RH]_0$ grows. It follows from equation 3.5.1 that a twofold decrease of the oxidation rate in comparison with the maximum possible rate can exist at the alkane concentration determined from the condition $\frac{k_2[\mathrm{CH_3CN}]}{k_1[\mathrm{RH}]}=1$, independently of the rate and mechanism of hydroxyl radical formation.

We have demonstrated in our kinetic experiments that the dependence modes of the ROOH formation rate upon the cyclohexane concentration are different for $Fe(ClO_4)_3$ and for $FeCl_3$ as catalysts (compare Fig. 3.5.3 and Fig. 3.5.6). We found a curve with a plateau in the first case, whereas a linear dependence can be noticed for the second catalyst in the same concentration interval. This difference means that the ratios between the rate constants for the CH_3CN and RH oxidations are different for each catalyst and, consequently, that oxidizing species are different for the two catalysts. The rate constant ratio found for $Fe(ClO_4)_3$ is close to that calculated on the

basis of radiation-chemical measurements [11]. The rate constant ratio is noticeably higher for $FeCl_3$.

Selectivity parameters obtained in the oxidation of branched alkanes (*cf.* Table 3.5.1) also support the conclusion about different active species operating in the studied systems. The selectivity obtained in the oxidation catalyzed by $Fe(ClO_4)_3$ is close to that determined in oxidations induced by hydroxyl radicals. The corresponding parameters for $FeCl_3$-catalyzed oxidations are higher.

We have also found striking differences in selectivity of the dec-1-ene oxidation by the two systems. The data obtained are summarized in Table 3.5.5. It can be clearly seen that, if $Fe(ClO_4)_3$ is used as a catalyst, the main product of the dec-1-ene oxidation is (after reduction of the reaction mixture with PPh_3) the allylic alcohol, which is formed by the hydroperoxidation of allylic C–H bonds. By contrast, when the catalyst is $FeCl_3$, the predominant product is the epoxide.

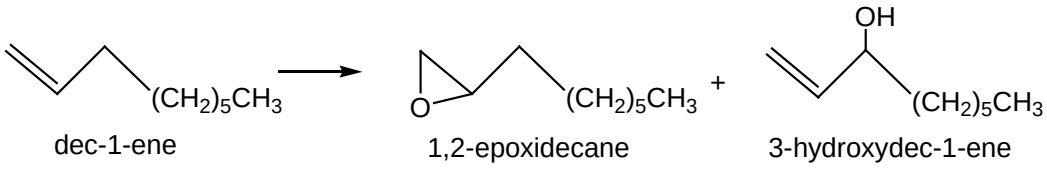

dec-1-ene 1,2-epoxidecane 3-hydroxydec-1-ene

Scheme 3.5.1. The products from the oxidation of dec-1-ene with hydrogen peroxide and air catalyzed by $Fe(ClO_4)_3$ and $FeCl_3$ after treatment with PPh_3.

Table 3.5.5. Oxidation products of dec-1-ene with hydrogen peroxide and air catalyzed by $Fe(ClO_4)_3$ and $FeCl_3$ in acetonitrile.

Catalyst, × mol dm^{-3}	**Time, min**	**Products, × 10^3 mol dm^{-3}**		
		1,2-epoxydecane	3-hydroxydec-1-ene	Epoxide:alcohol ratio
$Fe(ClO_4)_3$	0.5	0.13	0.33	0.39
	1	0.20	0.70	0.29
$FeCl_3$	0.5	1.04	0.22	4.72
	1	2.10	0.40	5.25

Conditions: [catalyst] = 5 × 10^{-4} mol dm^{-3}; [dec-1-ene] = 0.4 mol dm^{-3}; [H_2O_2] = 0.25 mol dm^{-3} for $Fe(ClO_4)_3$ and 0.05 mol dm^{-3} for $FeCl_3$; 25 °C; 10 ml total volume. Products concentration measured after treatment with PPh_3.

For the two systems based on $Fe(ClO_4)_3$ and $FeCl_3$, the modes of dependence of the initial rate on the initial hydrogen peroxide concentration are different (compare Fig. 3.5.1, graph B, curve *1* and Fig. 3.5.7, graph B, curve *1*). We assume that this situation is the result of a competition between the chloride anion, hydrogen peroxide and water for coordinating the iron(III). Changes in hydrogen peroxide concentration lead simultaneously to the corresponding changes in water concentration because we use 35% aqueous solution of H_2O_2.

The data obtained suggest that, in the case of $Fe(ClO_4)_3$, the properties of the oxidizing species are close to those of hydroxyl radicals. In these experiments the chloride anion was absent, and the concentrations of hydrogen peroxide and water

were 0.25 and 1.0 mol dm^{-3}, respectively. When $FeCl_3$ was used as catalyst, the concentrations of hydrogen peroxide and water were 0.05 and 0.2 mol dm^{-3}, respectively, and the experimental data showed that the oxidation was induced by a less reactive, consequently, more selective species. One can assume that this species is an iron(IV) species. Both oxidizing species, the hydroxyl radical and the iron (IV) species, that we can schematize as $Fe^{IV}O(L)_i$, (where L are various ligands, for example, Cl^-, H_2O_2, H_2O, i being the number of these ligands) are formed from the interaction of Fe^{2+} with hydrogen peroxide *via* two different mechanisms (Scheme 3.5.2).

$$[Fe(L)_i]^{2+} + H_2O_2 \rightleftharpoons [FeO(L)_i]^{2+} + H_2O \qquad (3.5.2\ a)$$

$$[Fe(L)_i]^{2+} + H_2O_2 \rightleftharpoons [Fe(L)_i]^{3+} + OH^- + OH\cdot \qquad (3.5.2\ b)$$

Scheme 3.5.2. The two possible oxidizing species formed from the interaction of an iron catalyst with hydrogen peroxide.

It is probable that the ratio between the two-electron channel (Scheme 3.5.2, Eq. 3.5.2 a) and the one-electron channel (Scheme 3.5.2, Eq. 3.5.2 b) for the oxidation of the complex $[Fe(L)_i]^{2+}$ with H_2O_2 depends on the coordination sphere of iron(III). Given these two possibilities, the fewer water ligands are present in the coordination sphere of the iron complex, the higher will be the yield of the oxo species $[FeO(L_i)]^{2+}$. This is confirmed by our experimental data. In the reaction with perchlorate salt containing water, the one-electron channel is the predominant route.

3.6 Catalysis by Iron(III) Complexes Containing *N*- and *N,O*-Chelating Ligands

Oxygen-activating proteins and especially enzymes containing non-heme diiron sites such as methane monooxygenase (*cf.* Section 2.2) and oxygen-transporting proteins as hemerythrin have attracted considerable interest over the last decades [166–180, 8a–c, 79, 137].

Hemerythrin is a non-heme enzyme which transports oxygen in a variety of marine invertebrates (spiculindians) in the same way as haemoglobin does in mammalians. In its inactive form (deoxyhemerythrin), the μ-hydroxo diiron(II) core is bonded to the protein by five histidines, one asparagine and one glutamine residues. In the active form (oxyhemerythrin) the dinuclear iron core is oxidized to iron(III) by bonding to dioxygen [164, 165] (Figure 3.6.1).

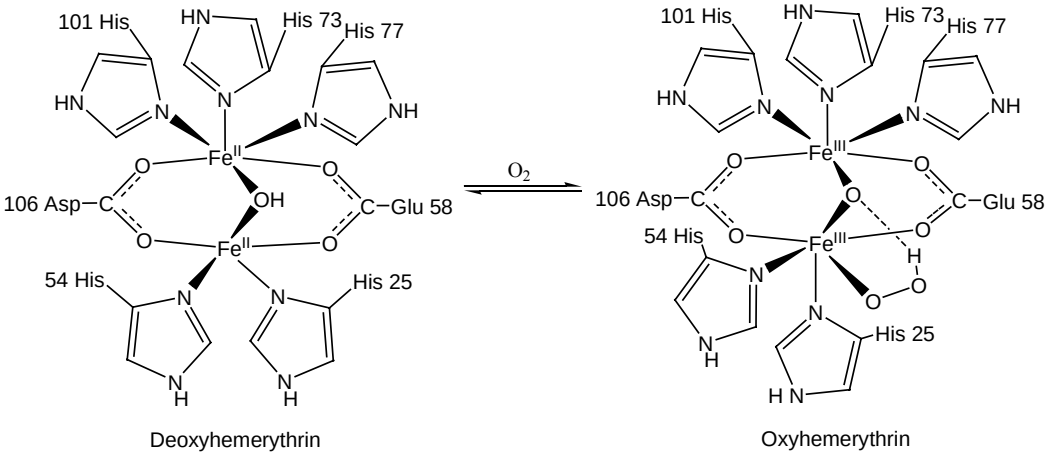

Figure 3.6.1. The two forms of hemerythrin.

Various dinuclear iron complexes have been synthesized as structural models of diiron non-heme enzymes, and their properties have been studied. In some cases, the activity of such complexes as catalysts for the oxidation of saturated and aromatic hydrocarbons was reported [26, 49, 137, 176, 181-190]. Usually polydentate nitrogen-containing ligands were used in these complexes, and either molecular oxygen or hydrogen peroxide was employed as oxidants. The efficiency of these systems was rarely high, the turnover numbers varying between 2 and 30.

In this subchapter we report on the catalytic alkane oxidation activity of two diiron(III) complexes, one containing a *N,O*-chelating ligand and another containing a *N*-chelating ligand that can be considered as models of non-heme diiron-containing enzymes [191,192].

3.6.1 Alkane Oxidations Catalyzed by $[Fe_2(hptb)(\mu\text{-}OH)(NO_3)_2]^{2+}$ (9)

The known cationic diiron(III) complex (**9**) (Figure 3.6.2) was used in the form of its nitrate salt, [**9**] $(NO_3)_2 \cdot CH_3OH \cdot 2\ H_2O$ [193-199].

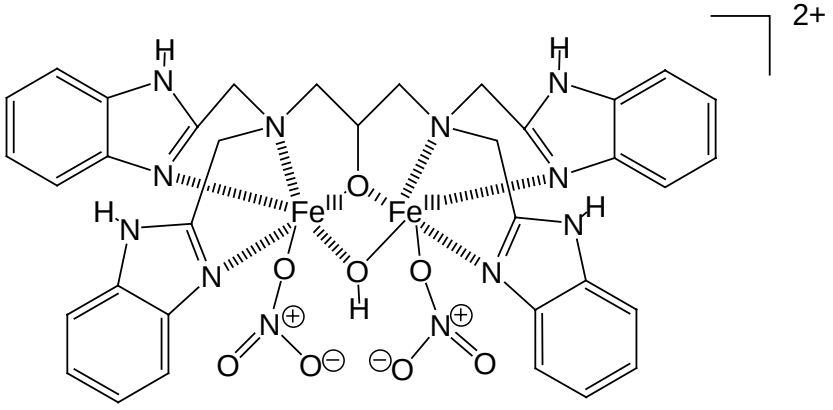

Figure 3.6.2. Cation **9**.

3.6.1.1 Oxidation of Cyclohexane

The nitrate salt of cation **9** was tested as a catalyst for the oxidation of cyclohexane with H_2O_2 in acetonitrile at room temperature.

$$C_6H_{12} + H_2O_2 + \tfrac{1}{2}\,O_2 \longrightarrow C_6H_{11}OOH + H_2O$$

$$2\,C_6H_{11}OOH \longrightarrow C_6H_{11}OH + C_6H_{10}O$$

Scheme 3.6.1. Reaction products of the oxidation of cyclohexane with H_2O_2 and air catalyzed by [**9**] $(NO_3)_2 \cdot CH_3OH \cdot 2\,H_2O$.

Complex **9** is not efficient as a catalyst when used alone in a relatively low concentration (4×10^{-4} mol dm^{-3}), however, when pyrazine-2-carboxylic acid (pcaH) or pyrazine-2,3-dicarboxylic acid (2,3-pdcaH_2) is used as co-catalyst in a 25 : 1 ratio, efficient cyclohexane oxidation is observed. With pcaH as co-catalyst, the total concentration of products attains 0.056 mol dm^{-3} after 8 hours, which corresponds to a TON of 140. The efficiency of 2,3-pdcaH_2 as co-catalyst is somewhat lower under the same conditions. Other aminoacids tested as co-catalysts are picolinic acid (picH) and pyridine-2,6-dicarboxylic acid (2,6-pycaH_2). Both proved to be inactive even in a ratio 1 : 100. In all cases, cyclohexyl hydroperoxide is the main product (90 %) in the oxidation of cyclohexane (Figure 3.6.3).

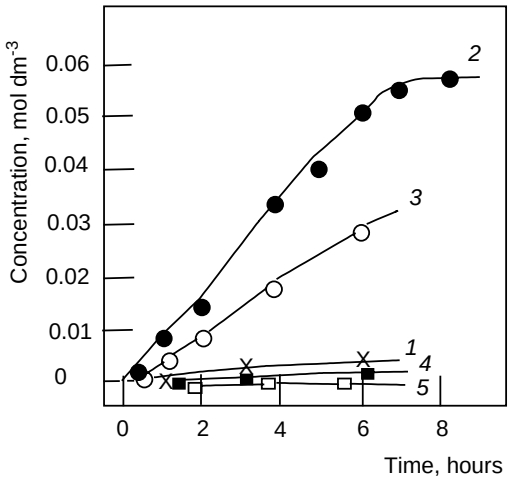

Figure 3.6.3. Sum of all products from the reaction of cyclohexane with hydrogen peroxide in acetonitrile at 25°C catalyzed by **9** in the absence of co-catalyst (1), and in the presence of pcaH (2), 2,3-pdcaH$_2$ (3), picH (4) and 2.6-pycaH$_2$ (5). Conditions: [cyclohexane] = 0.46 mol dm^{-3}; [H_2O_2] = 0.625 mol dm^{-3}; [catalyst] = 4 × 10^{-4} mol dm^{-3}; [co-catalyst] = 0.01 mol dm^{-3}; 25°C; 10 ml total volume; 1 atm air.

Complex **9** also shows a catalase activity, that is to say, the ability to catalyze the hydrogen peroxide decomposition to give molecular oxygen and water, like catalases enzymes do [204].

$$H_2O_2 \longrightarrow \tfrac{1}{2}\, O_2 + H_2O$$

Equation 3.6.1. The decomposition of hydrogen peroxide in molecular oxygen and water (catalase activity).

This catalase activity is measured in terms of the concentration of oxygen evolved with time in the cyclohexane oxidation catalyzed by **9** in the presence and in

the absence of pcaH as co-catalyst. The oxygen evolution is negligible in the absence of pcaH, but it is intensive in the initial period of the reaction when pcaH is present. This suggests that the first catalytically active species formed from **9** and hydrogen peroxide and pcaH is active in the decomposition of hydrogen peroxide, and that then this species is transformed into other species which oxygenates cyclohexane better than it decomposes hydrogen peroxide into oxygen and water.

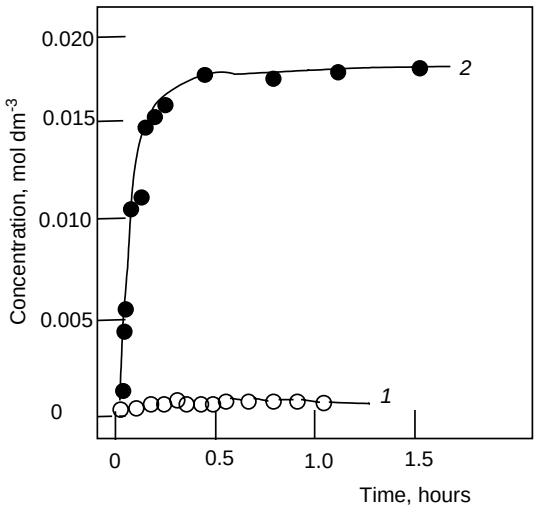

Figure 3.6.4. Oxygen evolution in the oxidation of cyclohexane with hydrogen peroxide and air in acetonitrile catalyzed by **9** without co-catalyst (1) and with pcaH (2). Conditions: [cyclohexane] = 0.46 mol dm^{-3}; [H_2O_2] = 0.625 mol dm^{-3}; [catalyst] = 4×10^{-4} mol dm^{-3}; [pcaH] = 0.01 mol dm^{-3}; 25°C; 10 ml total volume; 1 atm air.

The reaction requires a high concentration of pcaH as co-catalyst, the use of picH (same concentration) does not affect the yield of the reaction. Therefore, it was interesting to study the dependence of the initial reaction rate (W) on the concentration of the co-catalyst used, for both pcaH and picH. The reaction rate is calculated as the slope of the curve obtained from the representation of the total

concentration of products detected after reduction with PPh_3 versus time in the first minutes of the reaction. We found that the dependence of the reaction rate on the pcaH concentration has an S-like shape and the maximum *W* is attained starting from a pcaH concentration of 0.01 mol dm^{-3}. Surprisingly, we found that picH also accelerates the cyclohexane oxygenation, but in this case the co-catalyst should be used in much smaller concentration. Indeed, the curve for the *W* as a function of picH concentration has a maximum at approximately 4×10^{-4} mol dm^{-3}. At relatively high concentrations of picH no oxygenation occurs (*cf.* Figure 3.6.2).

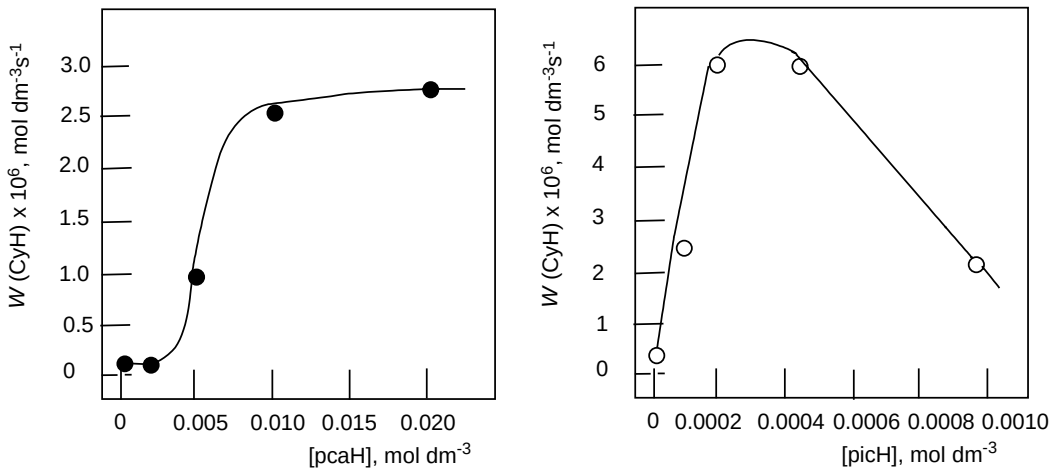

Figure 3.6.5. Reaction rate *vs* concentration of pcaH and picH added in the oxidation reaction of cyclohexane with hydrogen peroxide and air in acetonitrile catalyzed by **9**. Conditions: [cyclohexane] = 0.46 mol dm^{-3}; [H_2O_2] = 0.625 mol dm^{-3}; [catalyst] = 4×10^{-4} mol dm^{-3}; [pcaH] = 0.01 mol dm^{-3}; 25°C; 10 ml total volume; 1 atm air.

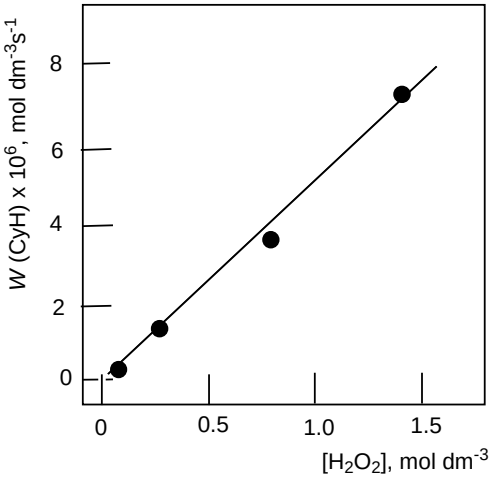

Figure 3.6.6. Reaction rate *vs* initial concentration of H_2O_2 in the oxidation reaction of cyclohexane with H_2O_2 and air in acetonitrile catalyzed by **9.** Conditions: [cyclohexane] = 0.46 mol dm^{-3}; [catalyst] = 4×10^{-4} mol dm^{-3}; [pcaH] = 0.01 mol dm^{-3}; 25°C; 10 ml total volume; 1 atm air.

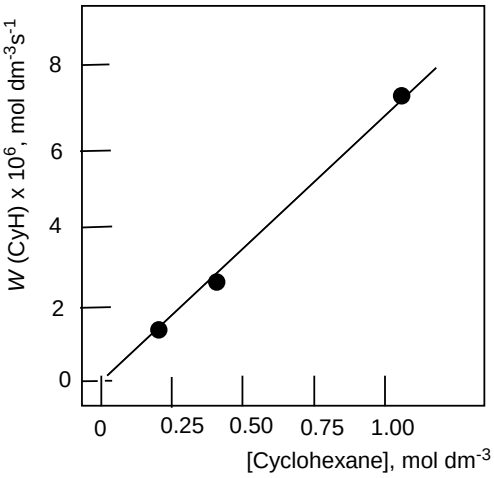

Figure 3.6.7. Reaction rate *vs* initial concentration of cyclohexane in the oxidation reaction of cyclohexane with H_2O_2 and air in acetonitrile catalyzed by **9.** Conditions: [H_2O_2] = 0.625 mol dm^{-3}; [catalyst] = 4×10^{-4} mol dm^{-3}; [pcaH] = 0.01 mol dm^{-3}; 25°C; 10 ml total volume; 1 atm air.

We studied also the dependence of *W* upon the concentration of hydrogen peroxide added and upon the concentration of cyclohexane used as substrate. In conclusion, the cyclohexane oxydation reaction catalyzed by **9** is of a first order with respect to both hydrogen peroxide and alkane concentration since the initial rate of the reaction is proportional to $[H_2O_2]_0$ and to $[\text{cyclohexane}]_0$.

3.6.1.2 Oxidation of Higher Alkanes

In order to get a mechanistic understanding of the reaction with saturated hydrocarbons catalyzed by **9** and pcaH, we also studied the oxidation of higher branched and cyclic alkanes with hydrogen peroxide and air. We used *n*-heptane, 3-methylhexane, 2,2,4-trimethylpentane (isooctane), methylcyclohexane and toluene in order to study the regioselectivity and bon selectivity of the oxidation (Scheme 3.6.2). The reaction was stopped after six hours, and the samples were analyzed by GC after reduction with PPh_3 (reducing the alkyl hydroperoxides, the major products, to the corresponding alcohols). The stereoselectivity of the oxidation was also studied, using the *cis*-and *trans*- isomers of decalin as substrates from which the *trans*/*cis* ratio was calculated (*cf.* Section 3.1). All results are shown in Table 3.6.1 and compared with those from other systems.

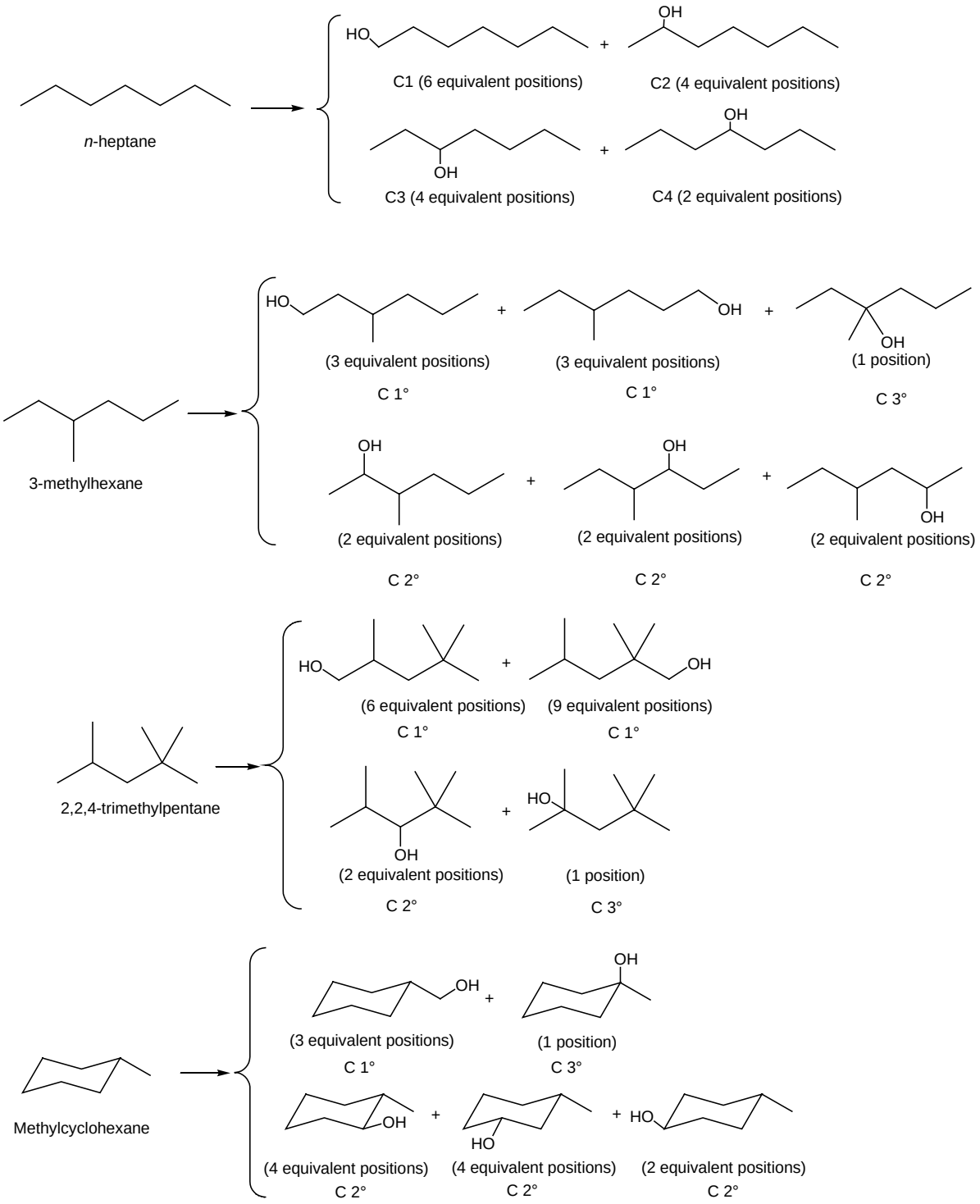

Scheme 3.6.2. Reaction products of the *n*-heptane, 3-methylhexane, 2,2,4-trimethylpentane and methylcyclohexane oxidations with H_2O_2 and air catalyzed by cation **9** after treatment with PPh_3.

Table 3.6.1. Selectivities of *n*-heptane, 3-methylhexane, 2,2,4-trimethylpentane, methyl-cyclohexane oxidations by various systems in acetonitrile.

System	**Hydrocarbon oxidized / selectivity parameter**			
	n-heptane	3-methyl-hexane	2,2,4-trimethyl-pentane	Methyl-cyclohexane
	1:2:3:4	1°:2°:3°	1°:2°:3°	1°:2°:3°
H_2O_2–**9**–pcaH	1:5.6:5.9:4.9	1:5.0:14	1:3.5:7.8	1:5.9:13
O_2–H_2O_2–hv [a]	1:7:6:7	1:4:12	1:2:6	
O_2–H_2O_2–$FeSO_4$ [a]	1:5:5:4.5		1:3:6	
H_2O_2–VO_3^-–pcaH [a]	1:6.2:6.3:5.3	1:5.7:22	1:4:9	1:6:18
H_2O_2–$Fe(ClO_4)_3$ [a]		1:4:30	1:5:45	1:7:43
H_2O_2–$Fe(ClO_4)_3$–pcaH [a]		1:5:45	1:5:45	1:8:30
H_2O_2–Mn(IV)–CH_3COOH [b]	1:46:35:34	1:22:200	1:5:55	1:26:200

Conditions for H_2O_2–**9**–pcaH: [*n*-heptane] = [3-methylhexane] = 0.34 mol dm^{-3}; [2,4,4-trimethylpentane] = 0.30 mol dm^{-3}; [methylcyclohexane] = 0.39 mol dm^{-3}; [H_2O_2] = 0.625 mol dm^{-3}; [catalyst] = 4×10^{-4} mol dm^{-3}; [pcaH] = 0.01 mol dm^{-3}; 25°C; 6 hours; total volume 10 ml. [a] Refs. [11, 48, 137, 146, 147, 151, 163, 176]. [b] Refs. [176, 200–203].

The ratio of alcohols obtained was normalized for each substrate taking into account the equivalent hydrogen atoms at each position. For comparison, the corresponding parameters measured for oxidations by certain other systems studied by us earlier are also given. All regioselectivity parameters for our H_2O_2–**9**–pcaH system are close to that obtained for the systems known to oxidize alkanes *via*

formation of hydroxyl radicals, such as O_2–H_2O_2–hv, O_2–H_2O_2–$FeSO_4$ and H_2O_2–NBu_4VO_3–pcaH [11, 48, 137, 146, 147, 151, 163, 176]. These systems are characterized with relatively low selectivity parameters. In contrast, the H_2O_2–$[LMn^{IV}(O)_3Mn^{IV}L]^{2+}$–acetic acid system (where L = 1,4,7-trimethyl-1,4,7-triazacyclononane), which apparently does not involve free hydroxyl radicals, exhibits noticeably higher regioselectivity parameters. The oxidation with the H_2O_2–**9**–pcaH system proceeds non-stereoselectively, as the *t*/*c* parameters for the oxidation of *cis*- and *trans*-decalin show (3.5 and 5.1 for *cis*- and *trans*-decalin, respectively). This is typical for systems operating *via* hydroxyl radicals, and very different from systems that do not operate *via* hydroxyl radicals, as the H_2O_2-$[LMn^{IV}(O)_3Mn^{IV}L]^{2+}$-acetic acid system, from which the *t/c* parameters reveals a remarkable stereoselectivity (*t/c* = 0.12 and 33 for the oxidation of *cis*- and *trans*-decalin, respectively). Toluene was also oxidized and its results and those from the oxidation of *cis*- and *trans*-decalin are shown in Table 3.6.2.

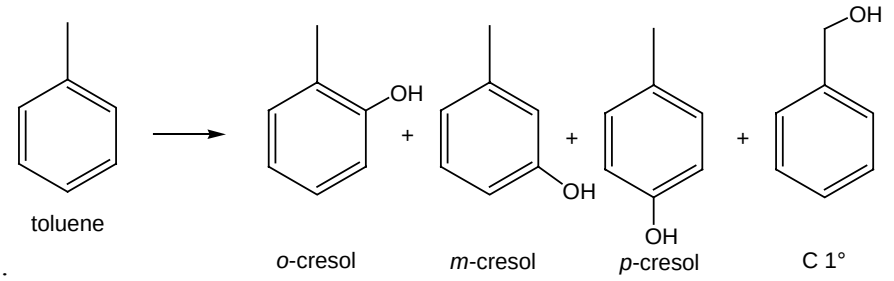

Scheme 3.6.3. Reaction products of the toluene oxidation with H_2O_2 and air catalyzed by cation **9** after treatment with PPh_3.

Table 3.6.2. Selectivities of *cis*-decalin, *trans*-decalin and toluene oxidations by various systems in acetonitrile. The parameter Me:Ar is the ratio between the primary alcohol and the total cresols (*o*-, *m*- and *p*-) obtained.

System	Hydrocarbon oxidized / selectivity parameter			
	Cis-decalin	*Trans*-decalin	Toluene	
	t:c	*t:c*	Me : Ar	*o:m:p*
H_2O_2–**9**–pcaH	3.5	5.1	0.5	38:33:29
O_2–H_2O_2–hν [a]	1.3	2.7		
O_2–H_2O_2–$FeSO_4$ [a]	3.4	8.8		
H_2O_2–VO_3^-–pcaH [a]	2.1	2.4	0.5	50:23:27
H_2O_2–$Fe(ClO_4)_3$ [a]			1.1	60:26:14
H_2O_2–$Fe(ClO_4)_3$–pcaH [a]			0.35	67:18:15
H_2O_2–Mn(IV)–CH_3COOH [b]	0.12	33	2.0	38:18:44

Conditions for H_2O_2–**9**–pcaH: [cis-decalin] = [trans-decalin] = 0.31 mol dm^{-3}; [toluene] = 0.47 mol dm^{-3}; [H_2O_2] = 0.625 mol dm^{-3}; [catalyst] = 4×10^{-4} mol dm^{-3}; [pcaH] = 0.01 mol dm^{-3}; 25°C; 6 hours; total volume 10 ml. [a] Refs. [11, 48, 137, 146, 147, 151, 163, 176]. [b] Refs. [176, 200–203].

3.6.1.3 Oxidation of Light Alkanes

We investigated the oxidation of light alkanes by the system under discussion. Ethane was transformed mainly to ethyl hydroperoxide as well as to a minor amount of acetaldehyde. Also acetic acid was detected in a very small concentration after 6 hours. After this time, the concentrations of ethyl hydroperoxide and acetaldehyde were measured to be 6.8×10^{-3} and 1.4×10^{-3} mol dm^{-3}. Thus a total TON attained for ethane is 21 after 6 hours. Results are shown in Figure 3.6.8 and Table 3.6.3.

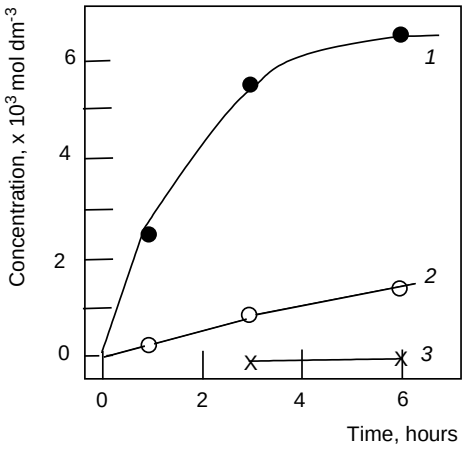

Figure 3.6.8. Accumulation of products in the oxidation of ethane with hydrogen peroxide in acetonitrile catalyzed by **9** in the presence of pcaH. Conditions: Ethane pressure = 30 bar; air pressure = 10 bar; $[H_2O_2]_0$ = 0.625 mol dm^{-3}; [catalyst] = 4 × 10^{-4} mol dm^{-3}; [pcaH] = 0.01 mol dm^{-3}; 25 °C, 10 ml total volume. Products: ethyl hydroperoxide (*1*), acetaldehyde (*2*), acetic acid (*3*).

Table 3.6.3. Oxidation products of methane and ethane with hydrogen peroxide and air catalyzed by **9** in the presence of pcaH in acetonitrile.

Substrate	**Products, × 10^2 mol dm^{-3}**			**TON**
	MeOOH	HCHO		
Methane	0.12	0.04		4
Substrate	**Products, × 10^2 mol dm^{-3}**			**TON**
	EtOOH	CH_3CHO	CH_3CO_2H	
Ethane	0.65	0.16	0.01	21

Conditions: methane pressure = 90 bar; ethane pressure = 30 bar; air pressure = 10 bar; [catalyst] = 4 × 10^{-4} mol dm^{-3}; [pcaH] = 0.01 mol dm^{-3}; $[H_2O_2]$ = 0.625 mol dm^{-3}; 25 °C; 10 ml total volume.

Methane (90 bar) was oxidized with hydrogen peroxide and air in acetonitrile at 25 °C in the presence of **9** and pcaH to produce after 6 hours methyl hydroperoxide and formaldehyde with a TON = 4 (Table 3.6.3).

3.6.1.4 Conclusions

On the basis of the results described above we can propose the following mechanism of alkane oxidation by the H_2O_2–**9**–pcaH system which is similar to the mechanism operating in other H_2O_2–Fe^{III} systems [176]. The first step of the process is the reduction of the dinuclear Fe^{III} core with two hydrogen peroxide molecules to produce hydroperoxy radicals and a dinuclear Fe^{II} core (Eqs. 1 – 2, Scheme 3.6.4). Subsequent reactions proceed partly *via* stages operative in Fenton's reagent and give rise to the formation of both molecular oxygen and hydroxyl radicals (Eqs. 3 – 6, Scheme 3.6.5).

$$[Fe^{III}\text{-}Fe^{III}]^{2+} + H_2O_2 \longrightarrow [Fe^{III}\text{-}Fe^{II}]^{+} + H^{+} + HOO\cdot \quad (1)$$

$$[Fe^{III}\text{-}Fe^{II}]^{+} + H_2O_2 \longrightarrow [Fe^{II}\text{-}Fe^{II}] + H^{+} + HOO\cdot \quad (2)$$

$$[Fe^{III}\text{-}Fe^{III}]^{2+} + HOO\cdot \longrightarrow [Fe^{III}\text{-}Fe^{II}]^{+} + H^{+} + O_2 \quad (3)$$

$$HOO\cdot + HOO\cdot \longrightarrow H_2O_2 + O_2 \quad (4)$$

$$[Fe^{III}\text{-}Fe^{II}]^{+} + H_2O_2 \longrightarrow [Fe^{III}\text{-}Fe^{III}]^{2+} + HO^{-} + HO\cdot \quad (5)$$

$$[Fe^{II}\text{-}Fe^{II}] + H_2O_2 \longrightarrow [Fe^{III}\text{-}Fe^{II}]^{+} + HO^{-} + HO\cdot \quad (6)$$

Scheme 3.6.4. Proposed mechanism for the formation of hydroxyl radicals in the system H_2O_2–**9**–pcaH.

The interaction of Fe^{II} with H_2O_2 possibly begins from the formation of a hydroperoxy derivative similar to that proposed for the hemerythrin oxidized form. We can assume that amino acids added to the reaction mixture play a very important role in this stage, facilitating the proton transfer between the coordinated H_2O_2

molecule and ligands at iron centers, as in the case of the alkane oxidations catalyzed by the NBu_4VO_3–pcaH system [11].

Furthermore, the hydroxyl radical formed from hydrogen peroxide attacks an alkane molecule and the alkyl radical thus formed adds rapidly an oxygen molecule affording the corresponding alkyl peroxy radical (Eqs. 1 – 2, Scheme 3.6.5). This alkyl peroxy radical can be reduced by one of the two iron(II) centers in the dinuclear complex in its reduced form and, after addition of a proton, a molecule of the alkyl hydroperoxide is formed (Eqs. 3 – 4, Scheme 3.6.5)

$$RH + HO\cdot \longrightarrow R\cdot + H_2O \quad (1)$$

$$R\cdot + O_2 \longrightarrow ROO\cdot \quad (2)$$

$$ROO\cdot + [Fe^{II}\text{-}Fe^{II}] \longrightarrow ROO^- + [Fe^{III}\text{-}Fe^{II}]^+ \quad (3)$$

$$ROO^- + H^+ \longrightarrow ROOH \quad (4)$$

Scheme 3.6.5. Proposed mechanism for the alkane oxidation with the system H_2O_2–**9**–pcaH.

This proposed mechanism involving hydroxyl radicals as the species which attack the alkane is very simplified, and we can assume that in addition or instead of hydroxyl radicals, metal-containing oxygen-centered radicals are species which can also abstract a hydrogen atom from an alkane forming an alkyl radical. In any case, the activation of inert C–H bonds in alkanes by these system proceeds with low selectivity that suggests a mechanism *via* strong oxygen-centered radicals. Such a mechanism is postulated for the alkane oxidations by MMO and, thus the system

described in the present paper can be considered as a structural and functional model of MMO (*cf.* Scheme 2.2.3).

3.6.2 Alkane Oxidations Catalyzed by $[Fe_2(tacn)_2(\mu\text{-}O)(CH_3CO_2)_2]^{2+}$ (10)

The known cationic diiron(III) complex (**10**), a structural model of hemerythrin, in which tacn = 1,4,7-trimethyltriazacyclononane, was used in the form of its iodide salt, [**10**] $I_2 \cdot 0.5\ CH_3CN$ [205, 206].

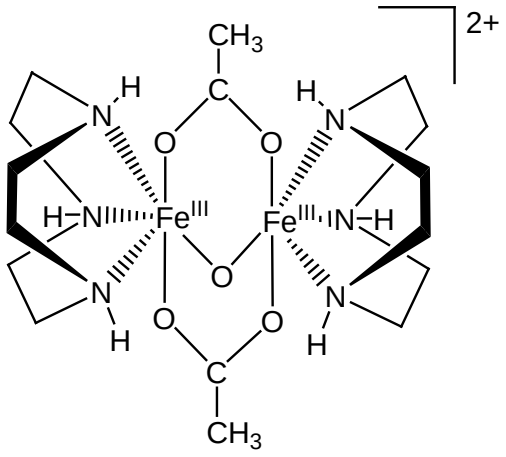

Figure 3.6.9. Cation **10**.

3.6.2.1 Oxidation of Cyclohexane

Catalyst **10** is almost inactive for the oxidation of cyclohexane in acetonitrile with hydrogen peroxide and air, giving a TON = 14 after 24 hours, but the addition of pcaH in a ratio 1 : 10 to the reaction solution enhances significantly the catalytic activity giving a TON = 251 after 24 hours. The products of the reaction were analyzed by GC and the major product detected was cyclohexyl hydroperoxide

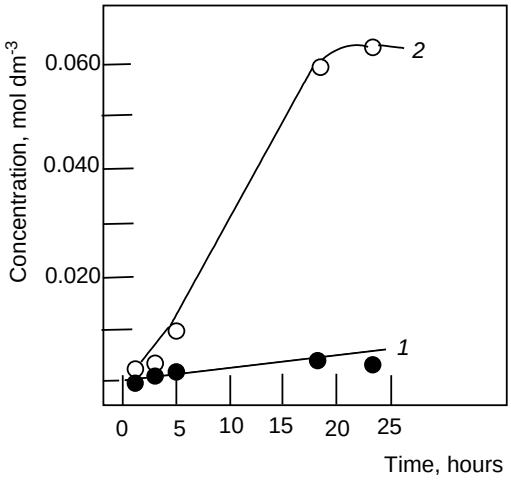

Figure 3.6.10. Sum of all products from the reaction of cyclohexane with hydrogen peroxide in acetonitrile at 25°C catalyzed by **9** in the absence of co-catalyst (1), and in the presence of pcaH (2). Conditions: [cyclohexane] = 0.46 mol dm^{-3}; [H_2O_2] = 0.59 mol dm^{-3}; [catalyst] = 2.5×10^{-4} mol dm^{-3}; [co-catalyst] = 2.5×10^{-3} mol dm^{-3}; 25°C; 10 ml total volume; 1 atm air.

The oxidation of cyclohexane with hydrogen peroxide and air catalyzed by **10** is accompanied by oxygen evolution, showing that catalyst **10** has a catalase activity (Equation 3.6.1) in addition to its peroxidase activity.

3.6.2.2 Oxidation of Higher Alkanes

The oxidation of several branched hydrocarbons and the calculation of their selectivity parameter in the usual way (*cf.* Section 3.6.1.2), provide information about the oxidation mechanism by the system H_2O_2–**10**–pcaH.

Table 3.6.4. Selectivities of 3-methylhexane, methyl-cyclohexane, 2,2,4-trimethylpentane, *cis*- and *trans*-decalin oxidations by various systems in acetonitrile.

System	**Hydrocarbon oxidized / selectivity parameter**				
	3-methyl-hexane	2,2,4-trimethyl-pentane	Methyl-cyclohexane	*Cis*-decalin	*Trans*-decalin
	1°:2°:3°	1°:2°:3°	1°:2°:3°	*t:c*	*t:c*
H_2O_2–**10**–pcaH	1:8.0:16	1:2.5:7.8	1:8:34	9.8	3.2
O_2–H_2O_2–hν [a]	1:4:12	1:2:6		1.3	2.7
H_2O_2–VO_3^-–pcaH[a]	1:5.7:22	1:4:9	1:6:18	2.1	2.4
H_2O_2–Mn(IV)–CH_3COOH [b]	1:22:200	1:5:55	1:26:200	0.12	33

Conditions for H_2O_2–**10**–pcaH: [3-methylhexane] = 0.34 mol dm^{-3}; [2,4,4-trimethylpentane] = 0.30 mol dm^{-3}; [methylcyclohexane] = 0.39 mol dm^{-3}; [cis-decalin] = [trans-decalin] = 0.31 mol dm^{-3} [H_2O_2] = 0.59 mol dm^{-3}; [catalyst] = 2.5×10^{-4} mol dm^{-3}; [pcaH] = 2.5×10^{-3} mol dm^{-3}; 25°C; 6 hours; total volume 10 ml. [a] Refs. [11, 48, 137, 146, 147, 151, 163, 176]. [b] Refs. [176, 200–203].

The selectivity parameters of our system are indicative of a low-selectivity system, if we compare them with two systems which oxidize alkanes also in a low-selective way (O_2–H_2O_2–hν and H_2O_2–VO_3^-–pcaH) *via* hydroxyl radicals. However, the selectivity parameters for the system under consideration are somewhat higher than for these two other systems. This leads us to suggest that the H_2O_2–**10**–pcaH system yields not only low-selective hydroxyl radicals but also, by another channel, other species that can interact with alkanes in a more selective way, for instance, ferryl species. Nevertheless, the reaction involving hydroxyl radicals predominates, as can be deduced from the comparison of the selectivity parameters of our system with

those of the H_2O_2–Mn(IV)–CH_3COOH system, which oxidizes alkanes in a very selective way without participation of hydroxyl radicals.

3.6.2.3 Kinetic and Mechanistic Studies: Conclusions

The selectivity study of the alkane oxidation with hydrogen peroxide and air catalyzed by **10** suggests the formation of hydroxyl radicals as the species which attack the alkane to produce the corresponding alkyl hydroperoxide. This conclusion is further supported by a kinetic experiment, in which we measure the dependence of the initial oxidation rate, W_0, upon the initial cyclohexane concentration for our system, as compared to that obtained for the formation of cyclohexyl hydroperoxide under UV irradiation (λ = 253.0 nm) of a solution of cyclohexane in acetonitrile with hydrogen peroxide and air (O_2–H_2O_2–hν system), which doubtlessly proceeds *via* hydroxyl radicals [207]. The photolysis of hydrogen peroxide produces hydroxyl radicals (Reaction 1, Scheme 3.6.6). As neither acetonitrile, CH_3CN, nor cyclohexane, CyH, absorb in the specified spectral region, it can be assumed that the formation of cyclohexyl radicals, which will yield the cyclohexyl hydroperoxide observed in the photochemical experiment, is induced by OH· radicals and not by UV light (Reaction 2, Scheme 3.6.6). Hydroxyl radicals can also interact with the acetonitrile, used as solvent, giving several oxidation products such as formaldehyde and methanol (Reaction 3, Scheme 3.6.6).

$$H_2O_2 \longrightarrow 2\ HO\cdot \quad (1)$$

$$CyH + HO\cdot \xrightarrow{k_2} Cy\cdot + H_2O \quad (2)$$

$$CH_3CN + HO\cdot \xrightarrow{k_3} \text{products} \quad (3)$$

Scheme 3.6.6. Photolysis of hydrogen peroxide in acetonitrile in the presence of cyclohexane.

Taking these reactions into account, we can assume that an increase in the cyclohexane concentration should cause an increase in the rate of cyclohexane oxidation, whose limiting value corresponds to the rate of formation of hydroxyl radicals, W_1. An analysis of this kinetic scheme leads to the following equation for the initial stationary rate of formation of cyclohexyl hydroperoxide, CyOOH, where k_2 and k_3 are the rate constants for Reactions 2 and 3 (Scheme 3.6.6), respectively:

$$-\frac{d[\mathrm{CyH}]}{d\mathrm{t}} = \frac{d[\mathrm{CyOOH}]}{d\mathrm{t}} = W_1 / \left(1 + \frac{k_3[\mathrm{CH_3CN}]}{k_2[\mathrm{CyH}]}\right)$$

Equation 3.6.2. Kinetic expression for the rate of cyclohexyl hydroperoxide formation in the photolytic oxidation of cyclohexane with hydrogen peroxide in acetonitrile.

An analysis of the experimental dependence of W_0 on the initial concentration of CyH for the photolytic oxidation of cyclohexane (Figure 3.6.11), taking into account Equation 3.6.2, yields $k_3 / k_2 = 0.013$. If we assume in the oxidation of cyclohexane by the system H_2O_2–**10**–pcaH the formation of hydroxyl radicals to be the rate-determining step, we can use the same kinetic equation as Equation 3.6.2. The ratio between k_3 and k_2 calculated for this system, using the experimental data

(Figure 3.6.11 B), is 0.011. The two values of k_3 / k_2, obtained for O_2–H_2O_2–hν and for H_2O_2–**10**–pcaH are comparable, and also very close to the value determined from radiation chemical measurements, $k_3 / k_2 = 0.012$ [208, 209].

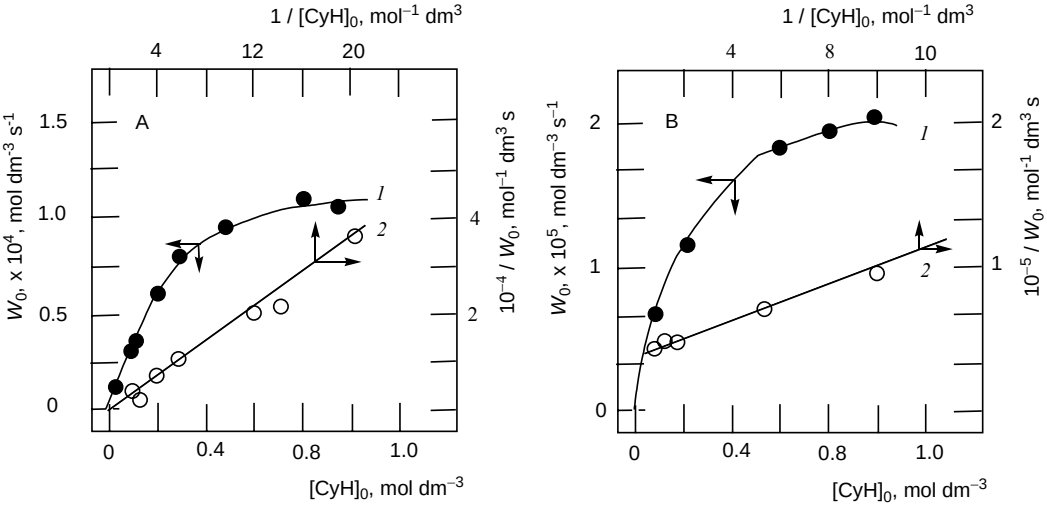

Figure 3.6.11. Initial reaction rate of the oxidation products formed *vs* initial concentration of cyclohexane in the photolytic oxidation reaction of cyclohexane with H_2O_2 and air in acetonitrile (A) and in the oxidation reaction of cyclohexane with H_2O_2 and air in acetonitrile catalyzed by **10** (B). Curves *1* are the measured data and lines *2* are the anamorphosis for these data. Conditions: $[H_2O_2] = 0.59$ mol dm^{-3}; [catalyst] = 2.5×10^{-4} mol dm^{-3}; [pcaH] = 2.5×10^{-3} mol dm^{-3}; 25°C; 10 ml total volume; 1 atm air.

Hence it follows that the oxidation of cyclohexane in the presence of hydrogen peroxide catalyzed by **10** is doubtlessly induced by hydroxyl radicals resulting from hydrogen peroxide. The classical chain mechanism of induced cyclohexane oxidation at the rates equal to these observed experimentally is impossible at room temperature because of the low reactivity of cyclohexyl peroxyl radicals, which gives a low parameter of hydrocarbon oxidizability by the chain mechanism [11-supplemetary data].

The evolution of molecular oxygen is observed even at a high concentration of cyclohexane, when all hydroxyl radicals are certainly accepted by the alkane. This suggests that hydroxyl radicals do not participate in the decomposition of hydrogen peroxide into oxygen and water. We must therefore consider two parallel hydrogen peroxide decomposition processes: with and without the participation of hydroxyl radicals.

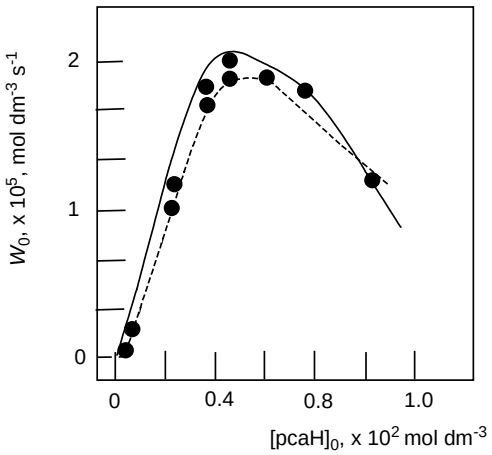

Figure 3.6.12. Initial reaction rate of the oxidation products *vs* initial concentration of pcaH in the oxidation reaction of cyclohexane with H_2O_2 and air in acetonitrile catalyzed by **10**. Conditions: [CyH] = 0.46 mol dm^{-3}; [catalyst] = 2.5×10^{-4} mol dm^{-3}; [H_2O_2] = 0.59 mol dm^{-3}; 25°C; 10 ml total volume; 1 atm air. Dashed line correspond to calculated data from Equation 3.6.3.

We studied the kinetics of cyclohexyl hydroperoxide formation and molecular oxygen evolution, in order to elucidate the details of the mechanism of the process. The increase of the initial rate of CyOOH formation upon addition of pcaH (Figure 3.6.12) suggests that the hydroxyl radical generation is associated with the formation of adducts between **10** and pcaH. Attempts to isolate such adducts were, however,

unsuccessful. We may consider that an adduct of one molecule of **10** and one pca molecule is formed (Eq. 4, Scheme 3.6.7), and that it is in equilibrium with an adduct containing two pca molecules (Eq. 5, Scheme 3.6.7).

$$[\mathbf{10}]^{2+} + \text{pcaH} \rightleftharpoons [\mathbf{10}(\text{pca})]^{+} + \text{H}^{+} \qquad (K_4) \qquad (4)$$

$$[\mathbf{10}(\text{pca})]^{+} + \text{pcaH} \rightleftharpoons [\mathbf{10}(\text{pca})_2] + \text{H}^{+} \qquad (K_5) \qquad (5)$$

$$[\mathbf{10}(\text{pca})]^{+} + \text{H}_2\text{O}_2 \rightleftharpoons [\mathbf{10}(\text{pca})\ \text{H}_2\text{O}_2]^{+} \qquad (K_6) \qquad (6)$$

$$[\mathbf{10}(\text{pca})\ \text{H}_2\text{O}_2]^{+} + \text{H}_2\text{O}_2 \rightleftharpoons [\mathbf{10}(\text{pca})\ (\text{H}_2\text{O}_2)_2]^{+} \qquad (K_7) \qquad (7)$$

$$[\mathbf{10}(\text{pca})\ (\text{H}_2\text{O}_2)_2]^{+} \longrightarrow [\mathbf{10}(\text{pca})]^{+} + \text{H}_2\text{O} + \text{HOO}\cdot + \text{HO}\cdot \ (k_8) \qquad (8)$$

Scheme 3.6.7. Kinetic pathway for the formation of hydroxyl and hydroperoxyl radicals from hydrogen peroxide by the action of catalyst **10** and co-catalyst pcaH in the oxidation of cyclohexane in acetonitrile.

The initial rate of CyOOH formation depends upon the initial concentration of hydrogen peroxide, $[H_2O_2]_0$, in a complex way (Figure 3.6.13). Initially, the process is close to second-order in hydrogen peroxide, and, at concentrations higher than 1 mol dm^{-3}, the reaction rate ceases to depend on $[H_2O_2]_0$. Such a behaviour is suggestive of the participation of an iron diperoxo complex at the stage of the generation of hydroxyl radicals. We may consider the formation of mono- and diperoxo complexes and assume that the rate-determining step of ·OH formation is the monomolecular decomposition of the diperoxo complex containing one pca molecule.

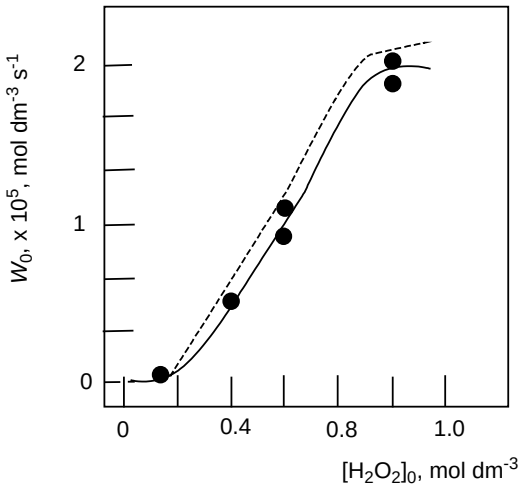

Figure 3.6.13. Initial reaction rate of the oxidation products formation *vs* initial concentration of H_2O_2 in the oxidation reaction of cyclohexane with H_2O_2 and air in acetonitrile catalyzed by **10.** Conditions: [CyH] = 0.46 mol dm^{-3}; [catalyst] = 2.5 × 10^{-4} mol dm^{-3}; [pcaH] = 2.5 × 10^{-3} mol dm^{-3}; 25°C; 10 ml total volume; 1 atm air.

Assuming the concentrations of the intermediary complexes to be in equilibrium (at high concentrations of CyH, when all hydroxyl radicals formed can interact with this hydrocarbon), the suggested kinetic scheme can be used to obtain the equation for the stationary rate of CyOOH formation, Equation 3.6.3.

$$-\frac{d[\mathrm{CyH}]}{d\mathrm{t}} = \frac{d[\mathrm{CyOOH}]}{d\mathrm{t}} =$$

$$= \frac{k_8 K_4 K_6 K_7 [\mathrm{H_2O_2}]_0^2 [\mathrm{pcaH}]_0 [\mathbf{10}]_0}{1 + K_4[\mathrm{pcaH}]_0 + K_4 K_5 [\mathrm{pcaH}]_0^2 + K_4 K_6 [\mathrm{pcaH}]_0 [\mathrm{H_2O_2}]_0 + K_4 K_6 K_7 [\mathrm{pcaH}]_0 [\mathrm{H_2O_2}]_0^2}$$

Equation 3.6.3. Kinetic expression for the rate of cyclohexyl hydroperoxide formation in the oxidation of cyclohexane with hydrogen peroxide in acetonitrile catalyzed by **10** in the presence of pcaH as co-catalyst.

Equation 3.6.3 describes satisfactorily the experimental data for the initial rate dependence of CyOOH formation upon $[pcaH]_0$ and on $[H_2O_2]_0$ with the following constant values: K_4 = 16 dm^{-3} mol^{-1}, K_5 = 6250 dm^{-3} mol^{-1}, K_6 = 12.5 dm^{-3} mol^{-1}, K_7 = 16 dm^{-3} mol^{-1}, k_8 = 0.13 s^{-1} (see Figures 3.6.12 and 3.6.13, dashed lines). We cannot say something definitely about the nature of the adduct between compound **10** and pcaH. It is for that, that in order to calculate the equilibrium constants for Equations 4 and 5, they were simplified to 4a and 5a.

10 + pcaH $\rightleftharpoons$ "**10**(pcaH)" (K_4) (4a)

"**10**(pca)" + pcaH $\rightleftharpoons$ "**10**$(pcaH)_2$" (K_5) (5a)

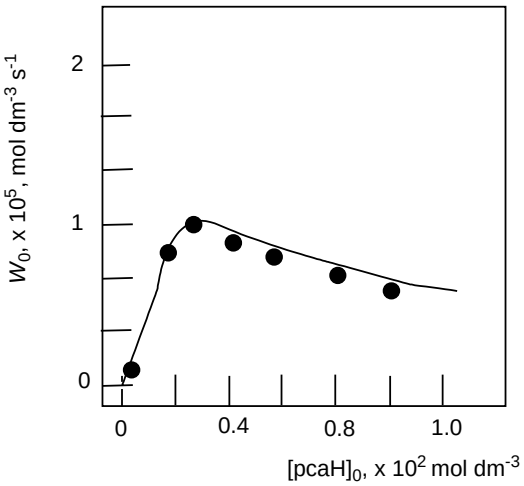

Figure 3.6.14. Initial reaction rate of the oxygen evolution *vs* initial concentration of pcaH in the oxidation reaction of cyclohexane with H_2O_2 and air in acetonitrile catalyzed by **10.** Conditions: [CyH] = 0.46 mol dm^{-3}; [catalyst] = 2.5 × 10^{-4} mol dm^{-3}; $[H_2O_2]$ = 0.59 mol dm^{-3}; 25°C; 10 ml total volume; 1 atm air. Dashed line correspond to calculated data from Equation 3.6.3.

The character of the dependence of the rate of molecular oxygen evolution on $[pca]_0$ is identical to that of the dependence of d[CyOOH] / dt upon $[pcaH]_0$ (Figure 3.6.14). Hence it follows that the same intermediary complex participates in the rate-determining steps of both processes, namely, the diperoxo derivative of compound **10** containing one pca molecule, [**10**(pca)$(H_2O_2)_2$]. The decomposition of this derivative can yield molecular oxygen (Equation.3.6.4) or hydroxyl and hydroperoxyl radicals (Eq. 8, Scheme 3.6.7).

$$[\mathbf{10}(pca)\ (H_2O_2)_2]^+ \longrightarrow 2\ H_2O\ +\ O_2\ +\ [\mathbf{10}(pca)]^+$$

Equation 3.6.4. The decomposition of hydrogen peroxide to molecular oxygen and water *via* a complex with catalyst **10** and pcaH as a secondary reaction of the oxidation reaction of cyclohexane in acetonitrile in the presence of air.

The process described by Equation 3.6.4 is similar to the decomposition of hydrogen peroxide by catalase enzymes. Both decomposition reactions of hydrogen peroxide, on the one hand to give hydroxyl and hydroperoxyl radicals and on the other hand to give molecular oxygen and water, are in competition in the cyclohexane oxidation reaction catalyzed by **10** in the presence of pcaH as co-catalyst in acetonitrile at atmospheric pressure (Figure 3.6.14).

Experimental Section

4.1 Solvents and Gases

Solvents for the catalytic experiments were of analytical grade (Fluka or Aldrich) and used without distillation, only stored over molecular sieve and under a nitrogen atmosphere. Solvents for synthesis were of technical grade and were purified by distillation under nitrogen atmosphere and dried according to standard laboratory practices [218]. Water was bidistilled and stored under nitrogen. Laboratory gases were purchased from Carbagas and used directly from the cylinders without further purification.

4.2 Starting Material

The compounds NBu_4VO_3 [219], $[NBu_4][VO_2(pca)_2]$ [10] hptb [199] and $pdcaH_2$ [220] were synthesized as described previously. Commercial salts of vanadium and iron were used as received (Fluka). Cathecol was recrystallized from a hot benzene solution and 1,4,7-trimethyl-1,4,7-triazacyclononane was received as a gift from Lonza AG (Visp-Switzerland). All other commercial organic compounds were of analytical grade and used as received (Fluka and Aldrich). Titanyl sulphate ($TiOSO_4$) was used as a solution in water according to DEV determination of hydrogen peroxides (Riedel de Haën). Hydrogen peroxide was used as a solution in water (35%) (Fluka) and stored at 4 °C. Peroxy acetic acid was used as a solution in acetic acid (39 %) (Fluka) and stored at 4 °C.

The tetrabutylammonium salts of anions $[PMo_{11}VO_{40}]^{4-}$ (**1**) and $[PMo_6V_5O_{39}]^{12-}$ (**2**) were synthesized according to references [133-135] at the Institute of Catalysis, Novosibirsk, Russia, and given to us for catalytic tests.

4.3 Instrumentation and Analyses

4.3.1 Infrared Spectroscopy

Infrared spectra were recorded with a Perkin-Elmer 1720X FT-IR spectrometer and with a Perkin-Elmer Spectrum One spectrometer in transmission mode where the absorptions are given in reciprocal centimetres (cm^{-1}). A standard press was used to produce KBr pellets. Intensity data are described with the following abbreviations: vs = very strong, s = strong, m = medium, w = weak, sh = shoulder.

4.3.2 NMR Spectroscopy

Nuclear magnetic resonance spectra were recorded using a Varian Gemini 200 BB instrument or a Bruker AMX 400 spectrometer and referenced by using the resonanaces of the residual non-deuterated solvents. ^{1}H NMR: internal standard solvent, external standard TMS; ^{31}P NMR: external standard 85% H_3PO_4. Chemical shifts are given in ppm and coupling constants *J* in Hz (s = singulet, d = doublet, t = triplet, dd = doublet of doublet, m = multiplet).

4.3.3 Gas Chromatography

Gas chromatography was performed on a Dani 86.10 gas chromatograph equipped with a split-mode capillary injection system and flame ionisation detector using a Cp-wax 52-CB capillary column (25m × 0.32 mm).

4.3.4 Elemental Analyses

Microanalyses were carried out by the Laboratory of Pharmaceutical Chemistry, University of Geneva (Switzerland) or by the Mikroelementaranalytisches Laboratorium, ETH Zürich (Switzerland).

4.3.5 Mass Spectra

ESI mass spectra were measured by Professor T. A. Jenny of the University of Fribourg (Switzerland) or by the mass service directed by Professor R. Tabacchi of the University of Neuchâtel (Switzerland) using a LCQ Finnigan spectrometer.

4.3.6 Crystallographic Analyses

The crystallographic analyses were done by Dr. Bruno Therrien and the crystallographic group of the University of Neuchâtel directed by Professor Helen Stoeckli-Evans. The experimental data for these analyses are shown in paragraph 4.6.

4.3.7 UV-Vis Spectrophotometry

Absorbances for the formaldehyde and hydrogen peroxide determinations were measured using a Novaspec II from Pharmacia Biotech. The samples were placed in glass cuves and the reference used was acetonitrile.

4.3.8 Kinetic Calculations

The kinetic parameters and equations from the experimental results of this work were calculated by Dr. Yuriy N. Kozlov from the Semenov Institute of Chemical Physics of the Russian Academy of Sciences (Moscow-Russia).

4.4 Catalytic Experiments

4.4.1 Apparatus and Catalytic Runs

The experiments using gases as methane, ethane or propane as substrates and synthetic air as oxidant were carried out in 100 ml autoclaves equipped with glass-lined steel vessels containing a magnetic bar. In a typical experiment, the glass tube containing the solvent, catalyst, co-catalyst and the hydrogen peroxide or peroxy acetic acid solution was introduced in the steel vessel of the autoclave, which was closed hermetically and purged with air twice. After that, the autoclave was pressurized with air and with the hydrocarbon, in this order, to the corresponding pressures and heated to the corresponding temperature under vigorous stirring. After the indicated reaction time, the autoclave was cooled in ice and the pressure was released. The experiments with higher alkanes were carried out in thermostated

cylindrical vessels connected to a reflux tube, when the reaction temperature is higher than 40 °C and open to air. In a typical experiment, a portion of hydrogen peroxide or peroxy acetic acid solution was added to the solution of the catalyst and substrate in acetonitrile or acetic acid. In all cases, the reaction mixture was filtered and two samples of 0.1ml each one were taken, and in the case of the reactions in acetic acid this samples were diluted 10 times in acetonitrile in order to avoid a broad peak of acetic acid in the chromatogram. To one of the samples was added solid triphenylphosphine to reduce the alkyl hydroperoxide to the corresponding alcohol, reaction which is complete after 15 minutes. Each sample was injected in GC twice, 0.5 μl each time.

4.4.2 Quantitative Determination of the Reaction Products

4.4.2.1 Normalization of GC Chromatograms

The chromatograms resulting from the GC injection of the oxidation reaction samples showed one peak for each alcohol, carboxylic acid and ketone (aldehyde) formed, except for formaldehyde, and one area for each peak, which correspond to its relative concentration. The concentrations of each product were calculated by comparison with the chromatogram from a calibration solution of the products in known concentrations. The concentration of a product i in the sample chromatogram (C_{is}) was defined as the quotient between its area (A_{is}) and the area of the acetonitrile peak in the sample (A_{Rs}) taken as the reference. The concentration of the same product in the calibration chromatogram (C_{ic}) is known from the prepared solution, and it can be defined in the same way, as the quotient between the area for i in the calibration chromatogram (A_{ic}) and the area of the reference peak (A_{Rc}). After

dividing the expression for C_{is} by that for C_{ic}, the resulting equation used to calculate the concentration of a product in the reaction was:

$$C_{is} = f_c \frac{A_{is}}{A_{Rs}} \qquad \text{where} \qquad f_c = \frac{A_{Rc}}{A_{ic}} C_{ic}$$

4.4.2.2 Determination of the Concentration of Alkyl Hydroperoxides

The concentration of alkyl hydroperoxides in the reaction (C_{ROOH}) cannot be determined directly from the GC chromatograms, as these compounds decompose in the GC column to give the corresponding alcohol and ketone; however in some experiments and in earlier work we were able to detect a peak of an alkyl hydroperoxide [46,47]. Its concentration was calculated comparing the concentrations of the corresponding alcohol (R-OH) and ketone (R_H=O) in the chromatograms resulting from samples injected directly (C'_{R-OH} and $C'_{R_H=O}$) and from samples injected after 15 minutes of reaction with solid triphenylphosphine (C''_{R-OH} and $C''_{R_H=O}$), which reduces all alkyl hydroperoxide to the corresponding alcohol [9a, 33, 34, 48, 136-137, 146-150, 153-154]. The alcohol / ketone ratio of the decomposition of alkyl hydroperoxide was assumed to be 1. The real concentration of ketone in the reaction ($C_{R_H=O}$) is equal to that calculated after reduction with PPh_3. The difference in ketone concentration between both samples, $\Delta C_{R_H=O} = C'_{R_H=O} - C''_{R_H=O}$, corresponds to the alkyl hydroperoxide that is decomposed to ketone in the GC column. As we assumed that both alcohol and ketone are formed in a 1 : 1 ratio in the GC, so the alcohol that comes from alkyl hydroperoxide decomposition will be equal to $\Delta C_{R_H=O}$, and its subtraction from the concentration of alcohol in the sample

injected directly gives the real concentration of alcohol formed in the reaction, C_{R-OH}. The concentration of alkyl hydroperoxide in the reaction is calculated as the difference between the concentration of alcohol in the sample with PPh_3 and the real concentration of alcohol in the reaction.

$$C_{R_{H=O}} = C''_{R_{H=O}}$$

$$C_{R-OH} = C'_{R-OH} - \Delta C_{R_{H=O}}$$

$$C_{ROOH} = C''_{R-OH} - C_{R-OH}$$

4.4.2.3 Determination of Formaldehyde Concentration

Formaldehyde concentration was determined by VIS-spectrophotometry after its reaction with the Nash reagent [224], a solution in water which contains 30.85 g of ammonium acetate, 0.62 ml of glacial acetic acid and 0.42 ml of acetylacetone for 100 ml. In this reaction, known as the Hantzsch reaction, the product formed was 3,5-diacetyl-2,6-dimethyl-1,4-dihydropyridine, a chromophore which was present in its zwitterionic form at the pH conditions of the experiment.

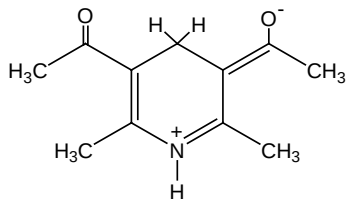

In a typical measurement, 1ml of the sample containing formaldehyde was mixed with 1 ml of the Nash reagent and the resulting light yellow solution was

diluted to 5 or10 ml with water and warm to 60 °C for 10 minutes. After this time, the absorbance of the resulting yellow solution was measured at 412 nm. We calculated the concentration on formaldehyde applying the Beer-Lambert's law, $A = \varepsilon\, c\, l$, where A is the absorbance measured at λ = 412 nm, l is the cuve length, 1 cm, and ε is the absorbance coefficient for the molecule formed, 8000 l $mol^{-1}cm^{-1}$; including the dilution of the formaldehyde sample, d, the equation results:

$$C_{CH_2O}\ (\text{mol dm}^{-3}) = \frac{A\ d}{8000}$$

4.4.2.4 Determination of H_2O_2 Concentration

The concentration of hydrogen peroxide in the oxidation reactions was determined by VIS-spectrophotometry after reaction with a titanyl sulphate solution in water. In a typical analysis, 0.5 ml of titanyl sulphate solution was mixed with 1 ml of H_2SO_4 2 M and with 0.1 ml of the sample containing hydrogen peroxide, and the mixture was diluted with water to 10 ml. The absorbance (A) of the resulting yellow solution was measured at 411 nm, and the concentration of hydrogen peroxide was calculated applying the Beer-Lambert's law, with l = 1 cm, ε = 950 l mol^{-1} cm^{-1} and the dilution of the sample, d = 100.

$$C_{H_2O_2}(\text{mol dm}^{-3}) = \frac{A}{9.5}$$

4.4.2.5 Determination of Oxygen Evolved

In experiments involving molecular oxygen evolution, the volume of molecular oxygen evolved was measured using a thermostated burette. The reaction system was connected to a manometric burette filled with water which was saturated with oxygen prior to use. After certain time intervals, the pressure was equilibrated using a separation funnel by adjusting the water level to the same heights.

4.5 Syntheses

4.5.1 Synthesis of $[VO_2(pca)(hmpa)]$ (3)

To an aqueous solution (10 ml) of 1.18 g (10 mmol) NH_4VO_3, a dichloromethane solution (60 ml) of 1.24 g (10 mmol) of pcaH and 3.5 ml (20 mmol) of hmpa was added, giving rise to the formation of a biphasic system composed of a bright yellow aqueous phase and a light yellow organic phase. After 15 minutes of vigorous stirring, 2 ml of HBF_4 (40 % in water) were added, which caused the aqueous phase to turn orange and the organic phase to turn bright yellow. The organic phase was then decanted and dried over Na_2SO_4. Slow evaporation of this solution yielded yellow crystals of **3** which were recrystallized from a mixture of CH_2Cl_2 and diethyl ether. Yield: 3 g (77%). IR (KBr, cm^{-1}): 935w, 945w ($\nu_{V=O}$), 1181m (ν_{P-O}), 1682vs ($\nu_{C=O}$). ^1H NMR (400 MHz, $CDCl_3$): δ 2.7 (d, 18 H), 8.9 (d, 2 H), 9.4 (s, 1H). ^{31}P NMR (400 MHz, $CDCl_3$): δ 32.4 (s). ESI MS: m/z 385.9 $[\mathbf{3} + H]^+$. Analysis: Calc. for $C_{11}H_{21}N_5O_5P_1V_1$: C, 34.30; H, 5.49; N, 18.18. Found: C, 34.06; H, 5.51; N, 18.15.

4.5.2 Synthesis of $[(VO_2)_2(pdca)(hmpa)_2]$ (4)

Complex **4** was synthesized by the same method described for **3,** using 234 mg (2 mmol) of NH_4VO_3 in 10 ml of water, and 168 mg (1 mmol) of $pdcaH_2$ and 0.7 ml (4 mmol) of hmpa in 10 ml of dichloromethane; 0.3 ml of HBF_4 were added in the course of the reaction. Yield: 0.5 g (36%). IR (KBr, cm^{-1}): 942w ($\nu_{V=O}$), 1198m (ν_{P-O}), 1678vs ($\nu_{C=O}$). ^1H NMR (400 MHz, $CDCl_3$): δ 2.77 (d, 36 H), 9.3 (dd, 2 H). ^{31}P NMR (400 MHz, $CDCl_3$): δ 27.4 (s). ESI MS: m/z 712.9 [**4** + Na]$^+$. Analysis: Calc. for $C_{18}H_{38}N_8O_{10}P_2V_2$: C, 31.32; H, 5.55; N, 16.23. Found: C, 31.84; H, 5.74; N, 15.97.

4.5.3 Synthesis of $[VO_2(pycaH)(hmpa)]$ (5)

Complex **5** was synthesized by the same method described for **3**, using 1.17 g (10 mmol) of NH_4VO_3 in 10 ml of water, and 1.67 g (10 mmol) of $pydcaH_2$ and 3.5 ml (20 mmol) of hmpa in 50 ml of dichloromethane; 2 ml of HBF_4 were added in the course of the reaction. Yield: 2.5 g (88%). IR (KBr, cm^{-1}): 942m ($\nu_{V=O}$), 1191s (ν_{P-O}), 1689s ($\nu_{C=O}$). ^1H NMR (400 MHz, $CDCl_3$): δ 2.7 (d, 18 H), 8.27 (d, 1 H), 8.7 (dd, 1H), 9.65 (s, 1H). ^{31}P NMR (400 MHz, $CDCl_3$): δ 28.3 (s). ESI MS: m/z 428.25 [**3** + Na]$^+$. Analysis: Calc. for $C_{19}H_{40}N_7O_8P_2V$ (**5** + hmpa): C, 37.57.46; H, 6.64; N, 16.14. Found: C, 36.97; H, 6.76; N, 16.27.

4.5.4 Synthesis of $[(VO)_4(hptb)_2(H_2O)_2(\mu\text{-}O)]\ [ClO_4]_4$ and $[(VO)_4(hptb)_2(H_2O)_2(\mu\text{-}O)]\ [CF_3SO_3]_4$ (cation 6)

To a solution of hptbH (120 mg, 0.2 mmol) in methanol (20 ml) was added an excess (100 mg) of $NaClO_4 \cdot n\ H_2O$, and then $VOSO_4$ (75 mg, 0.4 mmol). This mixture was stirred at room temperature: After a few minutes the solution become clear, after a few hours, the colour had turned from blue to green. After a few weeks, green crystals had formed mixed with white crystals of $NaClO_4$. The green crystals (**6**[ClO_4]) were separated manually for X-ray crystal structure analysis. For the isolation of **6** devoid of $NaClO_4$, the triflate salt was prepared in the same way, using 75 mg of KCF_3SO_3 instead of $NaClO_4$; in this case a green, analytically pure powder of **6**[CF_3SO_3]$_4$ precipitated. Yield: 50 mg (11%). IR (KBr, cm^{-1}): 845.77w ($\nu_{V=O}$). Analysis: Calc. for $C_{74}F_{12}H_{70}N_{20}O_{21}S_4V_4$: C, 41.62; H, 3.30; N, 13.12. Found: C, 41.98; H, 3.92; N, 13.22.

4.5.5 Synthesis of $[(tmtacn)VOCl_2]$ (7)

To a solution of VCl_3 (160 mg, 1mmol) in 10 ml of acetonitrile was added dropwise a solution of 1,4,7-trimethyl-1,4,7-triazacyclononane (176 mg, 1 mmol) in 10 ml of acetonitrile under nitrogen atmosphere at 0°C. An immediate colour change from dark brown to deep violet was observed. After stirring at room temperature under nitrogen atmosphere for 30 minutes, the mixture was refluxed for 18 hours in the presence of air and the resulting deep green solution was cooled, filtered, and evaporated to give a green solid. After redissolution in acetonitrile and filtration, slow crystallization at room temperature yielded after one week blue crystals of **5**. Yield: 57 mg (18%) IR (KBr, cm^{-1}): 749.40m, 790.76m ($\nu_{V\text{-}N}$), 965.79s ($\nu_{V=O}$), 1061.66m

(ν_{C-N}); MS (electrospray, positive mode): 331.1 ($[M + Na]^+$); Analysis: Calc.for $C_9Cl_2H_{21}N_3OV$: C: 34.97; H: 6.85; N: 13.59.Found: C: 34.46; H: 6.78; N: 13.43.

4.5.6 Synthesis of $[NBu_4][V(cat)_3]$ (anion 8)

To an acetonitrile solution (50 ml) of catechol (1.4204 g, 0.0129 mol) and triethylamine (10 ml) were added 1.4683 g (0.0043 mol) of NBu_4VO_3. The color of the solution immediately changed from colorless to black-blue. The reaction solution was refluxed in a nitrogen atmosphere for 5 hours and the reaction mixture was evaporated to 1/3 of its volume, giving a dark blue precipitate of $[NBu_4]$**8** · 0.5 CH_3CN · 1.5 H_2O, which was filtered and washed five times with small amounts of acetonitrile. Yield: 0.9 g (11 %). IR (KBr, cm^{-1}): 871m (ν_{V-O}) ^1H NMR (400 MHz, acetone-d_6): δ 0.9602 (d, 12 H, CH_3), 1.4204 (m, 8 H, CH_2), 1.8961 (m, 8H, CH_2), 3.4260 (m, 8 H, CH_2), 6.2480 (d, 6 H), 6.7085 (t, 6 H). ESI MS: (negative mode) m/z 375.0 $[V(cat)_3]^-$, (positive mode) m/z 242.29 $[NBu_4]^+$. Analysis: Calc. for $C_{35}H_{52.5}N_{1.5}O_{7.5}V$: C, 63.20; H, 7.90; N, 3.16. Found: C, 63.26; H, 7.83; N, 3.20.

4.5.7 Synthesis of $[Fe_2(hptb)(\mu\text{-}OH)(NO_3)_2]\,[NO_3]_2 \cdot CH_3OH \cdot 2\,H_2O$ (cation 9) and $[Fe_2(tacn)_2(\mu\text{-}O)(CH_3CO_2)_2]\,(I)_2 \cdot 0.5\,CH_3CN$ (cation 10)

The compound $[Fe_2(hptb)(\mu\text{-}OH)(NO_3)_2]\,[NO_3]_2 \cdot CH_3OH \cdot 2\,H_2O$ was synthesized and characterized by Prof. Bernt Krebs (Münster, Germany) and Prof. Siegfried Schindler (Erlangen, Germany) [199] and given to us for catalytic tests. The compound $[Fe_2(tacn)_2(\mu\text{-}O)(CH_3CO_2)_2]I_2 \cdot 0.5\,CH_3CN$ was synthesized by us as

found in the literature [206]. Analysis: Calc. for $Fe_2I_2O_5N_{6.5}C_{17}H_{37.5}$: C, 26.23; H, 4.86; N, 11.69. Found: C, 26.02; H, 4.97; N, 11.32.

4.6 Crystallographic Data

Intensity data were collected on a Stoe Image Plate Diffraction system using MoK_α graphite monochromated radiation. The structure was solved by direct methods using the programme SHELXS-97 [221]. The refinement and all further calculations were carried out using SHELXL-97 [222]. The H-atoms were included in calculated positions and treated as riding atoms using SHELXL default parameters. The non-H atoms were refined anisotropically, using weighted full-matrix least-squares on F^2. Structure calculations, checking for higher symmetry and preparations of molecular plots were performed with the PLATON package [223]. Further experimental details are given in following tables. Data for compound **7** are included even if its structure was published by Fiedler *et al*. during our work [157].

List of atomic coordinates, anisotropic displacement parameters and crystallographic data have been deposited with the Cambridge Crystallographic Data Centre, CCDC no. 209749 for **3**, CCDC 209751 for **4**, CCDC 209750 for **5** and CCDC 209752 for **6**. Copies of this information may be obtained free of charge from the Director, CCDC, 12 Union Road, Cambridge CB2 1EZ, UK (Fax: +44-1223-336033; e-mail: deposit@ccdc.cam.ac.uk or www: http://www.ccdc.cam.ac.uk).

Table 4.5.1. Summary of X-ray single-crystal data for **3**.

Chemical formula	$C_{11}H_{21}N_5O_5PV$
Formula weight	385.24
Crystal system	Orthorhombic
Space group	P ca21
a (Å)	15.0443(14)
b (Å)	7.9632(8)
c (Å)	14.430(3)
α (°)	90
β (°)	90
γ (°)	90
V (Å^3)	1728.7(4)
Z	4
T (K)	153(2)
D_{calc} (g cm^{-3})	1.480
μ (mm^{-1})	0.696
Scan range (°)	$2.56 < 2\theta < 25.92$
Collected reflections	5710
Unique reflections	2717
R_{int}	0.0344
Final R indices[$I > 2\sigma(I)$]	0.0438, wR_2 0.0911
R indices (all data)	0.0616, wR_2 0.0929
Goodness-of-fit	1.516
Max/min Δρ (e Å^{-3})	0.422, –0.296

Table 4.5.2. Summary of X-ray single-crystal data for **4**.

Chemical formula	$C_{36}H_{76}N_{16}O_{20}P_4V_4$
Formula weight	690.38
Crystal system	Monoclinic
Space group	P 21/c
a (Å)	7.7084(6)
b (Å)	11.4712(11)
c (Å)	16.6926(14)
α (°)	90
β (°)	92.796(10)
γ (°)	90
V ($Å^3$)	1441.6(3)
Z	2
T (K)	153(2)
D_{calc} (g cm^{-3})	1.591
μ (mm^{-1})	0.823
Scan range (°)	$2.18 < 2\theta < 25.77$
Collected reflections	9835
Unique reflections	2642
R_{int}	0.1791
Final R indices[$I > 2\sigma(I)$]	0.2095, wR_2 0.4966
R indices (all data)	0.2606, wR_2 0.5161
Goodness-of-fit	1.166
Max/min $\Delta\rho$ (e $Å^{-3}$)	3.472, –1.038

Table 4.5.3. Summary of X-ray single-crystal data for **5**.

Chemical formula	$C_{38}H_{80}N_{14}O_{16}P_4V_2$
Formula weight	1214.92
Crystal system	Triclinic
Space group	P-1
a (Å)	13.383(2)
b (Å)	14.329(2)
c (Å)	16.053(2)
α (°)	103.778(18)
β (°)	97.791(18)
γ (°)	101.048(19)
V (Å^3)	2881.0(8)
Z	2
T (K)	153(2)
D_{calc} (g cm^{-3})	1.401
μ (mm^{-1})	0.508
Scan range (°)	$1.91 < 2\theta < 25.78$
Collected reflections	21859
Unique reflections	10237
R_{int}	0.1410
Final R indices[$I > 2\sigma(I)$]	0.0626, wR_2 0.1331
R indices (all data)	0.1629, wR_2 0.1601
Goodness-of-fit	0.783
Max/min $\Delta\rho$ (e Å^{-3})	0.436, –0.536

Table 4.5.4. Summary of X-ray single-crystal data for **6**.

Chemical formula	$C_{35}H_{30}N_{10}O_{12.5}V_2$
Formula weight	961.45
Crystal system	Triclinic
Space group	P-1
a (Å)	12.9187(14)
b (Å)	14.3458(16)
c (Å)	16.8609(19)
α (°)	71.831(13)
β (°)	68.359(13)
γ (°)	70.054(13)
V (Å^3)	2667.7(5)
Z	2
T (K)	293(2)
D_{calc} (g cm^{-3})	1.199
μ (mm^{-1})	0.508
Scan range (°)	$2.00 < 2\theta < 24.1$
Collected reflections	19564
Unique reflections	9740
R_{int}	0.1145
Final R indices[$I > 2\sigma(I)$]	0.0773, wR_2 0.1722
R indices (all data)	0.2042, wR_2 0.2141
Goodness-of-fit	0.724
Max/min $\Delta\rho$ (e Å^{-3})	0.783, –0.495

Table 4.5.5. Summary of X-ray single-crystal data for **7**.

Chemical formula	$C_9H_{21}Cl_2N_3VO$
Formula weight	309.13
Crystal system	monoclinic
Space group	P 21/n
a (Å)	7.999(2)
b (Å)	13.682(3)
c (Å)	12.845(3)
α (°)	90
β (°)	97.50(3)
γ (°)	90
V (Å^3)	1393.8(6)
Z	4
T (K)	293(2)
D_{calc} (g cm^{-3})	1.473
μ (mm^{-1})	1.080
Scan range (°)	$2.18 < 2\theta < 25.12$
Collected reflections	4856
Unique reflections	2469
R_{int}	0.0599
Final R indices[$I > 2\sigma(I)$]	0.0626, $wR_2 = 0.1679$
R indices (all data)	0.0688, $wR_2 = 0.1755$
Goodness-of-fit	1.129
Max/min Δρ (e Å^{-3})	0.738, −0.985

Summary

The aim of this work was, on the one hand, to study the catalytic activity of new vanadium(IV) and (V) complexes for the oxidative alkane functionalization and, on the other hand, to extend the study to iron(III) complexes in the spirit of mimicking monooxygenase enzymes.

In the first part of this work, we present our studies on the catalytic activity of two known vanadium(V)-containing polyoxomolybdates for the alkane oxidation with hydrogen peroxide as well as the synthesis of new vanadium(IV) and (V) complexes and their catalytic potential for the alkane oxidation with hydrogen peroxide. A complete kinetic study for the alkane oxidation with peroxyacetic acid catalyzed by vanadium(V) compounds is also presented.

The known non-lacunary anion $[PMo_{11}VO_{40}]^{4-}$ (**1**) and the known lacunary anion $[PMo_6V_5O_{39}]^{12-}$ (**2**) were tested in the catalytic oxidation of alkanes using cyclooctane as a model substrate. The major product obtained was cyclooctyl hydroperoxide, and the most efficient catalyst was **1** with a total TON of 1180 after 9 hours *versus* 420 for **2**. The addition of pcaH in a 10 : 1 ratio to vanadium did not enhance significantly the final TON of the cyclooctane oxidation catalyzed by **1** or **2**, but it enhanced the initial reaction rate in the case of **1** as catalyst, and it allowed to attain the highest cyclooctyl hydroperoxide concentration after 5 hours *versus* 9 hours in its absence. Methane and ethane were also oxidized with **1** as catalyst with a total TON of 1 and 14, respectively. Studies about the selectivity of the oxidation with **1** using *n*-octane, adamantane, *cis*- and *trans*-decalin and comparison of the results

obtained to that for systems which oxidize alkanes *via* hydroxyl radicals, showed that the system **1**-H_2O_2-O_2 proceeds also with formation of hydroxyl radicals. The mechanism proposed for the alkane oxidation by **1** involves the dissociation of **1** to give Mo-O-V moieties which are the actual catalytic species. The vanadium(V) centre can be reduced to vanadium(IV) by bonding one hydrogen peroxide molecule and yielding a hydroperoxyl radical, a step in which the Mo-O fragment can help the vanadium centre either enhancing its oxidizing ability or accepting a hydrogen atom from hydrogen peroxide. The vanadium(IV) formed will bond a second hydrogen peroxide molecule yielding a hydroxyl radical, which will attack the alkane to form the major product, alkyl hydroperoxide, and the secondary products, alcohol and ketone.

$$2\ H_2O_2 \xrightarrow{\text{Mo-O-V}} HO\cdot + HOO\cdot + H_2O$$

$$RH + HO\cdot \longrightarrow R\cdot + H_2O$$

$$R\cdot + O_2 \longrightarrow ROO\cdot$$

$$ROO\cdot + HOO\cdot \longrightarrow ROOH + O_2$$

$$2\ ROO\cdot \longrightarrow ROH + R_H{=}O + O_2$$

The new vanadium(V) complexes **3**, **4** and **5** were synthesized by mixing pyrazine-2-carboxylic acid (pcaH), pyrazine-2,5-dicarboxylic ($pdcaH_2$) or pyridine-2,5-dicarboxylic acid ($pycaH_2$) with ammonium vanadate in the correct metal to ligand ratio and in the presence of excessive hexamethylphosphoramide in dichloromethane as solvent. They were recrystallized from a mixture of dichloromethane and diethyl ether and analyzed by X-ray diffraction techniques.

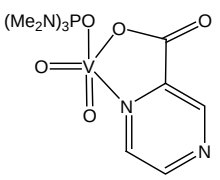

(**3**)

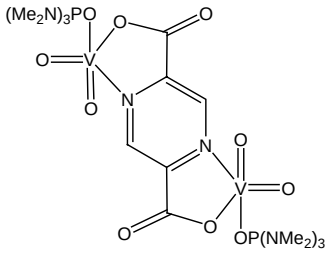

(**4**)

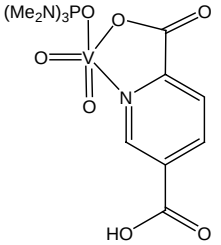

(**5**)

$$VO_3^- + pcaH + hmpa \longrightarrow [VO_2(pca)(hmpa)] + OH^-$$

(**3**)

$$2\ VO_3^- + pdcaH_2 + 2\ hmpa \longrightarrow [(VO_2)_2(pdca)(hmpa)_2] + 2\ OH^-$$

(**4**)

$$VO_3^- + pycaH_2 + hmpa \longrightarrow [VO_2(pycaH)(hmpa)] + OH^-$$

(**5**)

The new cation **6** was synthesized in the form of its perchlorate or triflate salt by the reaction of $VOSO_4$ with hptbH in methanol, the metal to ligand ratio being 2 : 1, in the presence of $NaClO_4 \cdot n\ H_2O$ or KCF_3SO_3. Green crystals of the perchlorate salt were structurally analyzed by X-ray diffraction techniques. The known vanadium(IV) complex **7** was synthesized by refluxing vanadium (III) chloride in wet acetonitrile with tmtacn in air. Blue crystals of **7** were obtained by recrystallization from acetonitrile and the X-ray analyses were done. The known vanadium(V) complex **8** was accessible as the tetrabutylammonium salt from [*n*-Bu_4N][VO_3] and catechol (1 : 3) in acetonitrile.

$$4\ [VO]^{2+} + 2\ hptbH + 3\ H_2O \longrightarrow [(VO)_4(hptb)_2(H_2O)_2(\mu\text{-}O)]^{4+} + 4\ H^+$$

(**6**)

$$2\ VCl_3 + 2\ tmtacn + H_2O + \tfrac{1}{2}\ O_2 \longrightarrow 2\ [VOCl_2(tmtacn)] + 2\ HCl$$

(**7**)

$$[VO_3]^- + 3\ catH_2 \longrightarrow [V(cat)_3]^- + 3\ H_2O$$

(**8**)

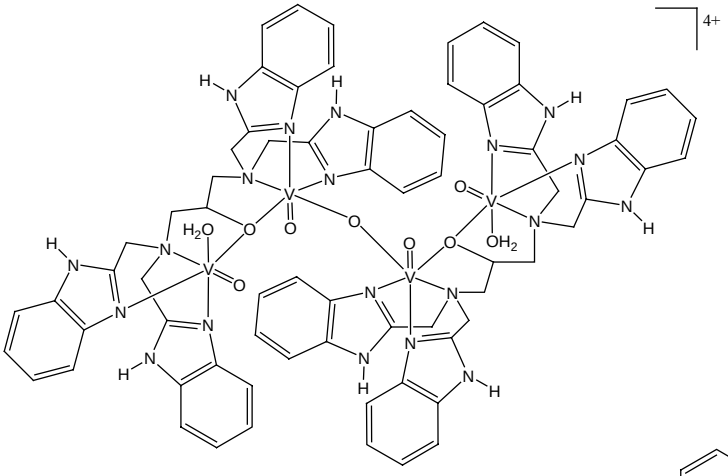

(**6**)

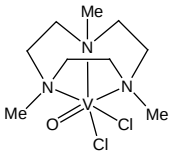

(**7**)

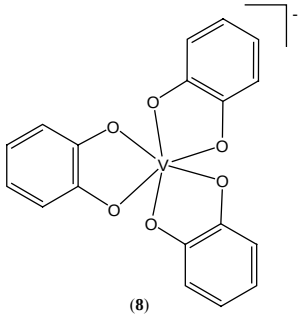

(**8**)

Complexes **3** to **8** were tested as catalysts for the cyclohexane oxidation with hydrogen peroxide and air in acetonitrile at 40 °C after 24 hours, using pcaH as co-catalyst in a 4 : 1 ratio with respect to vanadium. The most efficient catalysts turned out to be **3** and **5**, which oxidized cyclohexane with TONs of 1370 and 1440, respectively. The least efficient one was **7** which oxidizes cyclohexane with a TON of only 290. Complex **8** exhibits the highest initial rate, which can be explained assuming that catecholate ligands can be easily removed in the beginning of the reaction, reducing vanadium(V) to vanadium(IV), which will bind a molecule of hydrogen peroxide, producing a hydroxyl radical, the species which attacks the

alkane. The mechanism for the production of hydroxyl radicals by complexes **3** to **8** can be compared to that proposed for the system NBu_4VO_3-pcaH-H_2O_2-O_2.

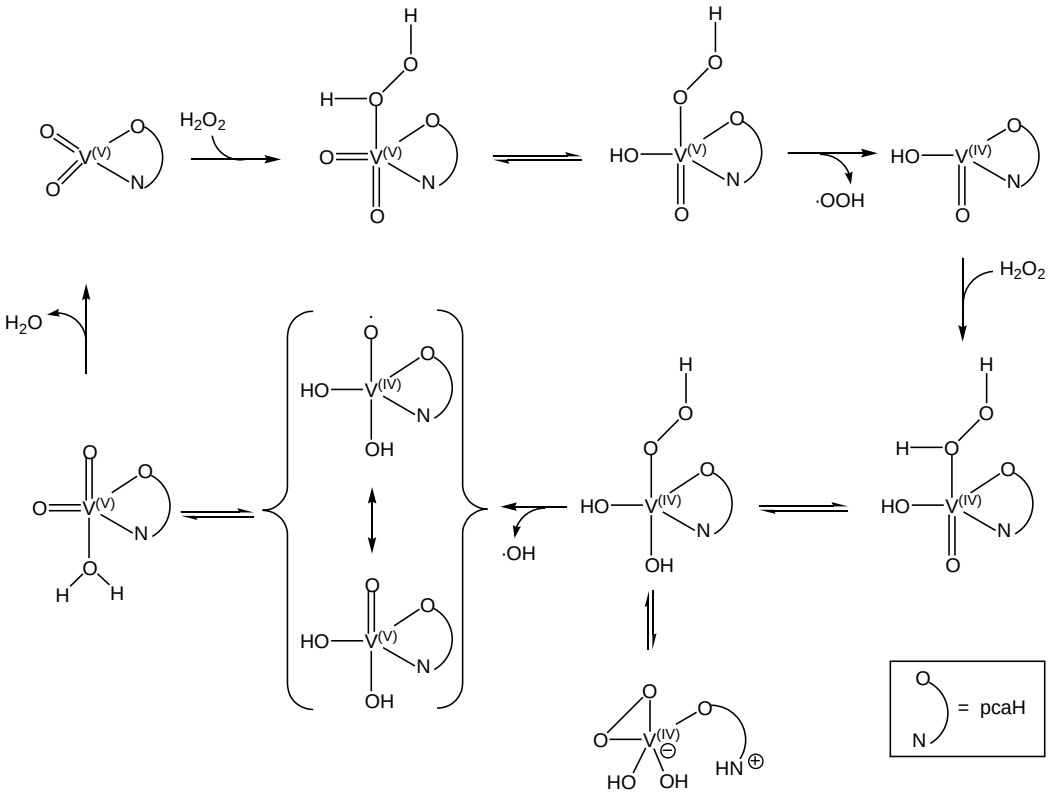

The alkane oxidation with peroxyacetic acid (paaH) and air catalyzed by *n*-tetrabutylammonium metavanadate has been studied kinetically. The conclusion is that vanadium(V), without needing any co-catalyst, reacts with paaH to give peroxyacetyl radicals, $CH_3COO\cdot$ which are the species that will attack the alkane giving an alkyl radical, which react with molecular oxygen from air to give the products: alkyl hydroperoxide, alcohol and ketone. Peroxyacetyl radicals react also with the solvent, acetonitrile or acetic acid, this reaction being in competition with the production of alkyl radicals from the alkane.

$$\text{“}V^{5+}\text{”} + CH_3C(O)OOH \rightleftharpoons \text{“}[V^{V}\text{–}OOC(O)CH_3]^{4+}\text{”} + H^{+}$$

$$\text{“}[V^{V}\text{–}OOC(O)CH_3]^{4+}\text{”} \longrightarrow \text{“}V^{4+}\text{”} + CH_3C(O)OO\cdot$$

$$\text{“}V^{4+}\text{”} + CH_3C(O)OOH \longrightarrow \text{“}V^{5+}\text{”} + CH_3C(O)O\cdot + OH^{-}$$

$$CH_3C(O)O\cdot + RH \longrightarrow R\cdot + CH_3C(O)OH$$

In the second part of this work we present our kinetic studies on the alkane oxidation with hydrogen peroxide and air using as catalysts simple iron(III) salts as well as two dinuclear iron(III) complexes which can be considered as models of methane monooxygenase and hemerythrin enzymes.

The iron(III) salts used as catalysts for the alkane oxidation were $Fe(ClO_4)_3$, $FeCl_3$ and $Fe(OAc)_2(OH)$. They differ inasmuch as, in the case of $Fe(ClO_4)_3$ and $FeCl_3$, the addition of pcaH decreases significantly the rate of the reaction, while $Fe(OAc)_2(OH)$ catalyzes the alkane oxidation only in the presence of pcaH. The selectivity parameters and the kinetic studies suggest that the catalysts $Fe(ClO_4)_3$ and $Fe(OAc)_2(OH)$ (this latter with pcaH as co-catalyst) produce hydroxyl radicals from hydrogen peroxide, which attack the alkane; however, in the case of $FeCl_3$ as catalyst, the oxidizing species formed is more selective than the hydroxyl radical, probably it is an oxoiron(IV) species. Both species, OH· and “$Fe^{IV}O$”, are formed from an iron(II) complex (accesible from the iron(III) salt after reaction with hydrogen peroxide) containing a number i of ligands L (with L = Cl^{-}, H_2O_2, H_2O).

$$[Fe(L)_i]^{2+} + H_2O_2 \rightleftharpoons [FeO(L)_i]^{2+} + H_2O$$
$$[Fe(L)_i]^{2+} + H_2O_2 \rightleftharpoons [Fe(L)_i]^{3+} + OH^{-} + OH\cdot$$

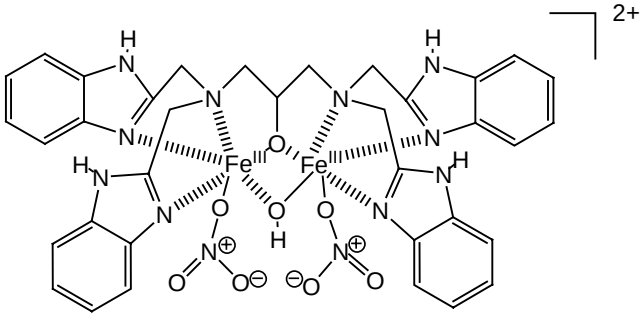

(**9**)

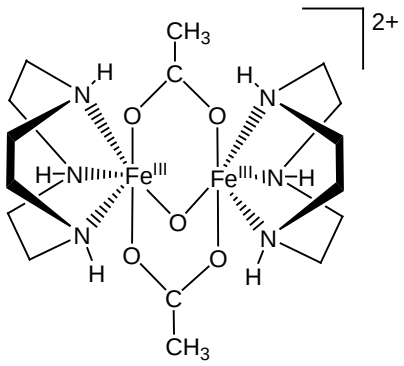

(**10**)

The cationic diiron(III) complexes **9** and **10** were tested as catalyst for the alkane oxidation with hydrogen peroxide and air. Both catalysts need the presence of an excess of pcaH as co-catalyst. It can be concluded from the kinetics that the dinuclear iron(III) core present in both complexes is reduced to iron(II) by hydrogen peroxide and reoxidized to give hydroxyl radicals, in a way reminiscent of that of Fenton's reagent. The hydroxyl radicals attack the alkane to produce an alkyl radical. The role of pcaH is thought to be to facilitate the proton transfer between the coordinated H_2O_2 molecule and ligands at iron centers, as in the case of the alkane oxidations catalyzed by the NBu_4VO_3–pcaH system.

$$[Fe^{III}\text{-}Fe^{III}]^{2+} + H_2O_2 \longrightarrow [Fe^{III}\text{-}Fe^{II}]^{+} + H^{+} + HOO\cdot$$

$$[Fe^{III}\text{-}Fe^{II}]^{+} + H_2O_2 \longrightarrow [Fe^{II}\text{-}Fe^{II}] + H^{+} + HOO\cdot$$

$$[Fe^{III}\text{-}Fe^{III}]^{2+} + HOO\cdot \longrightarrow [Fe^{III}\text{-}Fe^{II}]^{+} + H^{+} + O_2$$

$$HOO\cdot + HOO\cdot \longrightarrow H_2O_2 + O_2$$

$$[Fe^{III}\text{-}Fe^{II}]^{+} + H_2O_2 \longrightarrow [Fe^{III}\text{-}Fe^{III}]^{2+} + HO^{-} + HO\cdot$$

$$[Fe^{II}\text{-}Fe^{II}] + H_2O_2 \longrightarrow [Fe^{III}\text{-}Fe^{II}]^{+} + HO^{-} + HO\cdot$$

The mechanism postulated for the OH· radical formation from hydrogen peroxide catalyzed by **9** and **10** can be compared to that postulated for non-heme containing monooxygenases, like methane monooxygenase and hemerythrin. Therefore, complexes **9** and **10** can be considered as functional models for these two enzymes.

Résumé

Le but de ce travail était, d'une part, d'étudier l'activité catalytique des nouveaux complexes de vanadium(IV) et (V) pour la fonctionnalisation oxydante d'alcanes et, d'autre part, d'élargir l'étude aux complexes de fer(III) dans l'esprit de modeler des enzymes monooxygénases.

Dans la première partie de ce travail, nous présentons nos études sur l'activité catalytique de deux polyoxomolybdates connus, contenant du vanadium(V) pour l'oxydation d'alcanes avec du peroxyde d'hydrogène, aussi bien que la synthèse des nouveaux complexes de vanadium(IV) et (V), ainsi que leur potentiel catalytique pour l'oxydation d'alcanes avec du peroxyde d'hydrogène. Une étude cinétique complète sur l'oxydation d'alcanes avec de l'acide peroxyacétique catalysée par des composés de vanadium(V) est également présentée.

L'anion non-lacunaire connu $[PMo_{11}VO_{40}]^{4-}$ (**1**) et l'anion lacunaire connu $[PMo_6VO_{39}]^{12-}$ (**2**) ont été examinés dans l'oxydation catalytique des alcanes en utilisant le cyclooctane comme substrat modèle. Le produit principal obtenu était l'hydroperoxyde de cyclooctyl, et le catalyseur le plus efficace étant **1** avec un TON total de 1180 après 9 heures contre 420 pour **2**. L'addition de pcaH dans un rapport 10 : 1 au vanadium n'a pas augmenté de manière significative le TON final de l'oxydation de cyclooctane catalysée par **1** ou **2**, mais il a augmenté la vitesse initial de réaction dans le cas de **1** comme catalyseur, et il a permis d'atteindre la concentration la plus élevée en hydroperoxyde de cyclooctyl après 5 heures, par rapport à 9 heures en son absence. Le méthane et l'éthane ont été également oxydés avec **1** comme catalyseur

avec un TON total de 1 et de 14, respectivement. Des études au niveau de la sélectivité de l'oxydation avec **1** utilisant *n*-octane, adamantane, *cis* et *trans*-décaline ainsi que la comparaison de nos résultats avec ceux pour les systèmes oxydant les alcanes par l'intermédiaire de radicaux hydroxyles, prouvent que le système **1**-H_2O_2-O_2 se poursuit également par la formation des radicaux hydroxyles. Le mécanisme proposé pour l'oxydation d'alcanes par **1** implique la dissociation de **1** pour donner des fragments Mo-O-V qui sont les espèces catalytiques réelles. Le centre de vanadium(V) peut être réduit en vanadium(IV) par interaction avec une molécule de peroxyde d'hydrogène et en rapportant un radical hydroperoxyle, une étape dans laquelle le fragment de Mo-O peut aider le centre de vanadium à augmenter sa capacité oxydative ou accepter un atome d'hydrogène d'une molécule de peroxyde d'hydrogène. Le vanadium(IV) formé, lie une deuxième molécule de peroxyde d'hydrogène formant un radical hydroxyle, qui attaquera l'alcane pour donner le produit principal, l'hydroperoxyde d'alkyle, et les produits secondaires, l'alcool et la cétone.

$$2\ H_2O_2 \xrightarrow{\text{Mo-O-V}} HO\cdot + HOO\cdot + H_2O$$

$$RH + HO\cdot \longrightarrow R\cdot + H_2O$$

$$R\cdot + O_2 \longrightarrow ROO\cdot$$

$$ROO\cdot + HOO\cdot \longrightarrow ROOH + O_2$$

$$2\ ROO\cdot \longrightarrow ROH + R_H{=}O + O_2$$

Les nouveaux complexes de vanadium(V) **3**, **4** et **5** ont été synthétisés en mélangeant l'acide pyrazine-2-carboxylique (pcaH), l'acide pyrazine-2,5-dicarboxylique ($pdcaH_2$) ou l'acide pyridine-2,5-dicarboxylique ($pycaH_2$) au vanadate d'ammonium dans un rapport métal / ligand correct et en présence d'un excès d'

hexaméthylphosphoramide dans le dichlorométhane. La cristallisation a lieu dans un mélange de dichlorométhane et d'éther diéthylique et les cristaux ont été analysés par diffraction aux rayons-X.

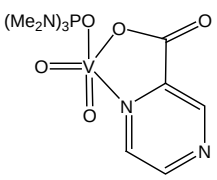

(**3**)

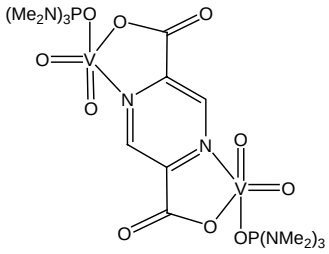

(**4**)

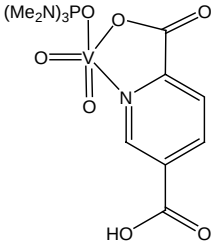

(**5**)

$$VO_3^- + pcaH + hmpa \longrightarrow [VO_2(pca)(hmpa)] + OH^-$$

(**3**)

$$2\ VO_3^- + pdcaH_2 + 2\ hmpa \longrightarrow [(VO_2)_2(pdca)(hmpa)_2] + 2\ OH^-$$

(**4**)

$$VO_3^- + pycaH_2 + hmpa \longrightarrow [VO_2(pycaH)(hmpa)] + OH^-$$

(**5**)

Le nouveau cation **6** a été synthétisé sous forme de sel de perchlorate ou sel de triflate par la réaction de $VOSO_4$ avec le hptbH en méthanol, le rapport métal au ligand étant 2 : 1, en présence de $NaClO_4 \cdot n\ H_2O$ ou KCF_3SO_3. Des cristaux verts de sel de perchlorate ont été structurellement analysés par diffraction aux rayons-X. Le complexe de vanadium(IV) connu **7** a été synthétisé en chauffant à reflux le chlorure du vanadium (III) dans l'acétonitrile humide avec le tmtacn à l'air. Des cristaux bleus de **7** ont été obtenus par recristallisation dans l'acétonitrile et les analyses aux rayons-X ont été effectuées. Le complexe de vanadium(V) connu **8** est accessible en tant que

le sel de tétrabutylammonium à partir de [*n*-Bu_4N][VO_3] et catéchol (1 : 3) dans l'acétonitrile.

$$4\ [VO]^{2+} + 2\ hptbH + 3\ H_2O \longrightarrow [(VO)_4(hptb)_2(H_2O)_2(\mu\text{-}O)]^{4+} + 4\ H^+$$

(**6**)

$$2\ VCl_3 + 2\ tmtacn + H_2O + \tfrac{1}{2}\ O_2 \longrightarrow 2\ [VOCl_2(tmtacn)] + 2\ HCl$$

(**7**)

$$[VO_3]^- + 3\ catH_2 \longrightarrow [V(cat)_3]^- + 3\ H_2O$$

(**8**)

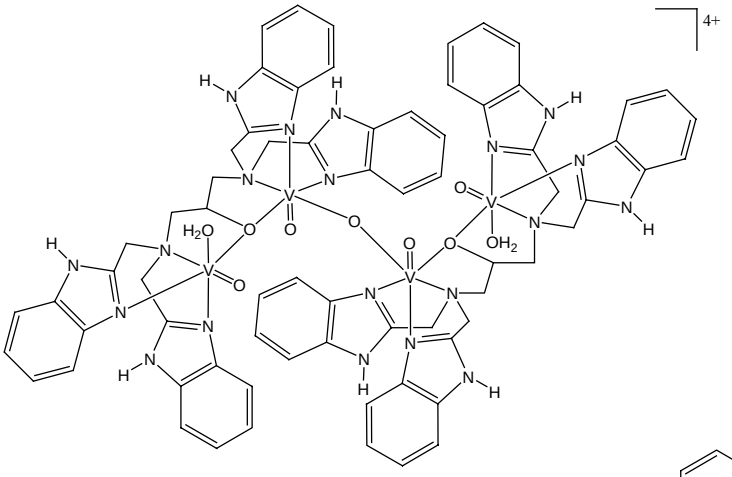

(**6**)

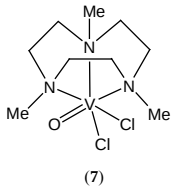

(**7**)

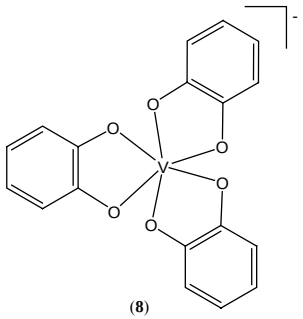

(**8**)

Les complexes **3** à **8** ont été examinés comme catalyseurs pour l'oxydation du cyclohexane avec du peroxyde d'hydrogène, à l'air, dans l'acétonitrile, à 40 °C et après 24 heures, en utilisant pcaH comme co-catalyseur dans un rapport 4 : 1 avec le vanadium. Les catalyseurs les plus efficaces se sont avérés être **3** et **5**, qui ont oxydé

le cyclohexane avec des TONs de 1370 et de 1440, respectivement. Le moins efficace était **7** qui oxyde le cyclohexane avec un TON de seulement 290. Le complexe **8** montre le taux initial le plus élevé, ce qui peut être expliqué supposant que des ligands de catécholate peuvent être facilement enlevés au début de la réaction, transformant le vanadium(V) en vanadium(IV), qui liera une molécule de peroxyde d'hydrogène, produisant un radical hydroxyle, l'espèce qui attaque l'alcane. Le mécanisme pour la production des radicaux hydroxyles par les complexes **3** à **8** peut être comparé au mécanisme proposé pour le système NBu_4VO_3-pcaH-H_2O_2-O_2.

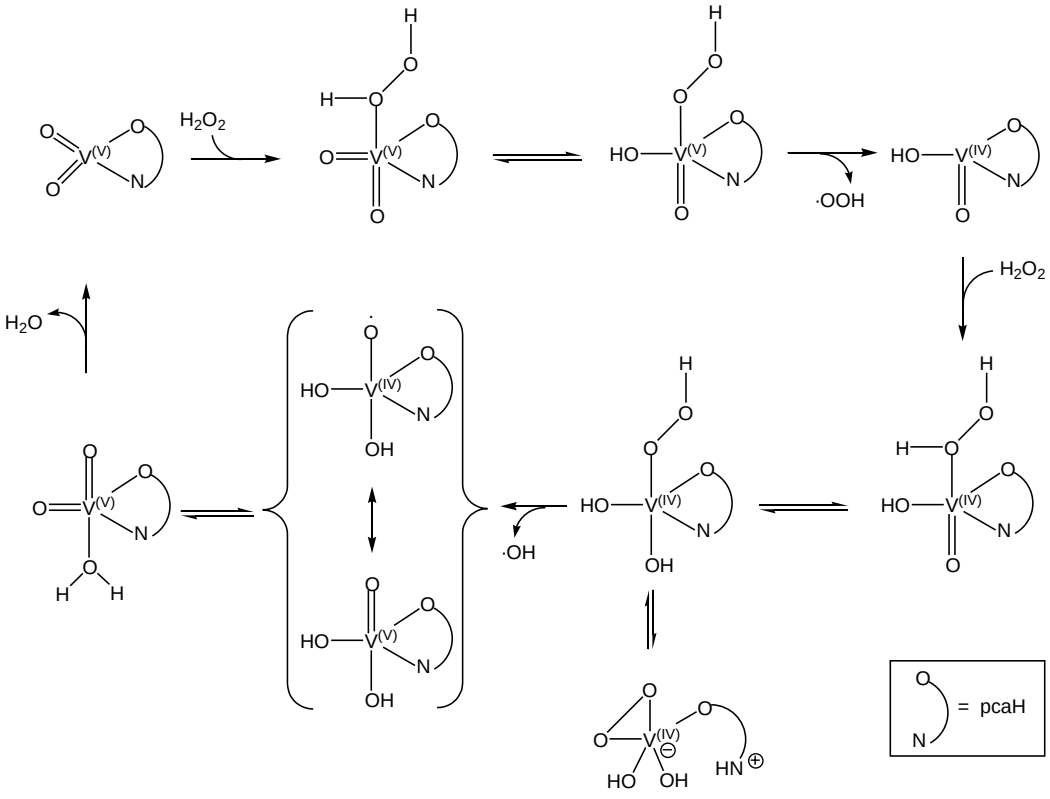

L'oxydation d'alcanes avec de l'acide peroxyacétique (paaH) et l'air catalysée par le métavanadate de *n*-tétrabutylammonium a été étudiée cinétiquement. La conclusion est que le vanadium(V), sans avoir besoin d'un co-catalyseur, réagit avec

paaH en donnant des radicaux de acétyle, $CH_3C(O)O\cdot$, ce qui sont les espèces qui attaqueront l'alcane en formant un radical alkyle, qui réagira avec l'oxygène moléculaire de l'air pour donner les produits: hydroperoxyde d'alkyle, alcool et cétone. Les radicaux de acétyle réagissent également avec le solvant, l'acétonitrile ou l'acide acétique, étant donné que cette reaction est en concurrence avec la production des radicaux alkyliques à partir d'alcane.

$$\text{“}V^{5+}\text{”} + CH_3C(O)OOH \rightleftharpoons \text{“}[V^{V}\text{–}OOC(O)CH_3]^{4+}\text{”} + H^+$$

$$\text{“}[V^{V}\text{–}OOC(O)CH_3]^{4+}\text{”} \longrightarrow \text{“}V^{4+}\text{”} + CH_3C(O)OO\cdot$$

$$\text{“}V^{4+}\text{”} + CH_3C(O)OOH \longrightarrow \text{“}V^{5+}\text{”} + CH_3C(O)O\cdot + OH^-$$

$$CH_3C(O)O\cdot + RH \longrightarrow R\cdot + CH_3C(O)OH$$

Dans la deuxième partie de ce travail nous présentons nos études cinétiques sur l'oxydation d'alcanes avec le peroxyde d'hydrogène et l'air en utilisant des sels simples de fer(III) comme catalyseurs aussi bien que deux complexes dinucléaires de fer(III) qui peuvent être considérés comme modèles des enzymes méthane monooxygénase et hémérythrine. Les sels de fer(III) utilisés comme catalyseurs pour l'oxydation d'alcanes sont $Fe(ClO_4)_3$, $FeCl_3$ et $Fe(OAc)_2(OH)$. Les résultats diffèrent puisque, dans le cas de $Fe(ClO_4)_3$ et de $FeCl_3$, l'addition de pcaH diminue de manière significative la vitesse de la réaction, alors que $Fe(OAc)_2(OH)$ catalyse l'oxydation d'alcanes seulement en présence du pcaH. Les paramètres de sélectivité et les études cinétiques suggèrent que les catalyseurs $Fe(ClO_4)_3$ et $Fe(OAc)_2(OH)$ (ce dernier avec pcaH comme co-catalyseur) produisent des radicaux hydroxyles à partir du peroxyde d'hydrogène, qui attaquent l'alcane; cependant, dans le cas de $FeCl_3$ comme catalyseur, l'espèce oxydante formée est plus sélective que le radical hydroxyle, qui

doit être probablement une espèce d'oxofer(IV). Les deux espèces, OH· et "$Fe^{IV}O$", sont formés à partir d'un complexe de fer(II) (accessible du sel de fer(III) après la réaction avec du peroxyde d'hydrogène) et contenant un numéro i des ligands L (avec L = Cl^-, H_2O_2, H_2O).

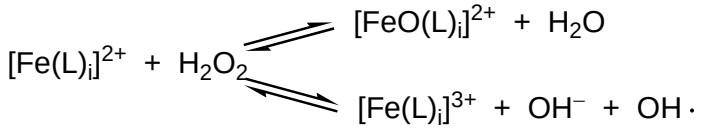

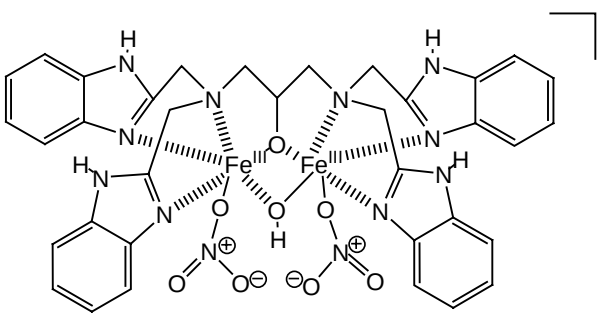

(**9**)

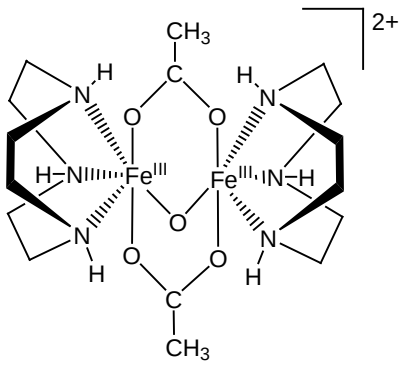

(**10**)

Les complexes cationiques de fer(III) **9** et **10** ont été examinés comme catalyseurs pour l'oxydation d'alcanes avec du peroxyde d'hydrogène et l'air. Les deux catalyseurs ont besoin de la présence d'un excès de pcaH comme co-catalyseur. Nous pouvons conclure de la cinétique, que le centre dinucléaire de fer(III) dans les deux complexes est réduit en fer(II) par le peroxyde d'hydrogène et oxydé de nouveau pour donner des radicaux hydroxyle, d'une manière rappellant celle du réactif de Fenton. Les radicaux hydroxyle attaquent l'alcane pour produire un radical d'alkyle. Le rôle de pcaH est probablement de faciliter le transfert de proton entre la molécule de H_2O_2 et les ligands coordinnés aux centres de fer, comme dans le cas des oxydations d'alcanes catalysées par le système NBu_4VO_3-pcaH.

$$[Fe^{III}\text{-}Fe^{III}]^{2+} + H_2O_2 \longrightarrow [Fe^{III}\text{-}Fe^{II}]^{+} + H^{+} + HOO\cdot$$

$$[Fe^{III}\text{-}Fe^{II}]^{+} + H_2O_2 \longrightarrow [Fe^{II}\text{-}Fe^{II}] + H^{+} + HOO\cdot$$

$$[Fe^{III}\text{-}Fe^{III}]^{2+} + HOO\cdot \longrightarrow [Fe^{III}\text{-}Fe^{II}]^{+} + H^{+} + O_2$$

$$HOO\cdot + HOO\cdot \longrightarrow H_2O_2 + O_2$$

$$[Fe^{III}\text{-}Fe^{II}]^{+} + H_2O_2 \longrightarrow [Fe^{III}\text{-}Fe^{III}]^{2+} + HO^{-} + HO\cdot$$

$$[Fe^{II}\text{-}Fe^{II}] + H_2O_2 \longrightarrow [Fe^{III}\text{-}Fe^{II}]^{+} + HO^{-} + HO\cdot$$

Le mécanisme postulé pour la formation de radicaux OH· à partir du peroxyde d'hydrogène, catalysée par **9** et **10**, peut être comparé à celui postulé pour les non-hèmes monooxygénases, comme la méthane monooxygenase et l'hémérythrine. Par conséquent, les complexes **9** et **10** peuvent être considérés comme modèles fonctionnels pour ces deux enzymes.

Resumen

La finalidad de este trabajo era, por una parte, estudiar la actividad catalítica de nuevos complejos de vanadio(IV) y (V) para la funcionalización oxidante de alcanos y, por otra parte, ampliar el estudio a complejos de hierro(III) con la finalidad de modelizar enzimas monooxigenasas.

En la primera parte de este trabajo, presentamos nuestra investigación sobre la actividad catalítica en la oxidación de alcanos con peróxido de hidrógeno de dos polioxomolibdatos conocidos que contienen vanadio(V) así como la síntesis de nuevos complejos de vanadio(IV) y (V) y de su potencial catalítico para la oxidación de alcanos con peróxido de hidrógeno. También se presenta un estudio cinético completo sobre la oxidación de alcanos con el ácido peroxiacético catalizada por compuestos de vanadio(V).

El anión saturado conocido $[PMo_{11}VO_{40}]^{4-}$ (**1**) y el anión insaturado conocido $[PMo_6VO_{39}]^{12-}$ (**2**) fueron probados como catalizadores en la oxidación de alcanos con el ciclooctano como sustrato modelo. El producto principal obtenido fue hidroperóxido de ciclooctilo, siendo **1** el catalizador más eficiente con un TON total de 1180 después de 9 horas contra 420 para **2**. La adición de pcaH en una relación de 10 : 1 respecto al vanadio no aumenta perceptiblemente el TON final de la oxidación de ciclooctano catalizada por **1** o **2**, sino que aumenta la velocidad inicial de la reacción en el caso de **1** como catalizador, y permitió lograr la concentración más alta de hidroperóxido de ciclooctilo después de 5 horas frente a 9 horas en su ausencia. El metano y el etano también fueron oxidados usando **1** como catalizador con un TON

total de 1 y 14, respectivamente. Los estudios sobre la selectividad de la oxidación con **1** usando como sustratos *n*-octano, adamantano, y *cis*- y *trans*-decalina y la comparación de los resultados obtenidos con aquellos para los sistemas que oxidan alcanos mediante la formación de radicales oxhidrilo, demuestra que el sistema **1**-H_2O_2-O_2 da lugar también a la formación de radicales oxhidrilo. El mecanismo propuesto para la oxidación de alcanos por **1** implica la disociación de **1** para dar fragmentos Mo-O-V que son las especies catalíticas reales. El átomo de vanadio(V) se puede reducir a vanadio(IV) enlazando una molécula de peróxido de hidrógeno y dando un radical hidroperoxilo, un paso en el cual el fragmento Mo-O puede ayudar al vanadio realzando su capacidad oxidante o aceptando un átomo de hidrógeno del peróxido de hidrógeno. El vanadio(IV) formado enlazará una segunda molécula de peróxido de hidrógeno dando un radical oxhidrilo, que atacará el alcano para formar el producto principal, el hidroperóxido de alquilo, y los productos secundarios, el alcohol y la cetona.

$$2\ H_2O_2 \xrightarrow{\text{Mo-O-V}} HO\cdot + HOO\cdot + H_2O$$

$$RH + HO\cdot \longrightarrow R\cdot + H_2O$$

$$R\cdot + O_2 \longrightarrow ROO\cdot$$

$$ROO\cdot + HOO\cdot \longrightarrow ROOH + O_2$$

$$2\ ROO\cdot \longrightarrow ROH + R_H{=}O + O_2$$

Los nuevos complejos de vanadio(V) **3**, **4** y **5** fueron sintetizados mezclando el ácido pirazin-2-carboxílico (pcaH), pirazin-2,5-dicarboxilico (pdcaH2) o el ácido piridin-2,5-dicarboxilico (pycaH2) con el vanadato de amonio en la proporción metal : ligando correcta y en la presencia de un exceso de hexametilfosforamida en

diclorometano como disolvente. Fueron recristalizados en una mezcla de diclorometano y dietiléter y analizados por técnicas de difracción de rayos X.

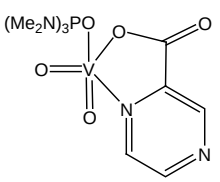

(**3**)

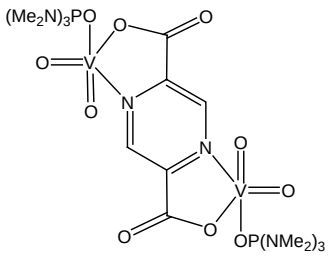

(**4**)

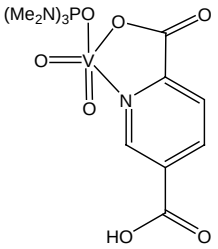

(**5**)

$$VO_3^- + pcaH + hmpa \longrightarrow [VO_2(pca)(hmpa)] + OH^-$$

(**3**)

$$2\ VO_3^- + pdcaH_2 + 2\ hmpa \longrightarrow [(VO_2)_2(pdca)(hmpa)_2] + 2\ OH^-$$

(**4**)

$$VO_3^- + pycaH_2 + hmpa \longrightarrow [VO_2(pycaH)(hmpa)] + OH^-$$

(**5**)

El nuevo catión **6** fue sintetizado en la forma de sal de perclorato o sal de triflato por reacción de $VOSO_4$ con el hptbH en metanol, siendo la proporción entre metal y ligando de 2 : 1, en la presencia de $NaClO_4 \cdot n\ H_2O$ o KCF3SO3. Los cristales verdes de la sal de perclorato fueron analizados estructuralmente por técnicas de difracción de rayos X. El complejo de vanadio(IV) conocido **7** fue sintetizado por reacción al aire del cloruro de vanadio (III) con tmtacn en acetonitrilo a reflujo. Los cristales azules de **7** fueron obtenidos por recristalización en acetonitrilo y analizados por difracción de rayos X. El complejo de vanadio(V) conocido **8** es accesible como

sal de tetrabutilamonio por reacción entre [*n*-Bu_4N][VO_3] y catecol (1 : 3) en acetonitrilo.

$$4\ [VO]^{2+} + 2\ hptbH + 3\ H_2O \longrightarrow [(VO)_4(hptb)_2(H_2O)_2(\mu\text{-}O)]^{4+} + 4\ H^+$$

(**6**)

$$2\ VCl_3 + 2\ tmtacn + H_2O + \tfrac{1}{2}\ O_2 \longrightarrow 2\ [VOCl_2(tmtacn)] + 2\ HCl$$

(**7**)

$$[VO_3]^- + 3\ catH_2 \longrightarrow [V(cat)_3]^- + 3\ H_2O$$

(**8**)

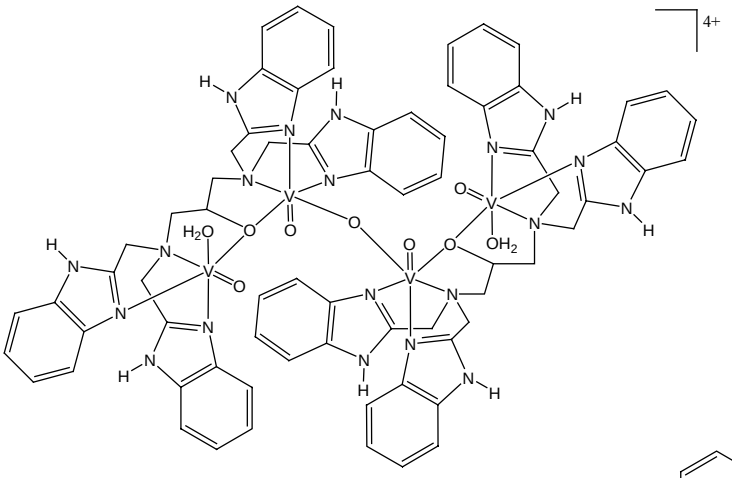

(**6**)

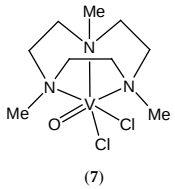

(**7**)

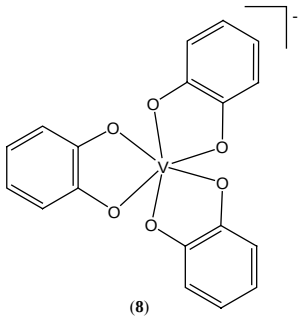

(**8**)

Los complejos **3** a **8** fueron probados como catalizadores en la oxidación de ciclohexano con peróxido de hidrógeno y aire en acetonitrilo a 40 °C después de 24 horas, usando pcaH como co-catalizador en una proporción de 4 : 1 con respecto al vanadio. Los catalizadores más eficientes resultaron ser **3** y **5**, que oxidaron el

ciclohexano con TON de 1370 y 1440, respectivamente. El catalizador menos eficiente fue **7** que oxida el ciclohexano con un TON de solamente 290. El complejo **8** exhibe la velocidad inicial más alta, que puede ser explicada si se asume que los ligandos catecolato se pueden descoordinar fácilmente en el principio de la reacción, reduciendo el vanadio(V) a vanadio(IV), que coordinará una molécula de peróxido de hidrógeno, produciendo un radical oxhidrilo, la especie que ataca el alcano. El mecanismo para la producción de los radicales oxhidrilo por los complejos **3** a **8** se puede comparar al propuesto para el sistema NBu_4VO_3-pcaH-H_2O_2-O_2.

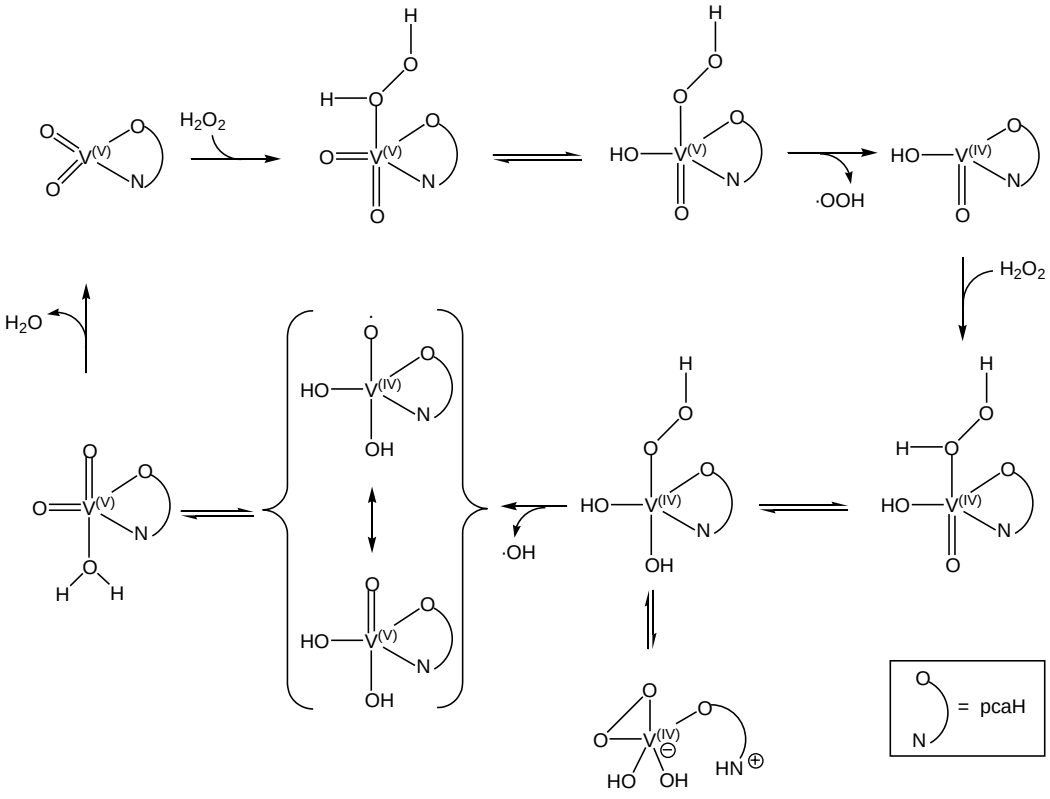

La oxidación de alcanos con el ácido peroxiacético (paaH) y aire catalizada por el metavanadato de *n*-tetrabutilamonio se ha estudiado cinéticamente. La conclusión es que el vanadio(V), sin necesitar ningún co-catalizador, reacciona con el

paaH dando radicales acetilo, $CH_3C(O)O\cdot$ que son las especies que atacarán el alcano dando un radical alquilo, que reacciona con oxígeno molecular proveniente del aire para dar los productos: hidroperóxido de alquilo, alcohol y cetona. Los radicales acetilo reaccionan también con el disolvente, acetonitrilo o ácido acético, estando esta reacción en competición con la producción de radicales alquilo a partir del alcano.

$$\text{“}V^{5+}\text{”} + CH_3C(O)OOH \rightleftharpoons \text{“}[V^{V}\text{–}OOC(O)CH_3]^{4+}\text{”} + H^{+}$$

$$\text{“}[V^{V}\text{–}OOC(O)CH_3]^{4+}\text{”} \longrightarrow \text{“}V^{4+}\text{”} + CH_3C(O)OO\cdot$$

$$\text{“}V^{4+}\text{”} + CH_3C(O)OOH \longrightarrow \text{“}V^{5+}\text{”} + CH_3C(O)O\cdot + OH^{-}$$

$$CH_3C(O)O\cdot + RH \longrightarrow R\cdot + CH_3C(O)OH$$

En la segunda parte de este trabajo presentamos nuestros estudios cinéticos en la oxidación de alcanos con el peróxido de hidrógeno y aire usando sales simples de hierro(III) como catalizadores así como dos complejos dinucleares de hierro(III) que pueden considerarse como modelos de enzimas monooxigenasas, como la metano monooxigenasa y la hemeritrina.

Las sales de hierro(III) usadas como catalizadores para la oxidación de alcanos son $Fe(ClO_4)_3$, $FeCl_3$ y $Fe(OAc)_2(OH)$. Se diferencian ya que en el caso de $Fe(ClO_4)_3$ y de $FeCl_3$, la adición de pcaH disminuye perceptiblemente la velocidad de la reacción, mientras que $Fe(OAc)_2(OH)$ cataliza la oxidación de alcanos solamente en la presencia de pcaH. Los parámetros de la selectividad y los estudios cinéticos sugieren que los catalizadores $Fe(ClO_4)_3$ y $Fe(OAc)_2(OH)$ (este último con pcaH como co-catalizador) producen radicales oxhidrilo a partir del peróxido de hidrógeno, que atacan el alcano; sin embargo, en el caso de $FeCl_3$ como catalizador, la especie

oxidante formada es más selectiva que el radical oxhidrilo y es probablemente una especie de oxohierro(IV). Ambas especies, OH· y "$Fe^{IV}O$", se forman a partir de un complejo de hierro(II) (formado por reducción a partir de la sal de hierro(III) después de la reacción con el peróxido de hidrógeno) que contiene un número i de ligandos L (con L = Cl^-, H_2O_2, H_2O).

$$[Fe(L)_i]^{2+} + H_2O_2 \rightleftharpoons [FeO(L)_i]^{2+} + H_2O$$
$$[Fe(L)_i]^{2+} + H_2O_2 \rightleftharpoons [Fe(L)_i]^{3+} + OH^- + OH\cdot$$

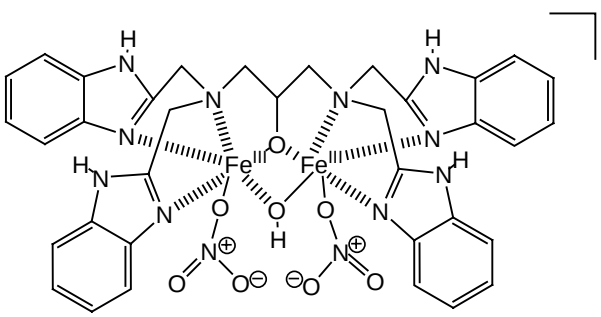

(**9**)

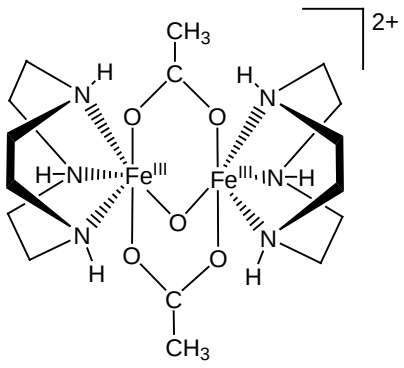

(**10**)

Los complejos catiónicos de hierro(III) **9** y **10** fueron probados como catalizadores para la oxidación de alcanos con el peróxido de hidrógeno y el aire. Ambos catalizadores necesitan la presencia de un exceso de pcaH como co-catalizador. Puede concluirse de la cinética que el centro dinuclear de hierro(III) presente en ambos complejos es reducido a hierro(II) por el peróxido de hidrógeno y oxidada de nuevo para dar radicales oxhidrilo, de una manera similar al reactivo de Fenton. Los radicales oxhidrilo atacan el alcano para producir un radical alquilo. El papel del pcaH parece ser el de facilitar la transferencia de protón entre la molécula de H_2O_2 y los ligandos coordinados a los átomos de hierro, del mismo modo que en el caso de las oxidaciones de alcanos catalizadas por el sistema NBu_4VO_3-pcaH.

$$[Fe^{III}\text{-}Fe^{III}]^{2+} + H_2O_2 \longrightarrow [Fe^{III}\text{-}Fe^{II}]^{+} + H^{+} + HOO\cdot$$

$$[Fe^{III}\text{-}Fe^{II}]^{+} + H_2O_2 \longrightarrow [Fe^{II}\text{-}Fe^{II}] + H^{+} + HOO\cdot$$

$$[Fe^{III}\text{-}Fe^{III}]^{2+} + HOO\cdot \longrightarrow [Fe^{III}\text{-}Fe^{II}]^{+} + H^{+} + O_2$$

$$HOO\cdot + HOO\cdot \longrightarrow H_2O_2 + O_2$$

$$[Fe^{III}\text{-}Fe^{II}]^{+} + H_2O_2 \longrightarrow [Fe^{III}\text{-}Fe^{III}]^{2+} + HO^{-} + HO\cdot$$

$$[Fe^{II}\text{-}Fe^{II}] + H_2O_2 \longrightarrow [Fe^{III}\text{-}Fe^{II}]^{+} + HO^{-} + HO\cdot$$

El mecanismo postulado para la formación de OH· a partir del peróxido de hidrógeno catalizada por **9** y **10** se puede comparar al postulado para las monooxigenasas que no contienen grupos hemo, como la metano monooxigenasa y la hemeritrina. Por lo tanto, los complejos **9** y **10** se pueden considerar como modelos funcionales de estas dos enzimas.

References

[1] (a) *Chemicals from Petroleum*, Waddams, A. L. (Ed.), Gulf Publ. Co, Houston, **1980**. (b) Absi-Halabi, M., Stanislaus, A., Qabazard, H., *Hydrocarbon processing*, Feb. **1997**, 45. (c) Weirauch, W., *Hydrocarbon Processing* **1997**, 23. (d) Weirauch, W., *Hydrocarbon Processing* **1997**, 27. (e) Manning, T. J., *Hydrocarbon Processing*, May **1997**, 85. (f) *Industrial Gases in Petrochemical Processing*, Gunardson, H., (Ed.), Dekker, New York, **1997**. (g) Morse, P. M., *Chem. & Eng. News* **1998**, *23*, 17. (h) *Natural Gas Conversion V*, Parmaliana, A., Sanfilippo, D., Frusteri, F., Vaccari, A., Arena, F. (Eds.), Elsevier, Amsterdam, **1998**. (i) Sedriks, W. *CHEMTECH*, Feb. **1998**, 47. (j) Wiltshire, J., *The Chemical Engineer*, 12 March **1998**, 20.

[2] (a) Nelson, C. R., Li, W., Lazar, I. M., Larson, K. H.; Malik, A., Lee, M. L., *Energy & Fuels* **1998**, *12*, 277. (b) Bonfanti, L., Comellas, L., Liberia, J., Vallhonrat-Matalonga, R., Pich-Santacna, M., Lopez-Pinol, D. J., *Anal. Appl. Pyrolysis* **1997**, *44*, 89. (c) Lapidus, A. L., Krylova, A. L., Eliseev, O.L., Khudyakov, D. S., *Khim. Tverd. Topl*. 1998, No. 1, 3 (in Russian).

[3] Demirel, B., Wiser, W. H., *Fuel Process. Technol*. **1998**, *55*, 83.

[4] *Industrielle Organische Chemie* Weissermel, K., Arpe, H.-J. (Eds.), Verlag Chemie, Weinheim, Germany, **1978**, 77.

[5] *Industrielle Organische Chemie* Weissermel, K., Arpe, H.-J. (Eds.), Verlag Chemie, Weinheim, Germany **1978**, 51.

[6] Hass, H. B., Hodge, E. B., Vanderbilt, B. M., *Ind. Eng. Chem*. **1936**, 339.

[7] *Industrielle Organische Chemie* Weissermel, K., Arpe, H.-J. Ed. Verlag Chemie, Weinheim, Germany **1978**, 46.

[8] Vincent, J. B., Olivier-Lilley, G. L., Averill, B. A., *Chem. Rev*. **1990**, *90*, 1447. (b) Wilkins, R. G., *Chem. Soc. Rev*. **1992**, 171. (c) Que, L., Jr., Dong, Y., *Acc. Chem. Res*. **1996**, 29, 190. (d) Liu, K. E., Lippard, S. J., *Adv. Inorg. Chem*. **1995**, *42*, 263. (e) Shteinman, A. A., *Russ. Chem. Bull*. **1995**, *44*, 975. (f) Valentine, A. M., Lippard, S. J., *J. Chem. Soc., Dalton Trans*. **1997**, 3925. (g) Shinohara, Y., Uchiyama, H., Yagi, O., Kusakabe, I., *J. Fermentation and Bioengineering* **1998**, *83*, 37.

[9] (a) Nizova, G. V., Süss-Fink, G., Shul'pin, G. B., *J. Chem. Soc., Chem. Commun.* **1997**, 397. (b) Süss-Fink, G., Yan, H., Nizova, G. V., Stanislas, S., Shul'pin, G. B., *Izv. Akad. Nauk Ser. Khim*. **1997**, *10*, 1897; *Russ. Chem. Bull*. **1997**, *46*, 1801. (c) Süss-Fink, G., Nizova, G. V., Stanislas, S., Shul'pin, G. B, *J. Mol. Catal. A* **1998**, *130*, 163.

[10] Süss-Fink, G., Stanislas, S., Shul'pin, G. B, Nizova, G. V., Stoeckli-Evans, H., Neels, A., Bobillier, C., Claude, S., *J. Chem. Soc., Dalton Trans*. **1999**, 3169.

[11] Shul'pin, G. B., Kozlov, Y. N., Nizova, G. V., Süss-Fink, G., Stanislas, S., Kitaygorodskiy, A., Kulikova, V. S., Shul'pina, L. S., *J. Chem. Soc., Perkin Trans*. *2* **2001**, 1351.

[12] a) Mizuno, N., Tateishi, M., Hirose, T., Iwamoto, M., *Chem. Lett*. **1993**, 2137. b) Murahashi, S.-I., Oda, Y., Naota, *J. Am. Chem. Soc*. **1992**, *114*, 7913.

[13] Hamamoto, M., Nakayama, K., Nishiyama, Y., Ishii, Y., *J. Org. Chem*. **1993**, 58, 6421.

[14] Ishii, Y., Iwahama, T., Sakaguchi, S., Nakayama, K., Nishiyama, Y., *J.Org. Chem.* **1996**, *61*, 4520.

[15] Ishii, Y. Kato, S., Iwahama, T., Sakaguchi, S., *Tetrahedron Lett*. **1996**, *37*, 4993.

[16] Sakaguchi, S., Kato, S., Iwahama, T., Ishii, Y., *Bull. Chem. Soc. Japan* **1998**, *71*, 1237.

[17] Ishii, Y., *J. Mol. Catal. A: Chem.* **1997**, *117*, 123.

[18] Murahashi, S., Oda, Y., Naota, T., *J. Am. Chem. Soc*. **1992**, *114*, 7913.

[19] Battioni, P., Iwanejko, R., Mansuy, D., Mlodnicka, T., Poltowicz, J., Sanches, F., *J. Mol. Catal. A: Chem.* **1996**, *109*, 91.

[20] Dell'Anna, M. M., Mastrorilli, P., Nobile, C. F., *J. Mol. Catal A: Chem*. **1998**, *130*, 65.

[21] Mastrorilli, P., Nobile, C. F., Suranna, G. P., Lopez, L., *J. Mol. Catal.* **1996**, *108*, 57.

[22] Kaneda, K., Haruna, S. Imanaka, T., Kawamoto, K., *J. Chem. Soc.: Chem. Commun*. **1990**, 1467.

[23] Nam, W., Kim, H. J., Kim, S.H., Ho, R. Y. N., Valentine, J. S., *Inorg. Chem*. **1996**, *35*, 1045.

[24] Murahashi, S. I., Saito, T., Naota, T. Kumobayashi, H., Akutagawa, S., *Tetrahedron Lett*. **1991**, *32*, 5991.

[25] Kuruse, Y., Neckers, D.C., *J. Org. Chem*. **1991**, *56*, 1981.

[26] Belova, V. S., Gimanova, I. M., Stepanova, M. K., Khenkin, A. M., Shilov, A. E., *Dokl. Akad. Nauk SSSR* **1991**, *316*, 653 (in Russian).

[27] Belova, V, S., Khenkin, A. M., Postnov, V. N., Prusakov, V. E., Shilov, A. E., Stepanolva, M. L., *Mendeleev Commun*. **1992**, 7.

[28] Davis, R., Durrant, J. L. A., Khan, M. A., *Polyhedron* **1988**, *7*, 425.

[29] Shul'pin, G. B., Kats, M. M., Lederer, P., *J. Gen. Chem. USSR* **1989**, *59*, 2450.

[30] Shul'pin, G. B., Kats, M. M., *React. Kinet. Catal. Lett*. **1990**, *41*, 239.

[31] Shul'pin, G. B., Kats, M. M., *Neftekhimiya* **1991**, *31*, 648 (in Russian).

[32] Shul'pin, G. B., Druzhinina, A. N., *Mendeleev Commun*. **1992**, 36.

[33] Shul'pin, G. B., Druzhinina, A. N., *Bull. Russ. Acad. Sci.,Div. Chem. Sci*. **1992**, *41*, 346.

[34] Shul'pin, G. B., Nizova, G. V., Kozlov, Yu. N., *New J. Chem*. **1996**, *20*, 1243.

[35] Druzhinina, A. N., Shul'pina, L. S., Shul'pin, G. B., *Bull. Acad. Sci. USSR, Div. Chem. Sci*. **1991**, *40*, 1492.

[36] Shul'pin, G. B., Nizova, G. V., Kats, M. M., *Neftekhimiya* **1991**, *31*, 658 (in Russian).

[37] Barton, D. H. R., Gastiger, M. J., Motherwell, W. B., *J. Chem. Soc., Chem. Commun*. **1983**, 41.

[38] (a) Barton, D. H. R., Doller, D., *Acc. Chem. Res*. **1992**, *25*, 514. (b) Barton, D. H. R., Taylor, D. K., *Russ. Chem. Bull.* **1995**, *44*, 575. (c) Barton, D. H. R., *Tetrahedron* **1998**, *54*, 5805. (d) Perkins, M. J., *Chem. Soc. Rev*. **1996**, 229. (e) Barton, D. H. R., *Chem. Soc. Rev*. **1996**, 237.

[39] (a) Barton, D. H. R., Bévière, S. D., Chavasiri, W., Csuhai, E., Doller, D., Liu, W.-G., *J. Am. Chem. Soc*. **1992**, *114*, 2147. (b) Barton, D. H. R., Bévière, S.D., Chavasiri, W. Csuhai, E. Doller, D., *Tetrahedron* **1992**, *48*, 2895. (c) Barton, D. H. R., Cshuai, E., Doller, D., *Tetrahedron* **1992**, *48*, 9195. (d) Barton, D. H. R., Bévière, S. D., Chavasiri, W., Doller, D., Hu, B., *Tetrahedron Lett*. **1993**, *34*, 567. (e) Barton, D. H. R., Chavasiri, W., Hill, D. R., Hu, B., *New J. Chem.* **1994**, *18*, 611. (f) Barton, D. H. R., Hill, D. R., *Tetrahedron Lett*. **1994**, *35*, 1431. (g) Barton, D. H. R., Chabot, B. M., Delanghe, N. C., Hu, B., Le Gloahec, V. N., Wahl, R. U. R., *Tetrahedron Lett*. **1995**, *36*, 7007. (i) Barton, D. H. R., Hu, B., Wahl, R. U. R., Taylor, D. K., *New J. Chem*. **1996**, *20*, 121. (j) Barton, D. H. R., Beck, .A. H., Delanghe, N. C., *Tetrahedron Lett.* **1996**, *37*, 1755. (l) Barton, D. H. R., Delanghe, N. C., *Tetrahedron*

Lett. **1996**, *37*, 1555. (k) Barton, d. H. R., Chabot, B. M., Hu, B., *Tetrahedron Lett*. **1996**, *37*, 8137. (m) Barton, D. H. R., Hu, B. Li, T. Mackinnon, J., *Tetrahedron Lett*. **1996**, *37*, 8329. (n) Barton, D. H. R., Hu, B., Taylor, D. K., Wahl, R. U. R., *J. Chem. Soc., Perkin Trans. 2* **1996**, 1031. (o) Barton, D. H. R., Chabot, B. M., *Tetrahedron* **1996**, *52*, 10287. (p) Barton, D. H. R., Chabot, B. M., Hu, B., *Tetrahedron* **1996**, *31*, 10301. (q) Barton, D. H. R., Hu, B., *Tetrahedron* **1996**, *31*, 10313. (r) Barton, D. H. R., Li. T., MacKinnon, J., *Chem. Commun*. **1997**, 557. (s) Barton, D. H. R., Delanghe, N. C., *Tetrahedron* **1998**, *54*, 4471. (t) Barton, D. H. R., Li, T., *Chem. Comm*. **1998**, 821.

[40] (a) *New Developments in Selective Oxidation*, Schuchardt, R., Mano, V., Centi, G., Trifiro, F., (Eds.), Elsevier, Amsterdam, **1990**, 185. (b) Schuchardt, U., Krähembühl, C. E. Z., Carvalho, W. A., *New J. Chem*. **1991**, *15*, 955. (c) Shul'pin, G. B., Kitaygorodskiy, A. N., *J. Gen. Chem. USSR* **1990**, *60*, 920. (d) Knight, C., Perkins, M. J., *J. Chem. Soc., Chem. Commun.* **1991**, 925. (e) Schuchardt, U., Carvalho, W. A., Spinacé, E. V., *Synlett* **1993**, 713. (f) Minisci, F., Fontana, F., Araneo, S., Recupero, F., *J. Chem. Soc., Chem. Commun*. **1994**, 1823. (g) Minisci, F., Fontana, F., *Tetrahedron Lett*. **1994**, *35*, 1427. (h) Minisci, F., Fontana, F., Zhao, L., Banfi, S., Quici, S., *Tetrahedron Lett*. **1994**, *35*, 8033. (i) Newcomb, M., Simakov, P. A., Park, S.-U., *Tetrahedron Lett*. **1996**, *37*, 819. (j) Sobolev, A. P., Babushkin, D. E., Shubin, A. A., Talsi, E. P., *J. Mol. Catal. A: Chem.* **1996**, *112*, 253. (k) Singh, B., Long, J. R., Papaefthymiou, G. C., Stavropoulos, P., *J. Am. Chem. Soc*. **1996**, *118*, 5824.

[41] Jones, P., *Inorg. Chim. Acta* **1983**, *79*, 177.

[42] Arasasingham, R. D., Balch, A. L., Hart, R. L., Latos-Grażyński, L., *J. Am. Chem. Soc.* **1990**, *112*, 7566.

[43] Fenton, H. J. H., *J. Chem. Soc.* **1894**, *65*, 899.

[44] Haber, F., Weiss, J. J., *Proc. Roy. Soc. London, Ser. A* **1934**, *147*, 332.

[45] a) Merz, J. H., Waters, W. A., *Discuss. Faraday Soc.* **1947**, *2*, 179. b) Merz, J. H. Waters, W. A., *J. Chem. Soc*. **1949**, *S15*, 2427.

[46] Walling, C., *Acc. Chem. Res*. **1975**, *8*, 125.

[47] Mimoun, H., Seree de Roch, I., *Tetrahedron* **1975**, *31*, 777.

[48] Shul'pin, G. B., Nizova, G. V., *React. Kinet. Catal. Lett.* **1992**, *48*, 333.

[49] Duboc-Toia, C., Menage, S., Lambeaux, C., Fontecave, M., *Tetrahedron Lett*. **1997**, *38*, 3727.

[50] (a) Kim, J., Harrison, R. G., Kim, C., Que, L., Jr., *J. Am. Chem. Soc* **1996**, *118*, 4373. (b) Kim, J., Kim, C., Harrison, R. G., Wilkinson, E. C., Que, L., Jr., *J. Mol. Catal. A: Chem.* **1997**, *117*, 83. (c) MacFaul, P. A., Arends, I. W. C. E., Ingold, K. U., Wayner, D. D. M. *J. Chem. Soc., Perkin Trans. 2* **1997**, 135.

[51] a) Nomura, K., Uemura, S., *J. Chem. Soc., Chem. Commun*. **1994**, 129. b) MacFaul, P. A., Wayner, D. D. M., Ingold, K. U., *Acc. Chem. Res*. **1998**, *31*, 159. c) Minisci, F., Fontana, F., Araneo, S., Recupero, F., Zhao, L., *Synlett* **1996**, 119. d) Rabion, A., Buchanan, R. M., Seris, J.-L., Fish, R. H., *J. Mol. Catal. A: Chem.* **1997**, *116*, 43.

[52] Kodera, M., Shimakoshi, H., Kano, K., *Chem. Comm*. **1996**, 1737.

[53] Gross, Z., Simkhovich, L., *Tetrahedron Lett*. **1998**, *39*, 8171.

[54] Mansuy, D., Bartoli, J.-F., Battioni, P., Lyon, D. K., Finke, R. G., *J. Am. Chem. Soc*. **1991**, *113*, 7222.

[55] Song, R., Sorokin, A., Bernadou, J., Meunier, B., *J. Org. Chem*. **1997**, *62*, 673.

[56] Shul'pin, G. B., Kats, M. M., Kozlov, Yu. N., *Bull. Acad. Sci. USSR, Div. Chem. Sci.* **1988**, *37*, 2396.

[57] Gross, Z., Simkhovich, L., *J. Mol. Catal. A: Chem*. **1997**, *117*, 243.

[58] *Activation and Catalytic Reactions of Saturated Hydrocarbons in the Presence of Metal Complexes* Shilov, A. E., Shul'pin, G. B., Kluwer Academic Publishers, Dordrecht, The Netherlands, **2000**, p. 470.

[59] Guengerich, F. P., Macdonald, T. L. *Acc. Chem. Res.* **1984**, *17*, 9.

[60] (a) *Activation and Catalytic Reactions of Saturated Hydrocarbons in the Presence of Metal Complexes* Shilov, A. E., Shul'pin, G. B.; Kluwer Academic Publishers (Eds.), Dordrecht, The Netherlands, **2000**, p. 474. (b) *Bioinorganic Chemistry* Valentine, J. S.; Bertini, I., Gray, H. B., Lippard, S. J., Valentine, J. S. (Eds.), University Science Books: Mill Valley, California, USA, **1994**, 253-314.

[61] Groves, J. T., McClusky, G. A., White, R. E., Coon, M. J., *Biochem. Biophys. Res. Commun.* **1978**, *81*, 154.

[62] Gelb, M. H., Heimbrook, D. C., Malkonen, P., Sligar, S. G. *Biochemistry* **1982**, *21*, 370.

[63] *Activation and Catalytic Reactions of Saturated Hydrocarbons in the Presence of Metal Complexes,* Shilov, A. E., Shul'pin, G. B.; Kluwer Academic Publishers (Eds.), Dordrecht, The Netherlands, **2000**, p. 482.

[64] (a) Khenkin, A. M., Shilov, A. E., *React. Kinet. Catal. Lett.* **1987**, *33*, 125. (b) Leduc, P., Battioni, P., Bartoli, J. F., Mansuy, D., *Tetrahedron Lett.* **1988**, *29*, 205.

[65] Belova, V.S., Nikonova, L. A., Raihkman, L. M., Borukaeva, M. R., *Dokl. Akad. Nauk SSSR* **1972**, *204*, 897 (in Russian).

[66] Tabushi, I., Yazaki, A., *J. Am. Chem. Soc.* **1981**, *103*, 7371.

[67] Karasevich, E. I., Khenkin, A. M., Shilov, A. E., *Dokl. Akad. Nauk SSSR* **1987**, *295*, 639 (in Russian).

[68] Shul'pin, G. B., Druzhinina, A. N. *Bull. Acad. Sci. USSR, Div. Chem. Sci*. **1991**, *40*, 2385.

[69] (a) Banfi, S., Maiocchi, A., Moggi, A., Montanari, F., Quici, S., *J. Chem. Soc., Chem. Commun.* **1990**, 1794. (b) Yamaki, S., Kobayashi, S., Kotani, E., Tobinaga, S., *Chem. Pharm. Bull*. **1990**, *38*, 1501. (c) Artaud, I., Ben-Aziza, K., Mansuy, D., *J. Org. Chem.* **1993**, *58*, 3373.

[70] (a) Mansuy, D., Battioni, P., Renaud, J.-P., *J. Chem. Soc., Chem. Commun.* **1984**, 1255. (b) Higuchi, T., Shimada, L., Maruyama, N., Hirobe, M., *J. Am. Chem. Soc.* **1993**, *115*, 7551.

[71] (a) Lindsay Smith, J. R., Sleath, P. S., *J. Chem. Soc., Perkin Trans. 2* **1982**, 1009. (b) Bartoli, J. F., Brigaud, O., Battioni, P., Mansuy, D., *J. Chem. Soc., Chem. Commun.* **1991**, 440. (c) Khanna, R. K., Pauling, R. M., Vajpayee, D., *Tetrahedron Lett.* **1991**, 440. (d) Battioni, P., Bartoli, J. F., Mansuy, D., Byun, Y. S., Traylor, T. G. *J. Chem. Soc., Chem. Commun.* **1992**, 1050. (e) Bartoli, J. F., Battioni, P., De Foor, W. R., Mansuy, D., *J. Chem. Soc., Chem. Commun*. **1994**, 23. (f) Nam, W., Valentine, J. S., *J. Am. Chem. Soc.* **1993**, *115*, 1772.

[72] (a) De Poorter, B., Ricci, M., Bortolini, O., Meunier, B., *J. Mol. Catal*. **1985**, *31*, 221. (b) Sorokin, A. B., Khenkin, A. M., *New J. Chem*. **1990**, *14*, 63.

[73] (a) Robert, A., Meunier, B., *New J. Chem.* **1988**, *12*, 885. (b) Meunier, B., *New J. Chem*. **1992**, *16*, 203. (c) Hoffmann, P., Robert, A., Meunier, B., *C. R. Acad. Sci., Ser. 2* **1992**, *314*, 51.

[74] Ohtake, H., Higuchi, T., Hirobe, M., *J. Am. Chem. Soc*. **1992**, *114*, 10660.

[75] (a) Querci, C., Ricci, M., *Tetrahedron Lett*. **1990**, *31*, 1779. (b) Artaud, I., Grennberg, H., Mansuy, D., *J. Chem. Soc., Chem. Commun*. **1992**, 1036.

[76] MacFaul, P. A., Ingold, K. U., Wayner, D. D. M., Que, L., Jr., *J. Am. Chem. Soc.* **1997**, *119*, 10594.

[77] Groves, J. T., Haushalter, R. C., Nakamura, M., Nemo, T. E., Evans, B. I., *J. Am. Chem. Soc*. **1981**, *103*, 2884.

[78] (a) Khenkin, A. M., Shteinman, A. A., *Kinet. Katal*. **1982**, *23*, 219 (in Russian). (b) Khenkin, A. M., Shteinman, A. A., *Izv. Akad, Nauk SSSR, Ser. Khim*. **1982**, 1668 (in Russian).

[79] Feig, A. L., Lippard, S. J., *Chem. Rev.* **1994**, *94*, 759.

[80] Lipscomb, J. D., *Annual Rev. Microbiol*. **1994**, *48*, 371.

[81] Rosenzweig, A. C., Frederick, C. A., Lippard, S. J., Nordlund, P., *Nature* **1993**, *366*, 537.

[82] Kopp, D. A., Lippard, S. J., *Current Opinion Chem.Biol.* **2002**, *6*, 568.

[83] Panov, G. I., Dubkov, K. A., Sobolev, V. I., Talsi, E. P., Rodkin, M. A., Watkins, N. H., Shteinman, A. A., *J. Mol. Cat A: Chemical* **1997,** *123,* 155.

[84] Miki, K., Furuya, T., *Chem. Comm.* **1998**, 97.

[85] *Chemistry of the Elements*, Greenwood, N. N., Earnshow, A., (Eds.), Butterworth-Heinemann, Oxford, **1997**.

[86] Milas, N. A., *J. Am. Chem. Soc*., **1937**, *59*, 2342.

[87] Conte, V., Di Furia, F., Licini, G., *Appl. Catal. A: General* **1997**, *157*, 335.

[88] Mimoun, H., Saussine, L., Daire, E., Postel, M., Fisher, J., Weiss, R., *J. Am. Chem. Soc*. **1983**, *105*, 3101.

[89] (a) Shul'pin, G. B., Attanasio, D., Suber, L., *Russ. Chem. Bull*. **1993**, *42*, 55. (b) Shul'pin, G. B., Druzhinina, A. N., Nizova, G. V, *Russ. Chem. Bull*. **1993**, *42*, 1327. (c) Shul'pin, G. B., Drago, R. S., Gonzalez, M., *Russ. Chem. Bull*., **1996**, *45*, 2386.

[90] Süss-Fink, G., Stanislas, S., Shul'pin, G. B., Nizova, G. V., *Appl. Organometal. Chem*. **2000**, *14*, 623.

[91] Remias, J. E., Pavlosky, T. A., Sen, A., *J. Mol. Catal. A: Chem*. **2003**, *203*, 179.

[92] Shul'pin, G. B., Lachter, E. R., *J. Mol. Catal. A: Chem*. **2003**, *197*, 65.

[93] Henze, M., *Hoppe Seyler's Z. Physiol. Chem*. **1911**, *72*, 494.

[94] Robson, R. L., Eady, R. R., Richardson, T. H., Miller, R. W., Hawkins, M., Postgate, J. R., *Nature* **1986**, *322*, 388.

[95] Rees, D. C., Howard, J. B., *Current Opinion in Chem. Biol*. **2000**, *4*, 559.

[96] Rehder, D., *Coord. Chem. Rev*. **1999**, *182*, 297.

[97] Vilter, H., *Phytochemistry* **1984**, *23*, 1387.

[98] Weyand, M., Hecht, H.-J., Kieß, M., Liaud, M.-F., Vilter, H., Schomburg, D., *J. Mol. Biol.* **1999**, *293*, 595.

[99] (a) Messerschmidt, A., Wever, R., *Proc. Natl. Acad. Sci. USA* **1996**, *93*, 392. (b) Messerschmidt, A., Prade, L., Wever, R., *Biol. Chem*. **1997**, *378*, 309.

[100] Colpas, G. J., Hamstra, B. J., Kampf, J. W., Pecoraro, V. L., *J. Am. Chem. Soc*. **1996**, *118*, 3469.

[101] Tsaramyrse, M., Kavousanaki, D., Raptopoulou, C. P., Terzes, A., Salifoglou, A., *Inorg. Chim. Acta* **2001**, *320*, 47.

[102] Willsky, G. R., Goldfine, A. B., Kostyniak, P., McNeill, J. H., Yang, L. Q., Khan, H. R., Crans, D. C., *J. Inorg. Biochem*. **2000**, *85*, 33.

[103] Baran, E. J., *J. Inorg. Biochem*. **2000**, *80*, 1.

[104] Stohs, S. J., Bagchi, D., *Free Radical Biol. Med*. **1995**, *18*, 321.

[105] Shi, X. L., Jiang, H. G., Mao, Y., Ye, J. P., Saffiotti, U., *Toxicology* **1996**, *106*, 27.

[106] Ding, M., Li, J. J., Leonard, S. S., Ye, J. P., Shi, X. L., Colburn, N. H., Castranova, V., Vallyathan, V., *Carcinogenesis* **1999**, *20*, 663.

[107] Castranova, V., Vallyathan, V., Shin, X. L., *J. Biol. Chem*. **2000**, *275*, 32516.

[108] Huang, C. S., Ding, M., Li, J. X., Leonard, S. S., Rojanasakul, Y., Castranova, V., Vallyathan, V., Ju, G., Shi, X. L., *J. Biol. Chem.* **2001**, *276*, 22397.

[109] Zhang, Z., Huang, C. S., Li, J. X., Leonard, S. S., Lanciotti, R., Butterworth, L., Shi, X. L., *Arch. Biochem. Biophys*. **2001**, *392*, 311.

[110] Zhang, Z., Huang, C., Li, J., Shi, X., *J. Inorg. Biochem*. **2002**, *89*, 142.

[111] Ding, M. Gannett, P. M., Rojanasakul, Y., Liu, K. J. Shi, X. L., *J. Inorg. Biochem.* **1994**, *55*, 101.

[112] Ferrer, E. G., Baran, E. J., *Biol. Trace Element Res*. **2001**, *83*, 111.

[113] Kotchevar, A. T., Ghosh, P., DuMez, D. D., Uckun, F. M., *J. Inorg. Biochem*. **2001**, *83*, 151.

[114] *Metal Ions in Biological Systems, vol. 31, Vanadium and Its Role in Life*, Djordjevic, C., Sigel, H., Sigel, A., Marcel Dekker (Ed.), New York, **1995**, pp. 595–616.

[115] Lyonett, B. M., Martin, E., *La Press Medicale 1*, **1899**, 191.

[116] *The Pharmacological Basis of Therapeutics*, Davis, S. N., Graner, D. K., Hardamn, J. G., Limbird, L. E., Ruddon, R. W., Gilman, A. G. (Eds.), Pergamon Press, New York, **1996**, p. 1487.

[117] Cohen, N., Halberstam, M., Shlimovich, P., Chang, C. J., Shamoon, H., Rosseti, J., *J. Clin. Invest*. **1995**, *95*, 2501.

[118] Boden, G., Chen, Z., Ruiz, J., van Rossum, G. D., Turco, S., *Metabolism* **1996**, *45*, 1130.

[119] Cusi, K., Cukeir, S., DeFronzo, R. A., Torres, M., *Diabetes* **1997**, *46*, 34A.

[120] Goldfine, A. B., Simonson, D. C., Folli, F., Patti, M.-E., Kahn, C. R., *J. Clin. Endocrinol. Metab*. **1995**, *80*, 3311.

[121] (a) Simons, T. J. B., *Nature* **1979**, *281*, 337. (b) Macara, I, G., *Trends Biochem. Sci.* **1980**, *5*, 92.

[122] Domingo, J. L., Paternain, J. L., Llobet, J. M., Corbella, J., *Life Science* **1986**, *39*, 819.

[123] Stacey, N. H, Klaassen, C. D., *Toxicol. Appl. Pharmacol*. **1981**, *58*, 8.

[124] Shi, X., Dalal, N. S., *Free Radic. Res. Commun*. **1992**, *17*, 369.

[125] Kozhevnikov, I. V., *Chem. Rev*. **1998**, *98*, 171.

[126] Attanasio, D., Orru', D., Suber, L., *J. Mol. Catal*. **1989**, *57*, L1.

[127] Neumann, R., de la Vega, M., *J. Mol. Catal*. **1993**, *84*, 93.

[128] Kuznetsova, N. I., Kuznetsova, L. I., Likholobov, V. A., *J. Mol. Catal. A: Chem.* **1996**, *108*, 135.

[129] Kuznetsova, L. I., Detusheva, L. G., Fedotov, M. A., Likholobov, V. A., *J. Mol. Catal. A: Chem.* **1996**, *111*, 81.

[130] Kuznetsova, N. I., Detusheva, L. G., Kuznetsova, L. I., Fedotov, M. A., Likholobov, V. A., *J. Mol. Catal. A: Chem*. **1996**, *114*, 131.

[131] Nomiya, K., Yanagivayashi, H., Nozaki, C., Kondoh, K., Hiramatsu, E., Shimizu, Y., *J. Mol. Catal. A: Chem*. **1996**, *114*, 181.

[132] Kuznetsova, L. I., Detusheva, L. G., Kuznetsova, N. I., Fedotov, M. a., Likholobov, V. A., *J. Mol. Catal. A: Chem*. **1997**, *117*, 389.

[133] Nomiya, K., Yagishita, K., Nemoto, Y., Kamataki, T., *J. Mol. Catal. A: Chem.* **1997**, *126*, 43.

[134] Nomiya, K., Nemoto, Y., Hasegawa, T., Matsuoka, S., *J. Mol. Catal. A: Chem*. **2000**, *152*, 55.

[135] Nomiya, K., Matsuoka, S., Hasegawa, Nemoto, Y., *J. Mol. Catal. A: Chem*. **2000**, *152*, 55.

[136] *Activation and Catalytic Reactions of Saturated Hydrocarbons in the Presence of Metal Complexes* Shilov, A. E., Shul'pin, G. B., Kluwer Academic Publishers, Dordrecht, The Netherlands, **2000**, p. 431.

[137] Shilov, A. E., Shul'pin, G. B., *Chem. Rev*. **1997**, *97*, 2879.

[138] Faraj, M., Hill, C., *J. Chem. Soc., Chem. Commun*. **1987**, 1487.

[139] Matsumoto, Y., Asami, M., Hashimoto, M., Misono, M., *J. Mol. Catal. A: Chem.* **1996**, *114*, 161.

[140] Mizuno, N., Nozaki, C., Hirose, T., Tateishi, M., Iwamoto, M., *J. Mol. Catal. A: Chem*. **1997**, *117*, 159.

[141] Cramarosa, M. R., Forti, L., Fedotov, M. A., Detusheva, L. G., Likholobov, V. A., Kuznetsova, L. I., Semin, G. L., Cavani, F., Trifirò, F., *J. Mol. Catal. A: Chem*. **1997**, *127*, 85.

[142] Mizuno, N., Nozaki, C., Kiyoto, I., Misono, M., *J. Am. Chem. Soc*. **1998**, *120*, 9267.

[143] Simões, M. M. Q., Conceição, c. M. M., Gamelas, J. A. F., Domingues, P. M. D. N., Cavaleiro, A. M. V., Cavaleiro, J. A. S., Ferrer-Correia, A. J. V., Johnstone, R. A. W., *J. Mol. Catal. A: Chem*. **1999**, *144*, 461.

[144] Hayashi, T., Kishida, A., Mizuno, N., *Chem. Commun*. **2000**, 381.

[145] Süss-Fink, G., Gonzalez, L., Shul'pin, G. B., *Applied Catalysis A: General* **2001**, *217*, 111.

[146] Shul'pin, G. B., Attanasio, D., Suber, L., *J. Catal*. **1993**, *142*, 147.

[147] Shul'pin, G. B., Guerreiro, M. C., Schuchardt, U., *Tetrahedron* **1996**, *52*, 13051.

[148] Guerreiro, M. C., Schuchardt, U., Shul'pin, G. B., *Russ. Chem. Bull*. **1997**, *46*, 749.

[149] Nizova, G. V., Süss-Fink, G., Shul'pin, G. B., *Tetrahedron* **1997**, *53*, 3603.

[150] Schuchardt, U., Guerreiro, M. C., Shul'pin, G. B., *Russ. Chem. Bull.* **1998**, *47*, 247.

[151] Shul'pin, G. B., Ishii, Y., Sakaguchi, S., Iwahama, T., *Russ. Chem. Bull***. 1999**, *48*, 887.

[152] Nizova, G. V., Süss-Fink, Stanislas, S., G., Shul'pin, G. B., *Chem. Commun*. **1998**, 1885.

[153] Shul'pin, G. B., Druzhinina, A. N., Shul'pina, L. S., *Petrol. Chem.* **1993**, *33*, 321.

[154] Shul'pin, G. B., Bochkova, M. M., Nizova, G. V., *J. Chem. Soc., Perkin Trans. 2* **1995**, 1465.

[155] Köppen, M., Fresen, G., Wieghardt, K., Llusar, R. M., Nuber, B, Weiss, J. *Inorg. Chem* **1988**, *27*, 721.

[156] Cooper, S. R., Koh, Y. B., Raymond, K. N., *J. Am. Chem. Soc.* **1982,** *104*, 5092.

[157] Fiedler, D., Miljanic, O. S, Welch, E. J., *Acta Cryst. E: Structure Reports* **2002,** m347.

[158] Neves, A., Rossi, L. M., Bortoluzzi, A. J., Mangrich, A. S. Haase, W., Nascimento, O., *Inorg. Chem. Comm.* **2002,** *5,* 418.

[159] Knopp, P., Wieghardt, K., Nuber, B., Weiss, J., *Z. Naturforsch*. **1991**, *B 46*, 1077.

[160] Jeske, P., Haselhorst, G., Weyhermüller, T., Wieghardt, K., Nuber, B., *Inorg. Chem.* **1994**, *33***,** 1987.

[161] Burger, K. S., Haselhorst, G., Stotzel, S., Weyhermüller, T., Wieghardt, K., Nuber, B., *J. Chem. Soc. Dalton Trans*. **1993**, 1987.

[162] de la Cruz, M. H. C., Kozlov, Yu. N., Lachter, E. R., Shul'pin, G. B., *New J. Chem.* **2003**, *27*, 634.

[163] Kozlov, Yu. N., Nizova, G. V., Shul'pin, G. B., *Russ. J. Phys. Chem*. **2001**, *75* 770.

[164] Ferrell, R. E., Kitto, G. B., *Biochem.* **1971**, *10*, 2923.

[165] Klippenstein, G. L., *Biochem.* **1972**, *11*, 372.

[166] Kurtz, D. M., Jr., *Chem. Rev*. **1990**, *90*, 585.

[167] Sychev, A. Ya., Isak, V. G., *Russ. Chem. Rev*. **1995**, *64*, 1105.

[168] Wallar, B. J., Lipscomb, J. D., *Chem. Rev*. **1996**, *96*, 2626.

[169] Siegbahn, P. E. M., Crabtree, R. H., *J. Am. Chem.Soc*. **1997**, *119*, 3103.

[170] Yoshizawa, K., Ohta, T. Yamabe, T., Hoffmann, R., *J. Am. Chem. Soc.* **1997**, *119*, 12311.

[171] van der Beuken, E. K., Ferenga, B. L., *Tetrahedron* **1998**, *54*, 12985.

[172] Fontecave, M., Ménage, S., Duboc-Toia, C., *Coord. Chem. Rev*. **1998**, *178-180*, 1555.

[173] Willems, J.-P., Valentine, A. M., Urbiel, R., Lippard, S. J., Hoffman, B. M., *J. Am. Chem. Soc.* **1998**, *120*, 9410.

[174] Deeth, R. J., Dalton, H., *JBIC* **1998**, *3*, 302-306 and subsequent papers in this issue.

[175] Valentine, A. M., Stahl, S. S., Lippard, S. J., *J. Am. Chem. Soc*. **1999**, *121*, 3876.

[176] *Activation and Catalytic Reactions of Saturated Hydrocarbons in the Presence of Metal Complexes* Shilov, A. E., Shul'pin, G. B., Kluwer Academic Publishers, Dordrecht, The Netherlands, **2000**, Chapter XI.

[177] Costas, M., Chen, K., Que, L., Jr., *Coord. Chem. Rev*. **2000**, *200-202*, 517.

[178] Solomon, E. I., Brunold, T. C., Davis, M. I., Demsley, J. N., Lee, S.-K., Lehnert, N., Neese, F., Skulan, A. J., Yang, Y.-S., Zhou, J., *Chem. Rev*. **2000**, *100*, 235.

[179] Solomon, E. I., *Inorg. Chem*. **2001**, *40*, 3656.

[180] Lee, D., Lippard, S. J., *Inorg. Chem*. **2002**, *41*, 827.

[181] Nishida, Y., Yamada, K., *J. Chem. Soc., Dalton Trans*. **1990**, 3639.

[182] Kitajima, N., Ito, M., Fukui, H., Moro-oka, Y., *J. Chem. Soc., Chem. Commun*. **1991**, 102.

[183] Fish, R. H., Konings, M. S., Oberhausen, K. J., Fong, R. H., Yu, W. M., Christou, G., Vincent, J. B., Coggin, D. K., Buchanan, R. M., *Inorg. Chem*. **1991**, *30*, 3002.

[184] Kulikova, V. S., Gritsenko, O. N., Shteinman, A. A. *Mendeleev Commun.* **1996**, *119*.

[185] Ménage, S., Galey, J.-B.,Hussler, G., Seité, M., Fontecave, M., *Angew. Chem. Int. Ed. Engl.* **1996**, *35*, 2353.

[186] Ito, S., Okuno, T., Itoh, H., Ohba, S., Matsushima, H., Tokii, T., Nishida, Y., *Z. Naturforsch.* **1997**, *52b*, 719.

[187] *3 rd World Congress on Oxidation Catalysis*, Knops- Gerrits, P. P., Dicks, S., Weiss, A., Genet, M., Rouxhet, P., Li, X. Y., Jacobs, P. A; Grasselli, R. K., Oyama, S. T., Gaffney, A. M., Lyons, J. E., Eds., Elsevier, Amsterdam, **1997**, 1061-1070.

[188] Ménage, S., Galey, J.-B., Dumats, J., Hussler, G., Seité, M., Luneau, I. G., Chottard, G., Fontecave, M., *J. Am. Chem. Soc*. **1998**, *120*, 13370.

[189] Nishino, S., Hosomi, H., Ohba, S., Matsushima, H., Tokii, T., Nishida, Y., *J. Chem. Soc., Dalton Trans*. **1999**, 1509.

[190] Roelfes, G., Lubben, M., Hage, R., Que, L., Jr., Feringa, B. L., *Chem. Eur. J*. **2000**, *6*, 2152.

[191] Nizova, G. V., Krebs, B., Süss-Fink, G., Schindler, S., Westerheide, L., Gonzalez Cuervo, L., Shul'pin, G. B., *Tetrahedron* **2002**, *58*, 9231.

[192] Kozlov, Yu. N., Gonzalez Cuervo, L., Süss-Fink, G., Shul'pin, G. B., *Russ. J. Phys. Chem*. **2003**, *77*, 652.

[193] Nishida, Y., Takeuchi, M., Shimo, H., Kida, S., *Inorg. Chim. Acta* **1984**, *96*, 115.

[194] Brennan, B., Chen, Q., Juarez-Garcia, C., Rue, A., O'Connor, C., Que, L., Jr., *Inorg. Chem*. **1991**, *30*, 1937.

[195] Tzou, J.-R., Chang, S.-C., Norman, R. E., *J. Inorg. Biochem*. **1993**, *51*, 480.

[196] Feig, A. L., Bautista, M. T., Lippard, S., *Inorg. Chem*. **1996**, *35*, 6892.

[197] Suzuki, M., Furutachi, H., Ōkawa, H., *Coord. Chem. Rev.* **2000**, *200-202*, 105.

[198] Satcher, J. H., Fr., Droege, M. W., Olmstead, M. M., Balch, A. L., *Inorg. Chem*. **2001**, *40*, 1454.

[199] Westerheide, L., Müller, F. K., Than, R., Krebs, B., Dietrich, J., Schindler, S., *Inorg. Chem*. **2001**, *40*, 1951.

[200] (a) Shul'pin, G. B., Lindsay Smith, J. R., *Russ. Chem. Bull.* **1998**, *47*, 2313. (b) Shul'pin, G. B., Lindsay Smith, J. R., *Russ. Chem. Bull.* **1998**, *47*, 2379.

[201] Shul'pin, G. B., Süss-Fink, G., Lindsay Smith, J. R., *Tetrahedron* **1999**, *55*, 5345.

[202] Shul'pin, G. B., Süss-Fink, G., Shul'pina, L. S., *J. Mol. Catal., A: Chem*. **2001**, *170*, 17.

[203] Lindsay Smith, J. R., Shul'pin, G. B., *Tetrahedron Lett.* **1998**, *39*, 4909.

[204] Heym, B., Alzari, P. M., Honoré, W., Cole, S. T., *Mol. Microbiol*. **1995**, *15*, 235.

[205] Wieghardt, K., Pohl, K., Gebert, W., *Angew. Chem. Int. Ed. Engl.* **1983**, *22*, 727.

[206] Spool, A., Williams, I. D., Lippard, S. J., *Inorg. Chem*. **1985**, *24*, 2156.

[207] Baxendale, J. H., Wilson, J. A., *Trans. Faraday Soc*. **1957**, *53*, 344.

[208] Khar'kova, T. V., Arest-Yakubovich, I. L., Lipes, V. V., *Kinet. Katal.* **1989**, *30*, 954.

[209] Anbar, M., Meyerstein, D., Neta, P.*, J. Chem. Soc.(B)* **1966**, 742.

[210] Vennat, M., Herson, P., Brégeault, J.-M., Shul'pin, G. B., *Eur. J. Inorg. Chem*. **2003**, 908.

[211] Shul'pin, G.B., Kozlov, Yu. N., *Org. Biomol. Chem*. **2003**, *1*, 2302.

[212] *Activation and Catalytic Reactions of Saturated Hydrocarbons in the Presence of Metal Complexes* Shilov, A. E., Shul'pin, G. B., Kluwer Academic Publishers, Dordrecht, The Netherlands, **2000**, Chapter X.

[213] Shul'pin, G. B., *Transition Metals for Organic Synthesis*, M. Beller and C. Bolm (Eds.), Wiley-VCH: Weinheim/New York, second edition, **2004**, vol. 2.

[214] Examples of non-catalysed oxidations with peroxy acids: (a) Ma, D., Xia, C., Tian, H., *Tetrahedron Lett*. **1999**, *40*, 8915. (b) Freccero, M., Gandolfi, R., Sarzi-Amadè, M., Rastelli, A., *Tetrahedron* **2001**, *57*, 9843.

[215] Non-metal-catalyzed oxidations with peroxy acids: Picard, M., Gross, J., Lübbert, E., Tölzer, S., Krauss, S., van Pée, K.-H., Berkessel, *Angew. Chem. Int. Ed.* **1997**, *36*, 1196.

[216] Base-induced oxidations with participation of peroxy acids: (a) Frank, W. C., *Tetrahedron: Asymmetry*, **1998**, *9*, 3745. (b) Ueno, S., Yamaguchi, K., Yoshida, K., Ebitani, K., Kaneda, K., *Chem. Commun*. **1998**, 295. (c) Yamaguchi, K., Ebitani, K., Kaneda, K., *J. Org. Chem*. **1999**, *64*, 2966. (d) Brauer, H.-D., Eilers, B., Lange, A., *J. Chem. Soc., Perkin Trans. 2* **2002**, 1288.

[217] Metal-catalyzed oxidations with peroxy acids: (a) Murahashi, S.-I., Oda, Y., Komiya, N., Naota, T., *Tetrahedron Lett*. **1994**, *35*, 7953. (b) Banfi, S., Montanari, F., Quici, S., Barkanova, S. V., Kaliya, O. L., Kopranenkov, V. N., Luk'yanets, E. A., *Tetrahedron Lett.* **1995**, *36*, 2317. (c) Kodera, M., Shimakoshi, H., Kano, K., *Chem. Comm.* **1996**, 1737. (d) Barkanova, S. V., Derkacheva, V. M., Dolotova, O. V., Li, V. D., Negrimovsky, V. M., Kaliya, O. L., Luk'yanets, E. A., *Tetrahedron Lett.* **1996**, *37*, 1637. (e) Yamaguchi, M., Kousaka, H., Yamagishi, T., *Chemistry Lett.* **1997**, 769. (f) Yamaguchi, M., Iida, T., Yamagishi, T., *Inorg. Chem. Commun.* **1998**, *1*, 299. (g) Beifuss, U., Herde, A., *Tetrahedron Lett.* **1998**, *39*, 7691. (h) Konoike, T., Araki, Y., Kanda, Y., *Tetrahedron Lett.* **1999**, *40*, 6971. (i) Banfi, S., Cavazzini, M., Pozzi, G., Barkanova, S. V., Kaliya, O. K., *J Chem. Soc., Perkin Trans 2* **2000**, 871. (j) Banfi, S., Cavazzini, M., Pozzi, G., Barkanova, S. V., Kaliya, O. K., *J Chem. Soc., Perkin Trans 2* **2000**, 879. (k) Komiya, N., Noji, S., Murahashi, S.-I., *Chem. Commun*. **2000**, *65*, 66. (l) Moody, C. J., O'Connell, J. L., *Chem. Commun.* **2000**, 1311. (m) Barkanova, S. V., Makarova, E. A., *J. Mol. Catal. A : Chem.* **2001**, *174*, 89. (n) Barkanova, S. V., Kaliya, O. K., Luk'yanets, E. A., *Mendeleev Commun*. **2001**, *11*, 116. (o) Murahashi, S.-I., Komiya, N., Hayashi, Y., Kumano, T., *Pure Appl. Chem.*

2001, *73*, 311. (p) Nam, W., Kim, I., Kim, Y., Kim. C., *Chem. Commun.* **2001**, 1262. (q) Le Bras, J., Muzart, J., *J. Mol. Catal. A : Chem.* **2002**, *185*, 113. (r) Khavasi, H. R., Davarani, S. S. H., Safari, N., *J. Mol. Catal. A : Chem*. **2002**, **188**, 115. (s) Sooknoi, T., Limtrakul, J., *Appl. Catal. A: General* **2002**, *233*, 227. (t) Yamaguchi, M., Ichii, Y., Kosaka, S., Masui, D., Yamagishi, T., *Chemistry Lett.* **2002**, 434. (u) Nam, W., Ryu, J. Y., Kim, I., Kim. C., *Tetrahedron Lett.* **2002**, *43*, 5487. (v) Grootboom, N., Nyokong, T., *J. Mol. Catal. A : Chem.* **2002**, *179*, 113.

[218] *Purification of Laboratory Chemicals*, Perrin, D. D., Armarego, W. L. F., Pergamon Press, Oxford, **1998**.

[219] Day, V.W., Klemperer, W. G., Yagasaki, A., *Chem. Lett.* **1990***,* 1267.

[220] Schut, W. J., Mager, H. I. X., Berends, W., *Recueil de Travaux Chimique des Pays-Bas* **1961**, *80*, 391.

[221] Sheldrick, G. M., SHELXS-97 'Program for Crystal Structure Determination', *Acta Cryst*. **1990**, *A46*, 467.

[222] Sheldrick, G. M., SHELXL-97, Universität Göttingen, Göttingen, Germany, **1999**.

[223] Spek, A. L., 'PLATON/PLUTON version Jan. 1999', *Acta Cryst.* **1999**, *A46*, C34.

[224] Nash, T., *Biochem. J*., **1953**, *55*, 416.